FORSCHUNGSZENTRUM
ROSSENDORF e.V.

FZR

FZR-150
September 1996

E. Grosse and B. Kämpfer

Internal Workshop on Kaon Production

Forschungszentrum Rossendorf e.V.
Postfach 51 01 19 · D-01314 Dresden
Bundesrepublik Deutschland

Telefon (0351) 260 3258
Telefax (0351) 260 3270
E-Mail kaempfer@fz-rossendorf.de

The **Internal Workshop on Kaon Production** took place on September 16, 1996 in the Research Center Rossendorf. This workshop was aimed at a survey on the experimental and theoretical status of kaon production in elementary hadron reactions and heavy-ion collisions. The experimental groups in the Institute for Nuclear and Hadron Physics reported on their activities in various collaborations at different accelerator facilities. Emphasis was put on our future abilities to achieve a substantial progress in the realm of strange particle production. From the theory side the previous results on kaon production and possible supports of the experimental research have been presented.

Please notice, the material presented here is in many cases very preliminary and is not suited for reference and should not be used in publications without explicit permission by the respective authors.

E. Grosse

B. Kämpfer

CONTENTS

E. Grosse Phenomenology

'elementary' process: $NN \to NYK^+$ $Y = \Lambda, \Sigma$

$pp \to K^+ + X$
Hogan et al.

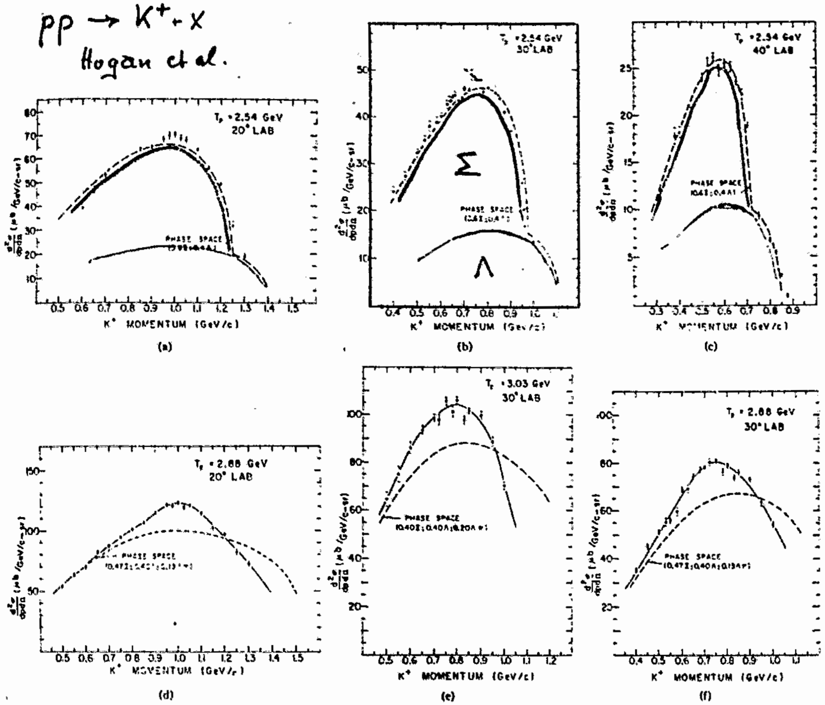

FIG. 4. Laboratory momentum spectra of K^+ mesons produced in hydrogen at the lab angles and incident proton kinetic energies indicated. Errors include statistical errors as well as uncertainties introduced through corrections, but do not include the ~16% uncertainty in the absolute calibration. Momentum resolution is ~2%. The dashed lines represent phase space (see text) normalized to the area under the data.

		$\sqrt{s}$	E_{Lab}^{kin}	
threshold:	$NN \to N\Lambda K^+$	2.548	1.582	
	$N\Sigma K^+$	2.620	1.780	GeV
	NNK^-K^+	2.864	2.494	

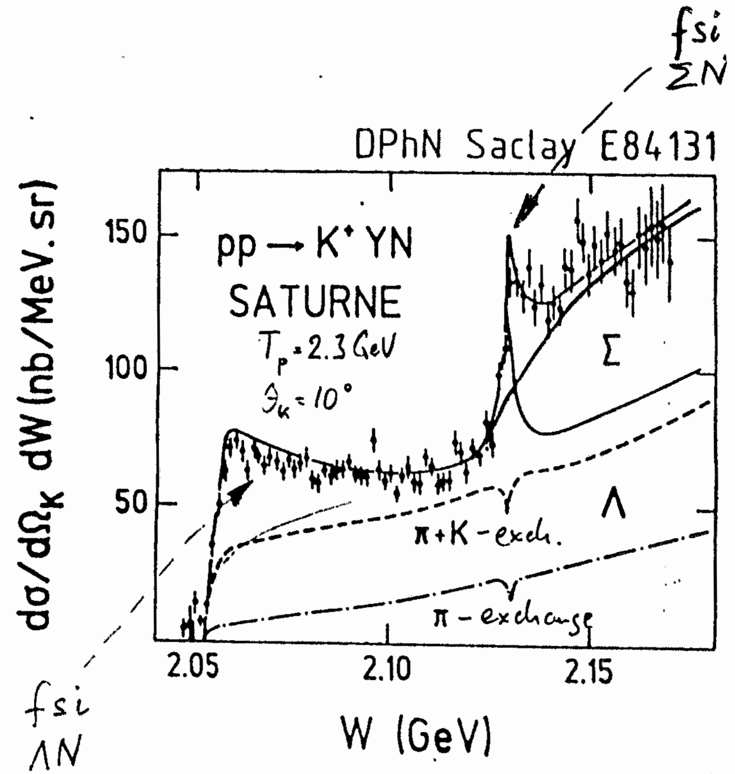

data: Siebert et al. ('8
fit: Laget PLB 259, 2

S. MROWSTINSKY

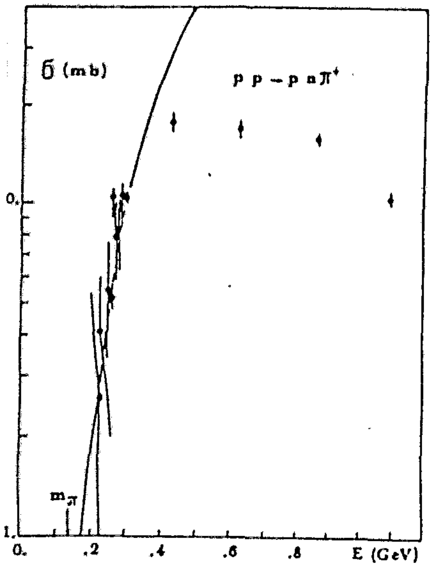

Fig. 2. The cross section of the reaction $pp\to pn\pi^+$ versus initial kinetic energy in the CM frame. The data are taken from ref. [5]. The solid line is the prediction of eq. (6) normalized at $E=0.3$ GeV.

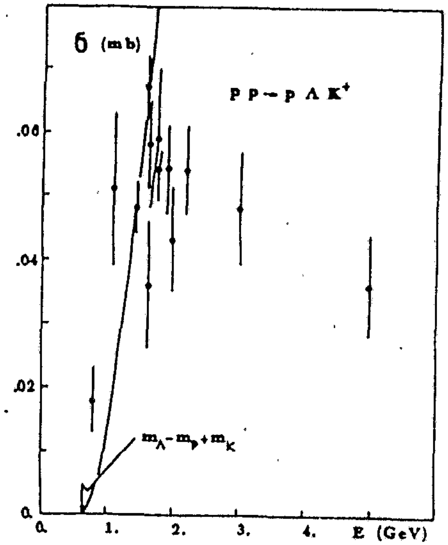

Fig. 3. The cross section of the reaction $pp\to p\Lambda K^+$ versus initial kinetic energy in the CM frame. The data are taken from ref. [5]. The solid line is the prediction of eq. (10) normalized at $E=1.5$ GeV.

Strangeness suppression at high energies

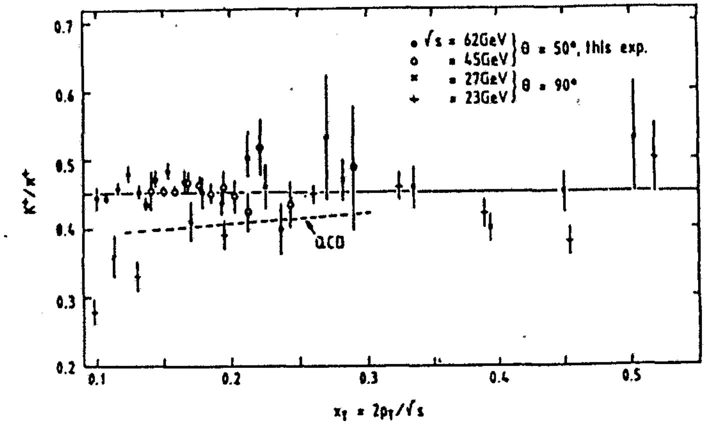

FIGURE 20

Experimental ratio of K^+ to π^+ production in proton-proton interactions at large $x_T = 2p_T/\sqrt{s}$. The dashed line shows a model prediction using $\lambda = 0.5$

λ: strangeness suppression factor W. Hofmann NP (90)

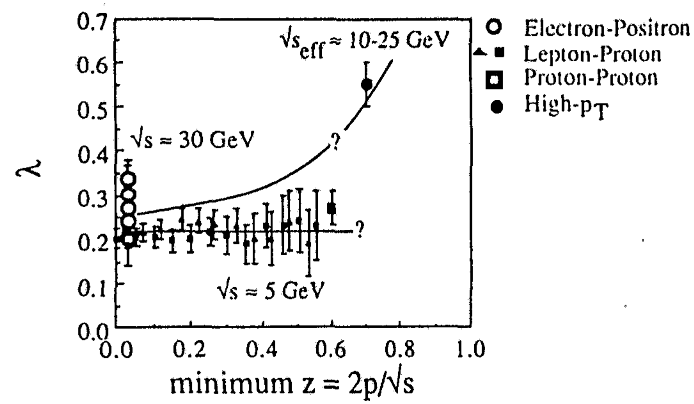

FIGURE 21

Values of λ as derived from K/π ratios, as a function of the minimum $z = P_{hadron}/P_{quark}$ above which hadrons are used in the analysis. Data are shown for e^+e^- annihilation (from several experiments), for neutrino-nucleon scattering, for low-p_T pp reactions and for high-p_T meson production in pp interactions.

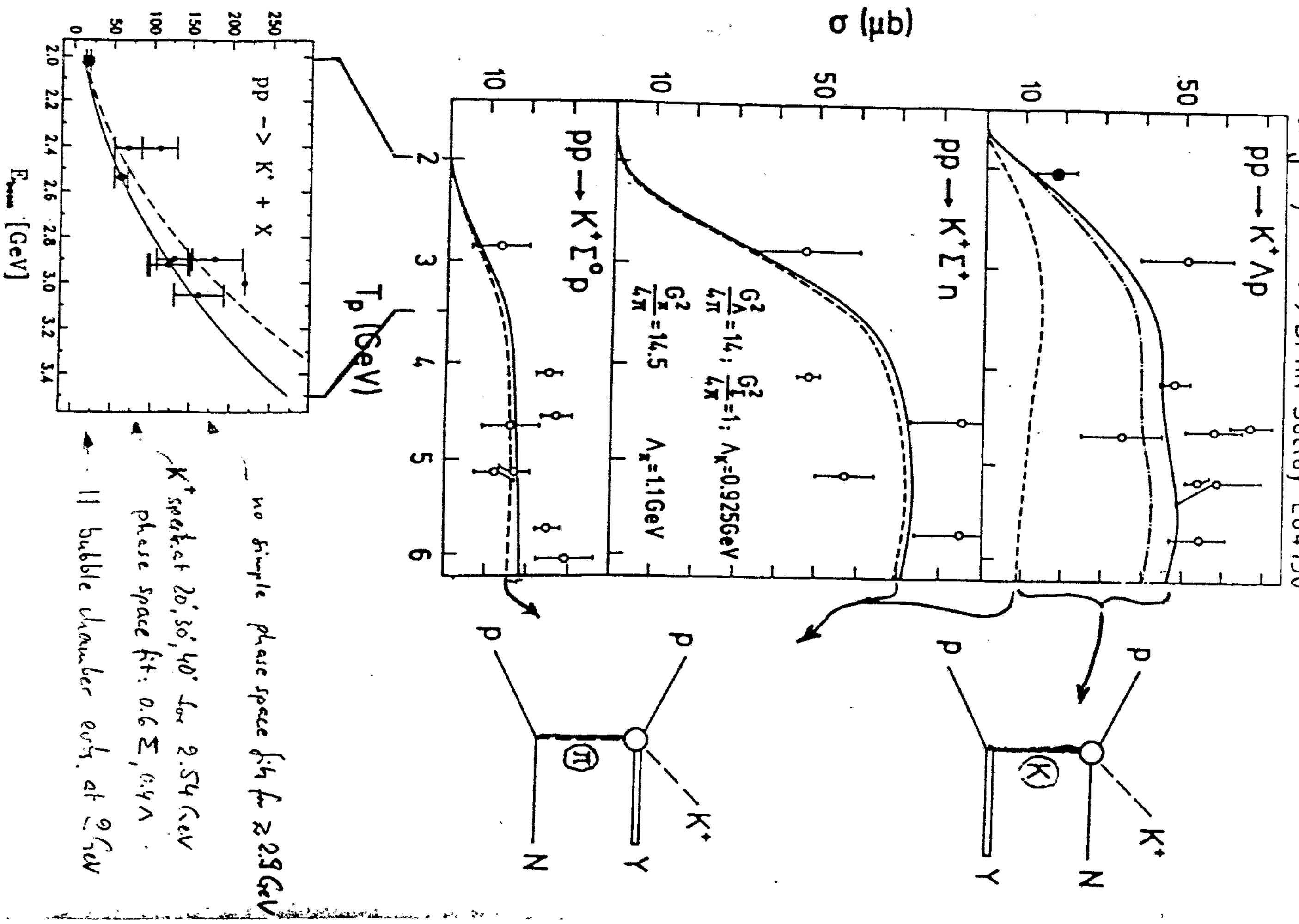

DPhN Saclay E84.130
σ (μb)
pp → K⁺Λp
pp → K⁺Σ⁺n
pp → K⁺Σ⁰p
Tp (GeV)
Λ_K = 0.925 GeV
Λ_π = 1.1 GeV
G²_π/4π = 14.5
pp -> K⁺ + X
K⁺
N
Y
p

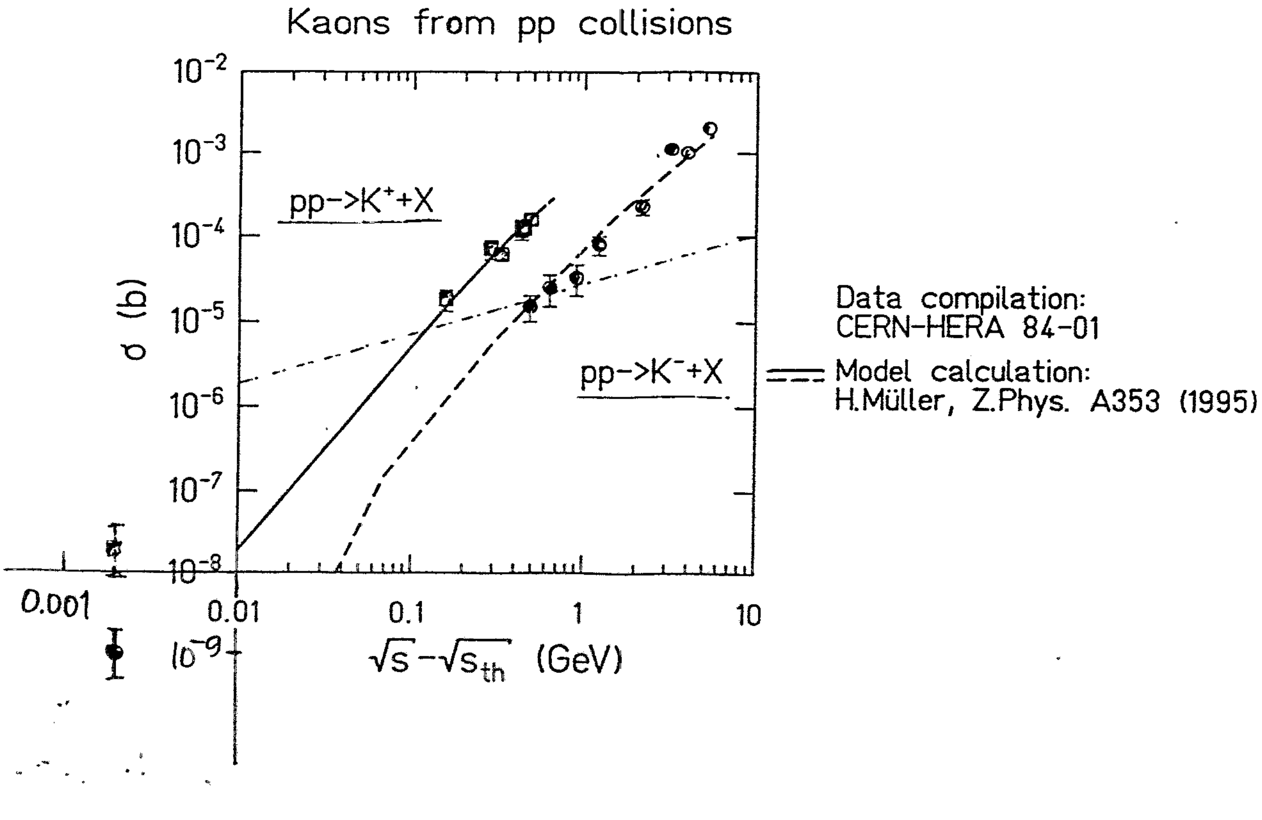

Kaons from pp collisions
pp->K⁺+X
pp->K⁻+X
σ (b)
√s−√s_th (GeV)
Data compilation:
CERN-HERA 84-01
Model calculation:
H.Müller, Z.Phys. A353 (1995)

The Light Hadrons

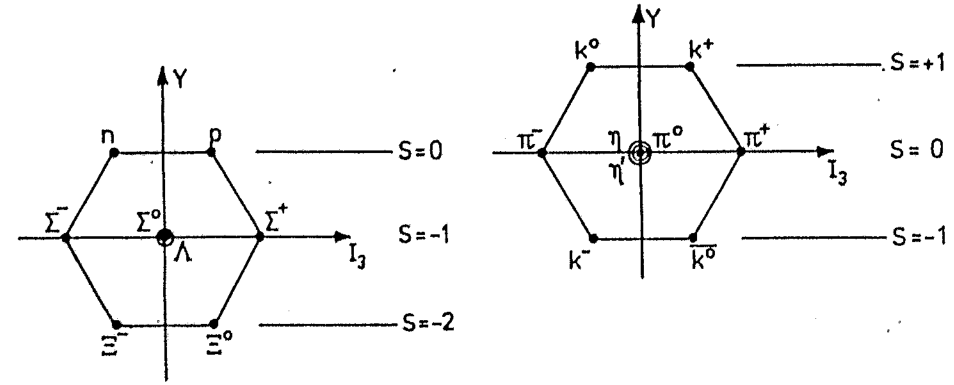

spin flip ⇓

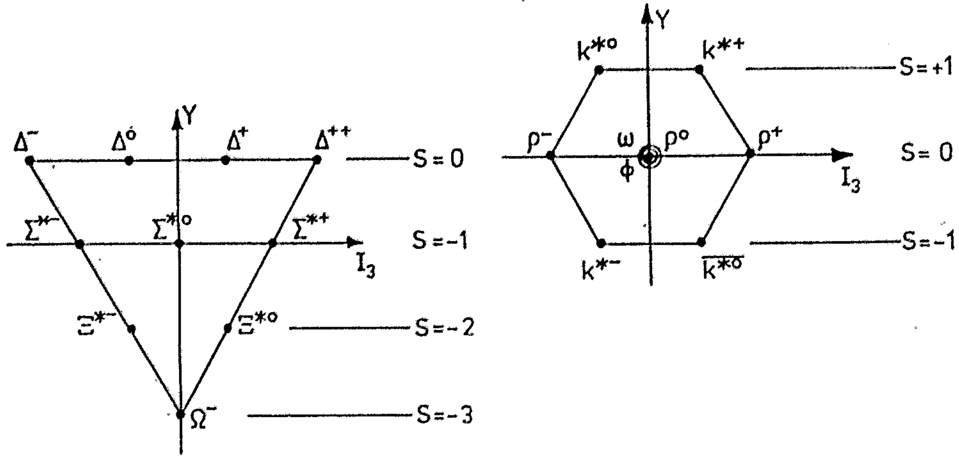

$Y = B + S$

Let's Make Strangeness

I. Elementary Cross Sections

fixed target ↓ ↓

BB, MB, MM → open strange mesons $M_{\bar{s}}$, M_s + anything

↑ GSI π beam

↑ COSY beam

					u ↓ d ↓	u ↓ d ↓		
$M_{\bar{s}}$	=	$q\bar{s}$	=		K^+, K^0	K^{*+}, K^{*0}	S = +1	K
M_s	=	$\bar{q}s$	=		$K^-, \bar{K}^0$	$K^{*+}, \bar{K}^{*0}$	S = −1	$\bar{K}$
					pseudo-scalar	vector		

weak interactions with nucleons → long mean free path in nuclei

→ $K^+ = u\,\bar{s}$: $K^+ N \leftrightarrow Z^* =$ high-lying

→ $K^- = \bar{u}\,s$: $K^- N \leftrightarrow Y^* =$ analog to $\pi N \leftrightarrow \Delta$

e.g., $\Lambda(1405) = \bar{K}\,N$ bound state or genuine 3q state?

BB, MB, MM $\longrightarrow$ hidden strange mesons $M_{s\bar{s}}$ + anything

$M_{s\bar{s}}$ = $s\bar{s}$ = (η), η'	Φ S = 0
pseudo-scalar	vector

vector Φ → K^+K^- (50%)
→ e^+e^- HADES

in strong interactions: strangeness is conserved

→ associated $s\bar{s}$ creation

detection possibilities:

$K^{\pm}$ → spectrometer ($c\tau$ = 371 cm)

or decays $\pi^{\pm}\pi^0$ (21%), $\mu^{\pm}\nu_{\mu}$ (63%) ⟵ $\Delta S = 1$

$K^0_{S/L}$ → decays ($c\tau$ = 2.6 / 1550 cm)

$K^0_S \rightarrow \pi^+\pi^-$ (68%), $\pi^0\pi^0$ (31%)

$K^0_L \rightarrow 3\pi^0$ (21%), $\pi^+\pi^-\pi^0$ (12%) ...

Constituent Quark Combinatoric

B = qqq, $M = q\,\bar{q}$, Y = qqs, $M_{\bar{s}} = q\,\bar{s}$, $M_s = \bar{q}\,s$

1) BB → K + anything

(i) BB → KYB

$$BB = \begin{matrix} qqq \\ + \, (s\bar{s}) \\ qqq \end{matrix} \rightarrow \begin{matrix} qqs \\ q\bar{s} \\ qqq \end{matrix} = \begin{matrix} Y \\ M_{\bar{s}} \\ B \end{matrix}$$

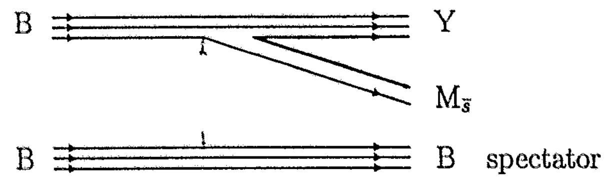

e.g. NN → KYN: $p^+ p^+ \rightarrow K^+ \Lambda p^+$, $K^+ \Sigma^+ n$, $K^0 \Sigma^+ p^+$

$p^+ n \rightarrow K^+ \Lambda n$, $K^+ \Sigma^- p^+$, $K^0 \Sigma^+ n$

$n\, n \rightarrow K^+ \Sigma^- n$, $K^0 \Lambda n$, $K^0 \Sigma^0 n$, $K^0 \Sigma^- p^+$

= the easiest way for open anti-strange mesons   Kaons

open strange mesons would require anti-hyperon

(too costly energetically)

(ii) BB → $K\bar{K}$BB

$$BB = \begin{matrix} qqq \\ \\ qqq \end{matrix} + (s\bar{s}) + (q\bar{q}) \rightarrow \begin{matrix} qqq \\ s\bar{q} + q\bar{s} \\ qqq \end{matrix} = \begin{matrix} B \\ M_s\, M_{\bar{s}} \\ B \end{matrix}$$

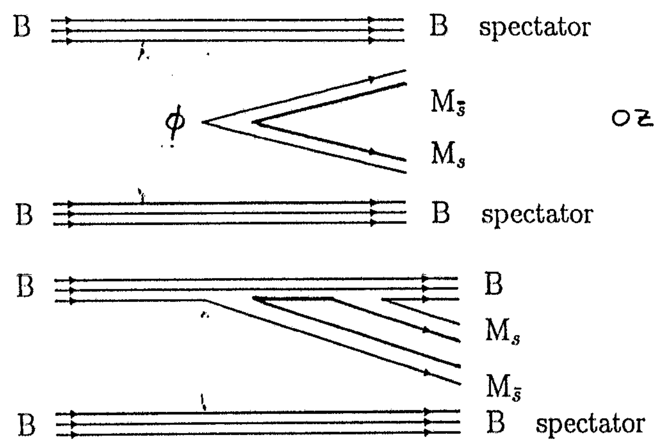

e.g. NN → $K\bar{K}$NN: $p^+ p^+ \rightarrow K^+ K^- p^+ p^+$

$p^+ n \rightarrow K^+ K^- p^+ n$

$n\, n \rightarrow K^+ K^- n\, n$

= the easiest way for <u>open strange mesons</u> anti-kaons

2) MB → K + anything

(i) MB → KY

$$MB = \begin{matrix} qqq \\ \dagger \\ q\bar{q} \end{matrix} + (s\bar{s}) \rightarrow \begin{matrix} qqs \\ \\ q\bar{s} \end{matrix} = \begin{matrix} Y \\ \\ M_{\bar{s}} \end{matrix}$$

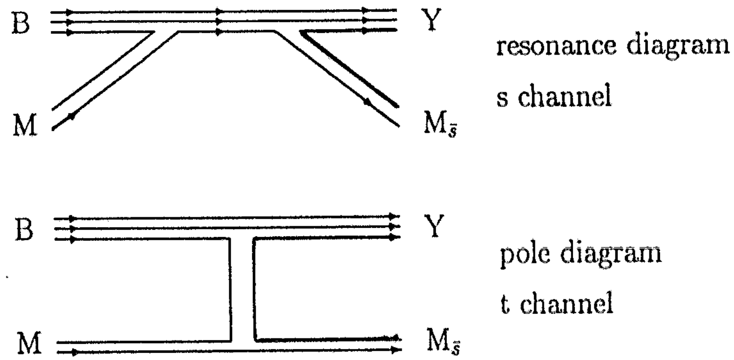

e.g. πN → KYN: $\pi^- p \rightarrow K^0\Lambda,\quad K^+\Sigma^-,\quad K^0\Sigma^0$

$\pi^0 p \rightarrow K^+\Lambda,\quad K^+\Sigma^0,\quad K^0\Sigma^+$

$\pi^+ p \rightarrow \quad K^+\Sigma^+$

$\pi^- n \rightarrow \quad K^0\Sigma^-$

$\pi^0 n \rightarrow K^0\Lambda,\quad K^+\Sigma^-,\quad K^0\Sigma^0$

$\pi^+ n \rightarrow K^+\Lambda,\quad K^+\Sigma^0,\quad K^0\Sigma^0,$

only open <u>anti-strange mesons</u> Kaons

(ii) MB → K $\bar{K}$ B

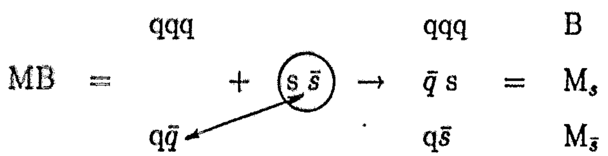

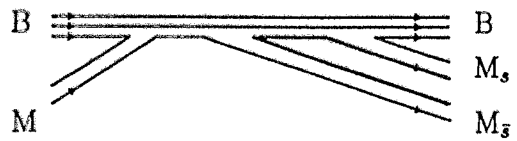

e.g. $\pi N \quad \rightarrow \quad K\bar{K}N: \quad \pi^0 p^+ \quad \rightarrow \quad K^+K^-p^+$

$\pi^- p^+ \quad \rightarrow \quad K^+K^-n$

$\pi^+ p^+ \quad \rightarrow \quad K^+K^-p^+$

and the same for πn

3) MM → $M_{\bar{s}}$ M_s

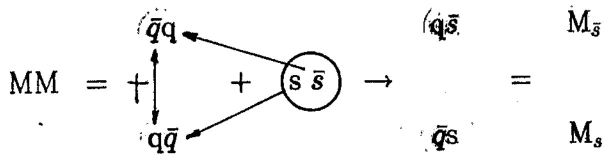

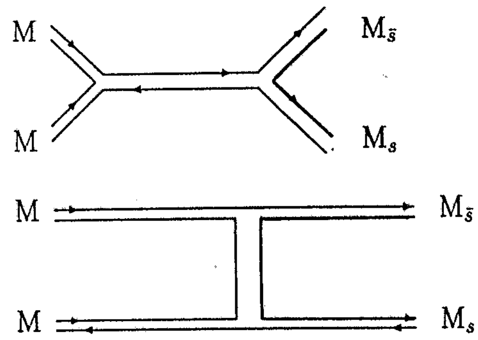

e.g. $\pi\pi \quad \rightarrow \quad K\bar{K}: \quad \pi^+\pi^- \rightarrow K^+K^-, \quad K^0\bar{K}^0$

$\pi^0\pi^0 \rightarrow K^+K^-, \quad K^0\bar{K}^0$

$\pi^-\pi^0 \rightarrow K^-K^0$

$\pi^+\pi^0 \rightarrow K^+\bar{K}^0$

at high energies also the heavier mesons contribute

Theory

does not exist; only models & parametrizations

one possibility: utilize OBE model philosophy

e.g. $NN \rightarrow NN$:

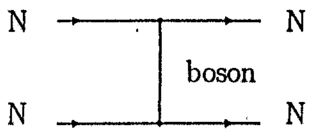

advantage: well defined via Lagrangian + Feynman diagramatics

+ extension possibilities → bremsstrahlung & di-electrons:

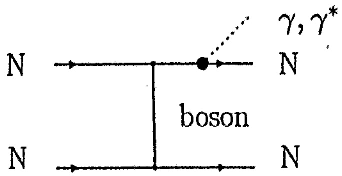

disadvantages: – effective theory,

– only tree level

– parameter fiddling: <u>masses, couplings, cut-offs</u>

e.g. NN scattering: 4 bosons

NN scattering + deuteron bound state: 6 bosons

– no simple initial/final state interaction corrections

nevertheless: try the same here

<u>1) $MM \rightarrow K\bar{K}$</u> is simplest

Brown/Ko/Wu/Li (1991):

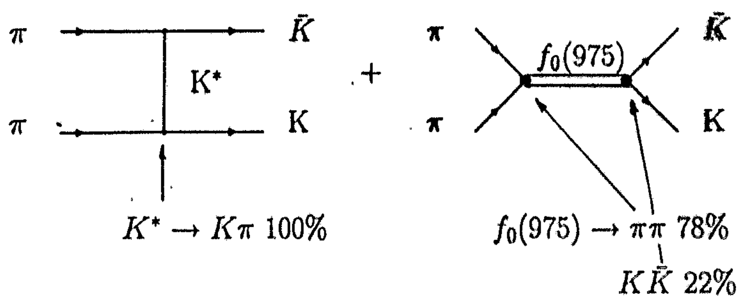

analog:

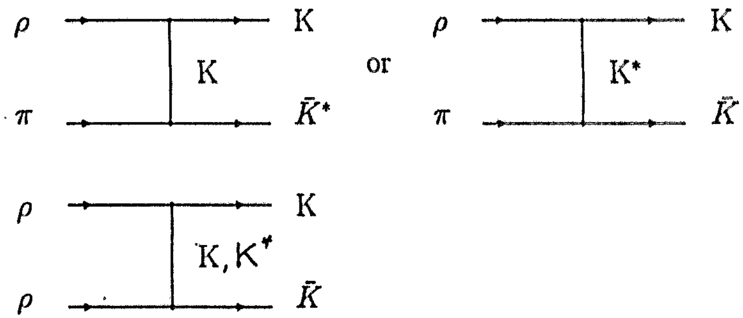

"for simplicity we neglect" ... diagrams → incomplete calculation

Technicalities

example: only the pole diagram

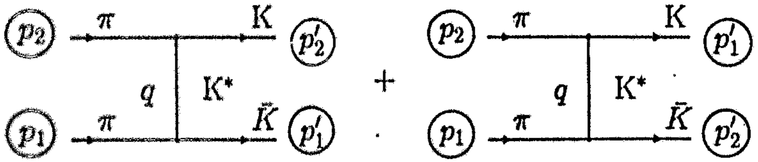

T_+ direct | T_- exchange

$$|M|^2 = |T_+|^2 + |T_-|^2 + \underline{2\mathrm{Re}(T_+^* T_-)}$$

↑ interference term

N diagrams $\rightarrow \frac{1}{2}N(N+1)$ terms $\rightarrow$ explosion of computational efforts

$$\boxed{\mathcal{L} = g\,(K_a^{*\mu}\vec{\tau}_{ab}K_b(\partial_\mu\vec{\pi}) - K^{*\mu}\vec{\tau}(\partial_\mu K)\vec{\pi})} \qquad a, b = 1, 2$$

$\mathcal{L}$ = Lorentz invariant, parity invariant, particle–anti-particle symmetric, iso-scalar

K^* = vector $\rightarrow K^{*\mu} \rightarrow$ derivative coupling is needed
$\rightarrow \partial_\mu\vec{\pi}$ and/or $\partial_\mu K$

π = iso-vector $\rightarrow \vec{\pi}$ in iso-spin 3 space

K = iso-dubletts $\rightarrow (K^+, K^0)$, $(K^-, \bar{K}^0)$, (K^{*+}, K^{*0}), $(K^{*-}, \bar{K}^{*0})$,

with $\vec{\tau} = 2 \times 2$ matrix contracted

formfactor at each vertex: $F(q) = \frac{m^2 - \Lambda^2}{q^2 - \Lambda^2}$

2) MB → KY

Brown/Ko/Wu/Li (1991): only rough estimates; no interference terms

Faessler & Huang, Tsushima, ... (1994 - 1996): systematic approach

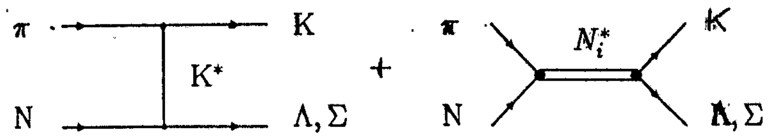

$\pi^+p^+ \rightarrow K^+\Sigma^+$	$\pi^-p^+ \rightarrow K^+\Sigma^-$	$\pi^0p^+ \rightarrow K^+\Sigma^0$
$\pi^+n \rightarrow K^+\Sigma^0$		$\pi^0n \rightarrow K^+\Sigma^-$
$\pi^0p^+ \rightarrow K^0\Sigma^+$		$\pi^0p^+ \rightarrow K^0\Sigma^+$
$\pi^0n \rightarrow K^0\Sigma^0$	$\pi^-n \rightarrow K^0\Sigma^-$	$\pi^0n \rightarrow K^0\Sigma^0$
$\pi^0p^+ \rightarrow K^0\Lambda$	$\pi^-p^+ \rightarrow K^0\Lambda$	$\pi^0p^+ \rightarrow K^+\Lambda$
		$\pi^0n \rightarrow K^0\Sigma^+$

+ inclusion of $\Delta \rightarrow$ Rarita-Schwinger fields

$\rightarrow \pi\Delta(1232) \rightarrow KY$

decays N^*, $\Delta \to MB$, KY

N(1650)	P=-1, j=$\frac{1}{2}$	π N	70%	1
		K Λ	7%	5
		$\pi\Delta$	5%	
N(1710)	P=+1, j=$\frac{1}{2}$	π N	15%	2
		K Λ	15%	6
		K Σ	6%	8
		$\pi\Delta$	17%	
N(1720)	P=+1, j=$\frac{3}{2}$	π N	15%	3
		K Λ	6%	7
		K Σ	3%	9
		$\pi\Delta$	10%	
Δ(1920)	P=+1, j=$\frac{3}{2}$	π N	12%	4
		K Σ	2%	10

interaction Lagrangians for $\pi N N^*$:

$$\mathcal{L}_1 = -g_{\pi N N_{1650}} \left(\underbrace{\bar{N}^*_a \vec{\tau}_{ab} N_b}_{\text{Dirac's matrices}} \vec{\pi} + \bar{N}\vec{\tau}N^*\vec{\pi} \right), \quad a,b = 1,2$$

$$\mathcal{L}_2 = -i g_{\pi N N_{1710}} \left(\underbrace{\bar{N}^*\gamma_5\vec{\tau}N}\vec{\pi} + \bar{N}\gamma_5\vec{\tau}N^*\vec{\pi} \right)$$

$$\mathcal{L}_3 = \frac{1}{m_\pi} g_{\pi N N_{1720}} \left(\bar{N}^{*\mu}\vec{\tau}N(\partial_\mu\vec{\pi}) + \bar{N}\vec{\tau}N^{*\mu}(\partial_\mu\vec{\pi}) \right)$$

$$\mathcal{L}_4 = \frac{1}{m_\pi} g_{\pi N \Delta_{1920}} \left(\bar{\Delta}^\mu \vec{I} N(\partial_\mu\vec{\pi}) + \bar{N}\vec{I}^\dagger\Delta^\mu(\partial_\mu\vec{\pi}) \right)$$

↑ isospin transition operator

interaction Lagrangians for KYN^*:

$$\mathcal{L}_5 = -g_{K\Lambda N_{1650}} \left(\underbrace{\bar{N}^*_a \Lambda} K_a + \bar{K}\bar{\Lambda}N^* \right)$$

$$\mathcal{L}_6 = -i g_{K\Lambda N_{1710}} \left(\underbrace{\bar{N}^*\gamma_5\Lambda} K + \bar{K}\bar{\Lambda}\gamma_5 N^* \right)$$

$$\mathcal{L}_7 = \frac{1}{m_K} g_{K\Lambda N_{1720}} \left(\bar{N}^{*\mu}\Lambda(\partial_\mu K) + (\partial_\mu\bar{K})\bar{\Lambda}N^* N^{*\mu} \right)$$

$$\mathcal{L}_8 = -i g_{K\Sigma N_{1710}} \left(\bar{N}^*\gamma_5\vec{\tau}\vec{\Sigma}K + \bar{K}\bar{\vec{\Sigma}}\vec{\tau}\gamma_5 N^* \right)$$

$$\mathcal{L}_9 = \frac{1}{m_K} g_{K\Sigma N_{1720}} \left(\bar{N}^{*\mu}\vec{\tau}\vec{\Sigma}(\partial_\mu K) + (\partial_\mu\bar{K})\bar{\vec{\Sigma}}\vec{\tau}N^* \right)$$

$$\mathcal{L}_{10} = \frac{1}{m_K} g_{K\Sigma\Delta_{1720}} \left(\bar{\Delta}^\mu\vec{I}\vec{\Sigma}(\partial_\mu K) + (\partial_\mu\bar{K})\bar{\vec{\Sigma}}\vec{I}\Delta^\mu \right)$$

QED, QCD look simpler

also for couplings for K^*

Σ = iso-triplet: $\vec{\Sigma} = (\Sigma^\pm, \Sigma^0)$

+ formfactors on each vertex

→ results of Faessler's group → figs.

Huang et al.

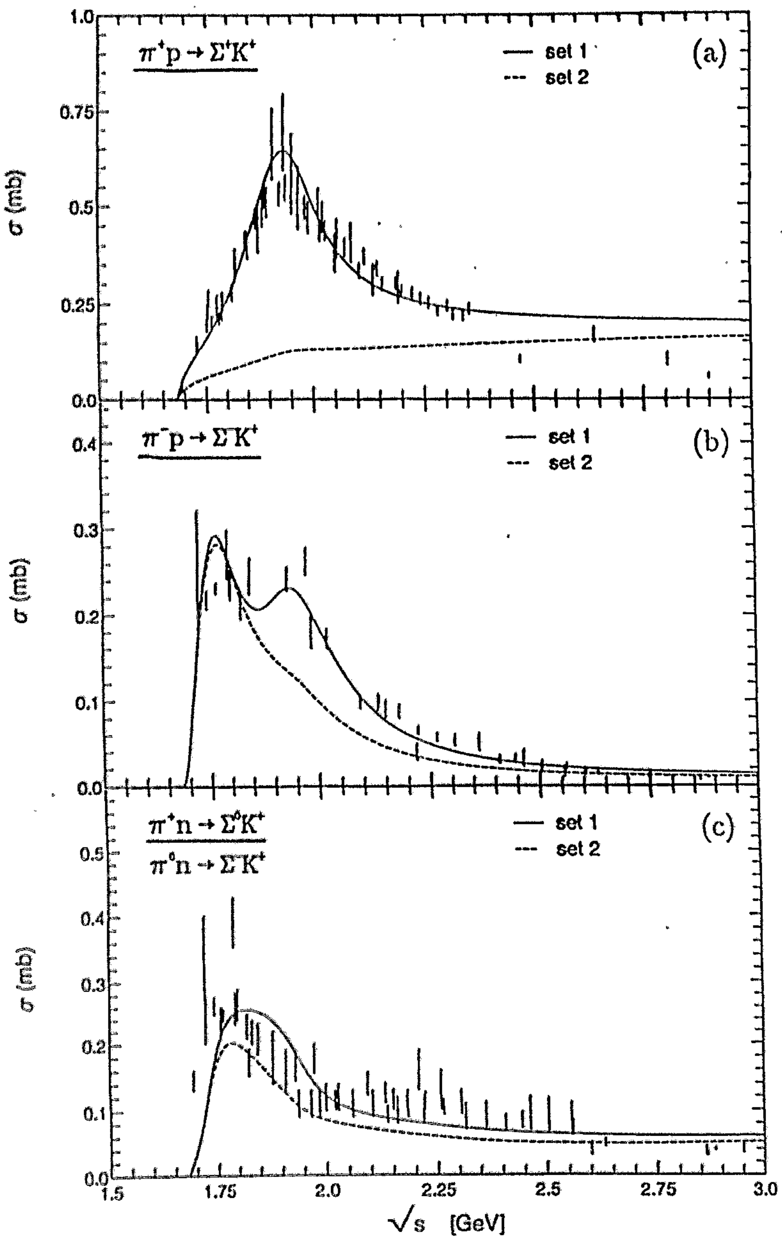

Huang et al.

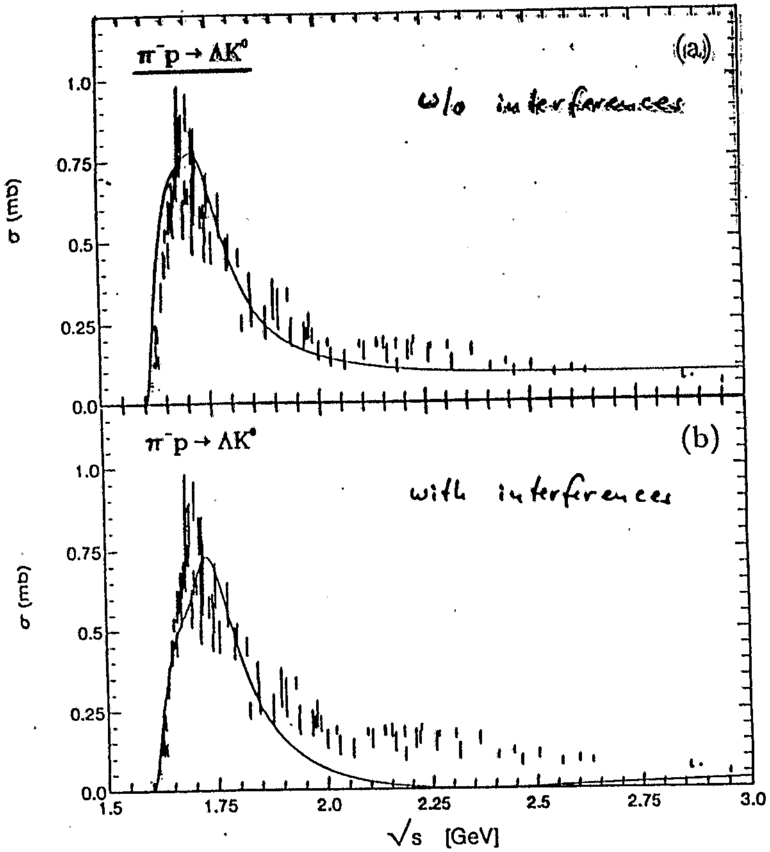

Huang et al.

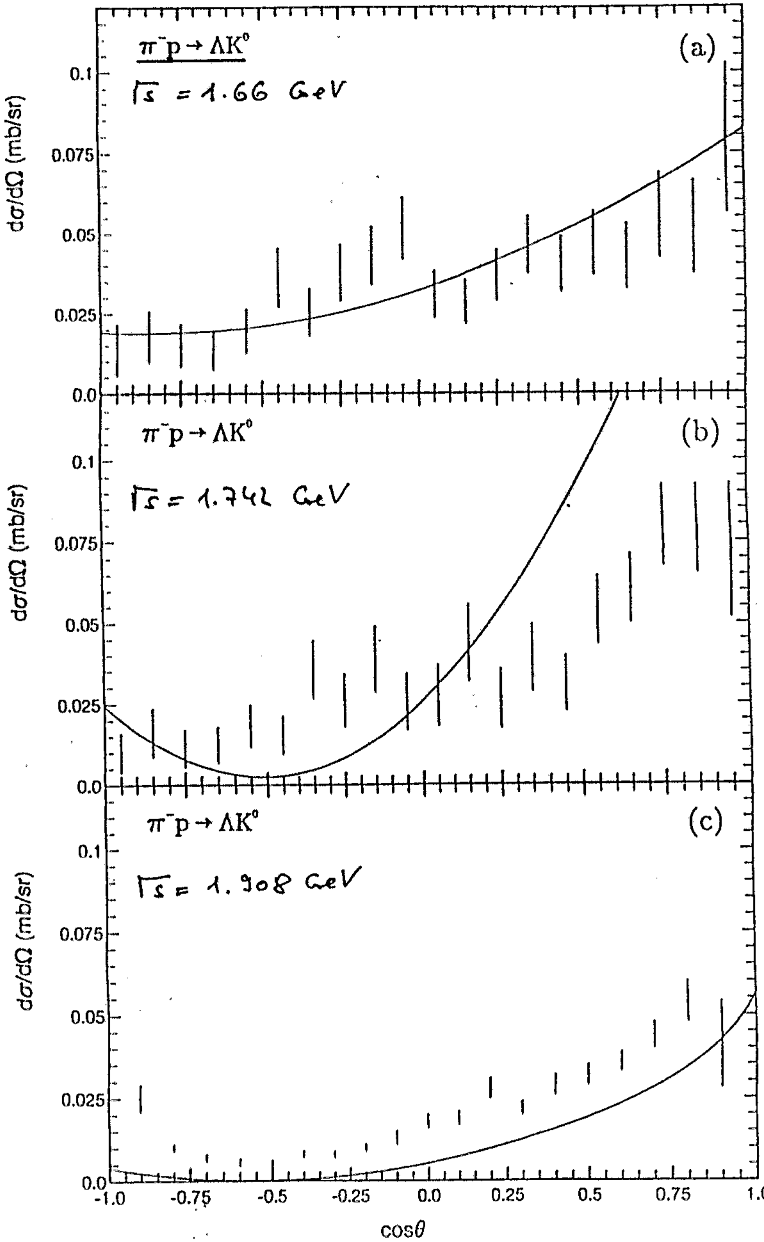

3) $MB \to K \bar{K} B$

nothing exists

however: using the above vertices one can continue with

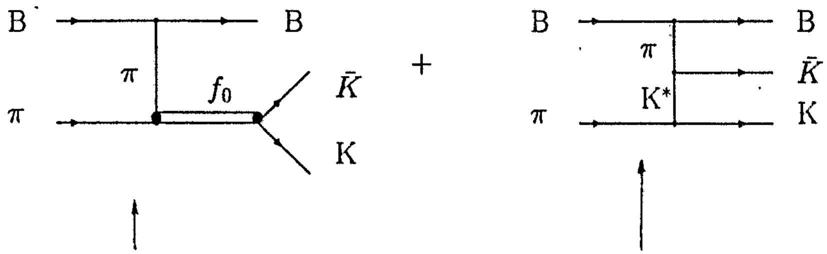

$\pi\pi \to f_0(965) \to K\bar{K}$

$\pi\pi \to K\bar{K}$

should one measure this at GSI with Kaos ?

4) BB → KYB

(i) nothing complete exists

announcement of A. Faessler: continue with the above OBE model

the above MB → KY diagrams = subprocesses here

should we start also such work? (e.g., Ph.D. work for M. Hentschel?)

(e.g., postdoc work of E.E. Kolomeitsev?)

(ii) earlier attempts:

	exchange	interference	Δ	FSI
Ferrari (1960)	π or K	+	−	−
Yao (1960)	π	−	−	−
Randrup/Ko (1980)	π	−	−	−
Wu/Ko (1989),	-"-	-"-	-"-	-"-
Brown/Ko/Wu/Xia (1991)	-"-	-"-	-"-	-"-
Deloff (1989) Laget (1991)	π, K	?	−	+
Sibirtsev (1995) Li/Ko (1996)	π, K	−	+	−

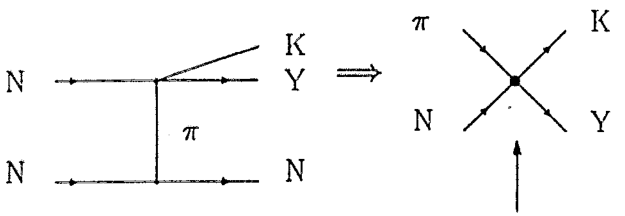

= subprocesses from MB → KY

= on-shell exp./theor. cross section

also for N Δ → KNY

● without spinor dynamics

$$M \propto (\bar{u}_3 \Gamma_6 u_1)\, \mathcal{D}_\pi(6)\, (\bar{u}_4 \Gamma_6 u_2)\, K_5$$

● without interference terms

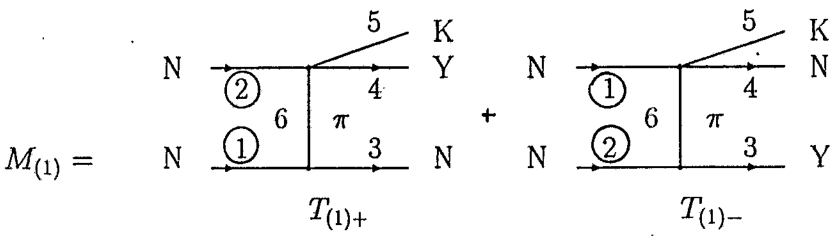

$$|M|^2 = T^2_{(1)+} + T^2_{(1)-} - \underline{2\mathrm{Re}(T^*_{(1)+} T_{(1)-})}$$

neglected

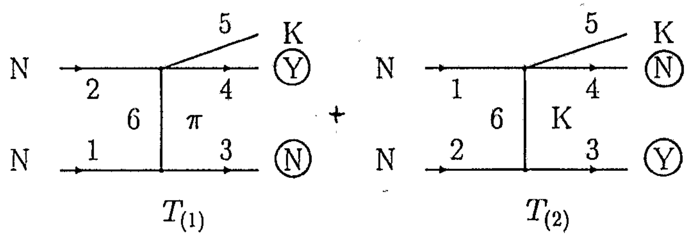

any $T_{(1)} T_{(2)}$ interference is neglected (→ 10 terms)

● subprocesses (1) $\pi N \to KY$, (2) $KN \to KN$ are put by hand on mass shell

results of Li/Ko → figs.

Li/Ko

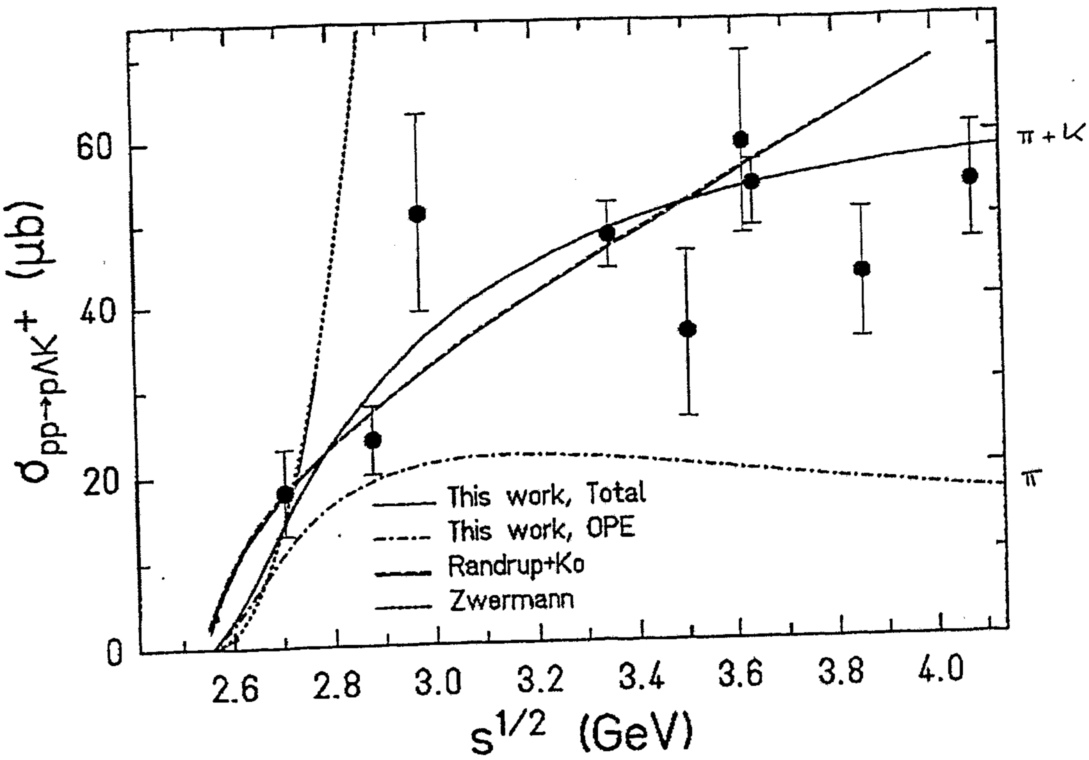

$\sigma_{pp\to p\Lambda K^+}$ (μb)
$s^{1/2}$ (GeV)
This work, Total
This work, OPE
Randrup+Ko
Zwermann
π + K
π
0
20
40
60
2.6
2.8
3.0
3.2
3.4
3.6
3.8
4.0

Li/Ko

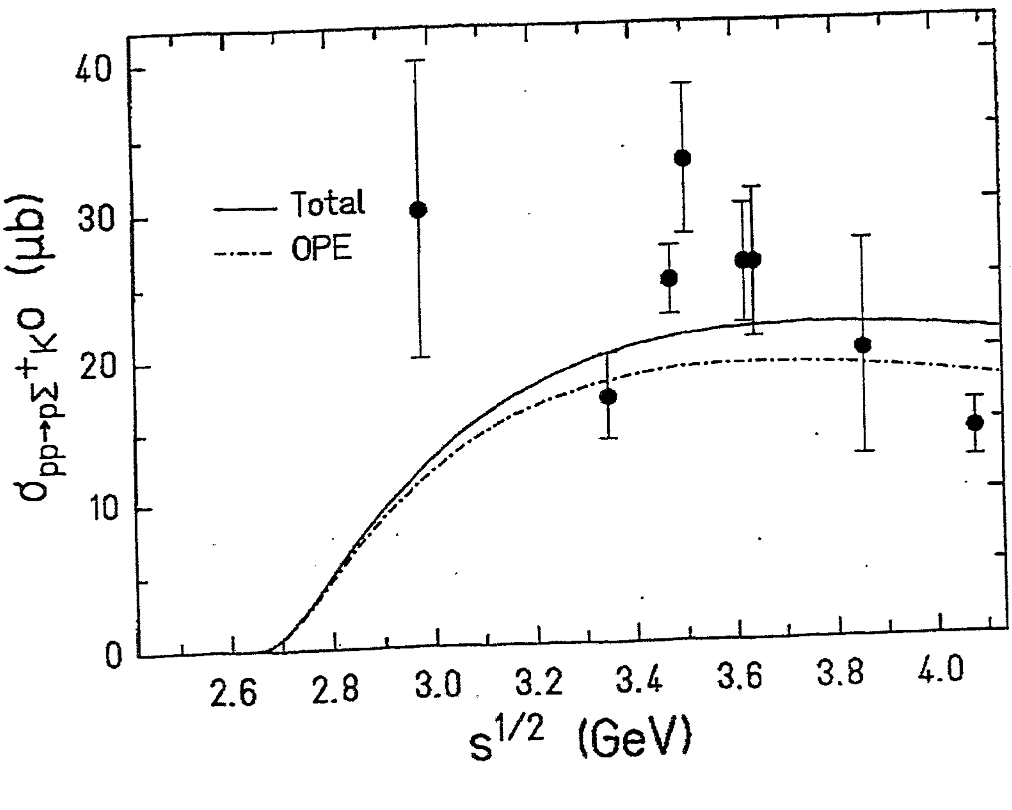

$\sigma_{pp\to p\Sigma^+K^0}$ (μb)
$s^{1/2}$ (GeV)
Total
OPE
0
10
20
30
40
2.6
2.8
3.0
3.2
3.4
3.6
3.8
4.0

Li/Ko

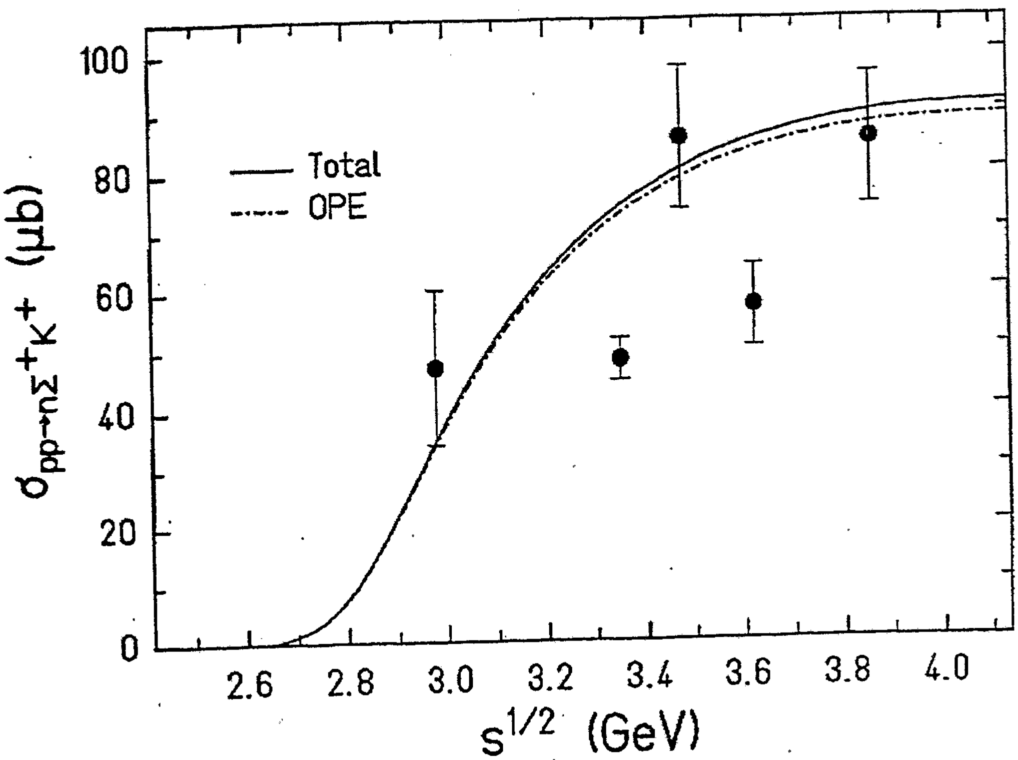

Total
OPE
$\sigma_{pp\to n\Sigma^+K^+}$ (μb)
$s^{1/2}$ (GeV)

Li/Ko

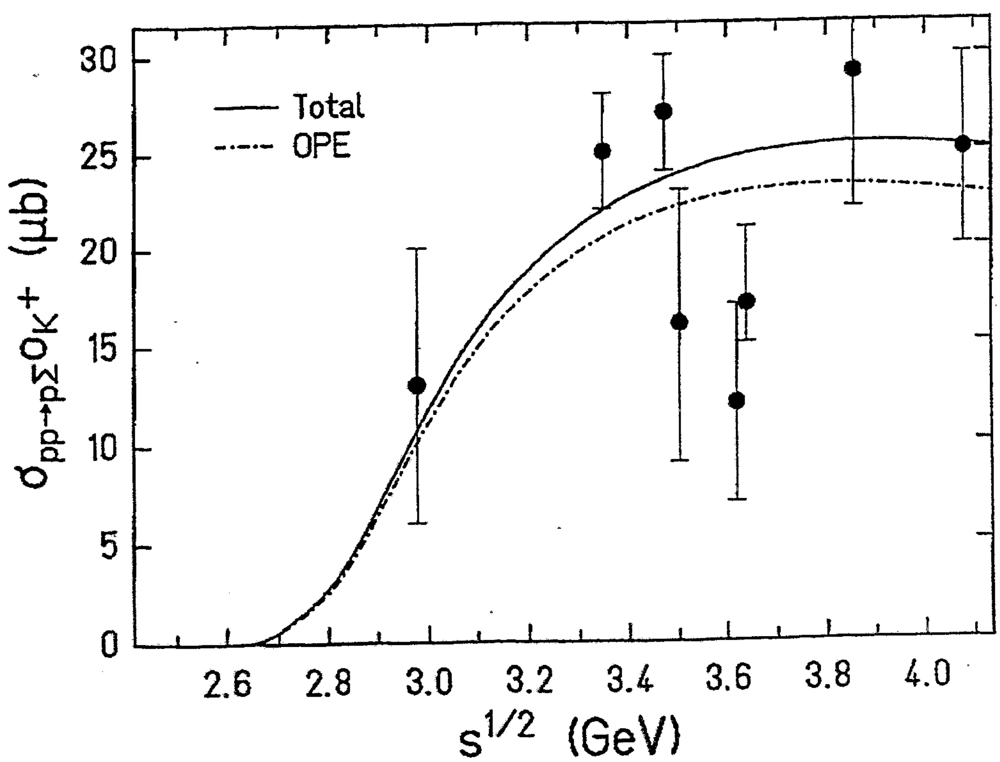

Total
OPE
$\sigma_{pp\to p\Sigma^0K^+}$ (μb)
$s^{1/2}$ (GeV)

$E_{lab}^{kin} = 2.3$ GeV , $\Theta_{K^+} = 10°$

missing mass spectrum

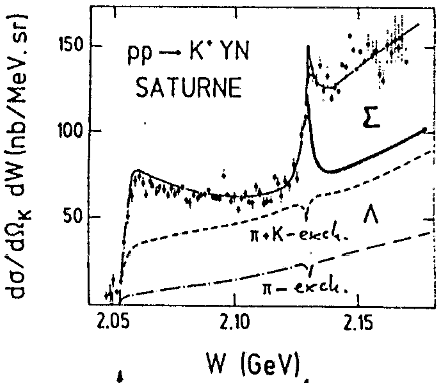

Laget (1991)

FSI, coupl. chan.

thr. $pp \to K^+ \Lambda p$ 2.053 GeV

thr. $pp \to K^+ \Sigma N$ 2.131 GeV $\Sigma^0 p$, $\Sigma^+ n$

cf. Deloff (1989)

W = NY eff. mass

5) BB → K $\bar{K}$ BB

nothing exists

but one can continue with the above strategy

→ rather extended work

Philosophy

earlier motivation (Bonn/Jülich group):

careful study of interactions on the hadronic level

→ separation of subnuclear (= quark-gluon) degrees of freedom

However: χPT + effective, low-energy models

→ express QCD entirely in terms of hadron observables

→ less space to "check" QCD

hadron interactions = low-energy QCD

to day: lattice QCD → $M_{hadrons}$

future: lattice QCD → σ ?

let's accumulate as much as possible details

---

models are needed, e.g. $\pi \Delta \to K Y$ ...

for HICs

W. Weise: s = < heaviest light quark uds / lightest heavy quark sctb

---

vacuum structure: $\langle q\bar{q}\rangle$, $\langle q\bar{s}\rangle$, $\langle \bar{q}s\rangle$

H. Müller	The Rossendorf Collision Model
H. Müller	K^- data from COSY

A quark model for hadron production

Basic assumptions

- Lorentz-invariant phase-space of n particles

$$\mathrm{d}L_n(s) = \prod_{i=1}^{n} \frac{\mathrm{d}^3 p_i}{2e_i} \delta^4(p - \sum_{i=1}^{n} p_i)$$

- Probability of populating final channel $\vec{\alpha}$

$$\mathrm{d}W(s;\vec{\alpha}) \propto \mathrm{d}L_n(s;\vec{\alpha})\, A^2$$

- Differential cross section for channel $\vec{\alpha}$

$$\mathrm{d}\sigma(s;\vec{\alpha}) = \sigma_{\mathrm{in}}(s) \frac{\mathrm{d}W(s;\vec{\alpha})}{\sum_{\vec{\alpha}} \int \mathrm{d}W(s;\vec{\alpha})}$$

Physical quantities are derived by summing up all channels $\vec{\alpha}$ and integrating over the unobserved variables

Matrix element

$$A^2(\vec{\alpha}_N) = A^2_{ex}(\vec{\alpha}_N)A^2_{sc}(\vec{\alpha}_N)A^2_{qs}(\vec{\alpha}_N)A^2_{st}(\vec{\alpha}_N)$$

Cluster excitation:

$$A^2_{ex}(\vec{\alpha}_N) = \prod_{I=1}^{N} \left(\frac{M_I}{\Theta_I}\right) K_1 \left(\frac{M_I}{\Theta_I}\right)$$

Scattering:

$$A^2_{sc}(\vec{\alpha}_N) = \exp\left(\beta\,(t_{a1}+t_{b2})\right) \times \prod_{I=3}^{N} \exp\left(-(Q_I/\overline{Q})^2\right)$$

Quark statistics:

$$A^2_{qs}(\vec{\alpha}_N) \longrightarrow algorithm$$

Statistics:

$$A^2_{st}(\vec{\alpha}_N) = \left\{\prod_{I=1}^{N} g(\alpha_I)\left(\frac{V_I}{(2\pi)^3}\right)^{n_I-1} \times \left[\prod_{i=1}^{n_I}(2\sigma_i+1)2m_i\right]\right\}\left(\frac{V_N}{(2\pi)^3}\right)^{N-1}$$

Decomposition of phase-space Hadron-Hadron

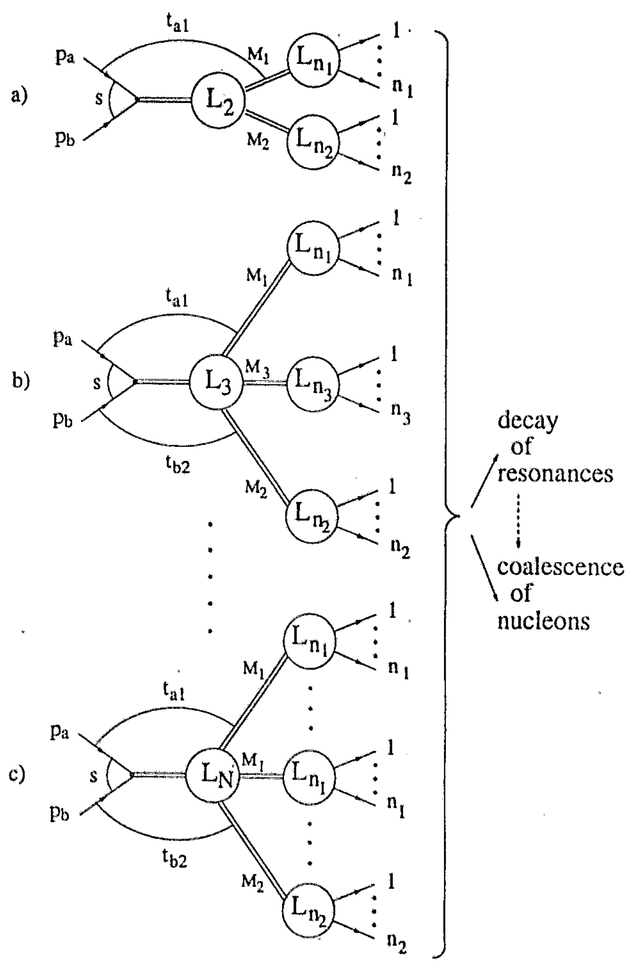

Excitation

$$A^2_{ex}(\vec{\alpha}_N) = (M/\Theta)\, K_1\,(M/\Theta)$$
$$\xrightarrow{M\to\infty} \sqrt{M/\Theta}\, \exp\,(-M/\Theta)$$
$$\xrightarrow{M\to 0} 1$$

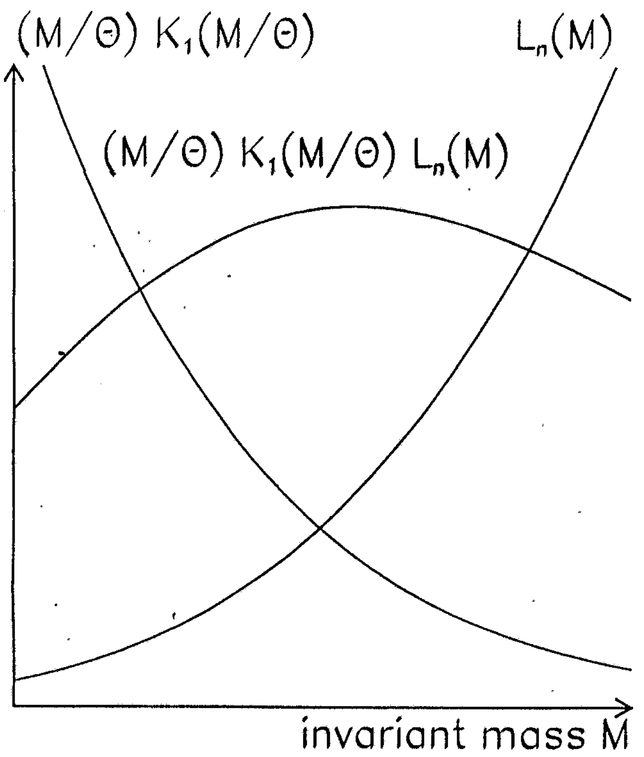

Quark statistics

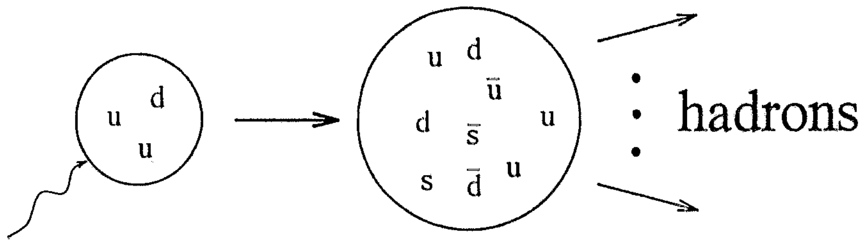

rules:

$q\bar{q}$	⟶	meson
$qq\bar{q}$	⟶	meson + q
qqq	⟶	baryon
⋮		

Hadrons consisting of the same quarks are sampled according to

$$\exp\,(-m\,/\,\Theta)$$

Number of states in the decay channel α_I of one cluster

$$\mathrm{d}\mathcal{Z}_I(\alpha_I) = g(\alpha_I)\left(\frac{V_I}{(2\pi)^3}\right)^{n_I-1} \left\{\prod_{i=1}^{n_I}(2\sigma_i+1)2m_i\right\} \mathrm{d}M_I \left(\frac{M_I}{\Theta_I}\right) K_1\left(\frac{M_I}{\Theta_I}\right) \mathrm{d}L_{n_I}(M_I;\alpha_I)$$

Number of "cluster states"

$$\mathrm{d}\mathcal{Z}_N(s) = \left(\frac{V_N}{(2\pi)^3}\right)^{N-1}\left\{\prod_{i=1}^{N}(2M_I)\right\} \exp\left(\beta\left(t_{a1}+t_{b2}\right)\right) \prod_{I=3}^{N}\exp\left(-(Q_I/\overline{Q})^2\right) \mathrm{d}L_N(s;M_1,\ldots,M_N)$$

Probability of populating channel $\vec{\alpha}_N = (\alpha_1,\ldots,\alpha_N)$

$$\mathrm{d}W(s;\vec{\alpha}_N) \propto \left\{\prod_{I=1}^{N}\mathrm{d}\mathcal{Z}_I(\alpha_I)\right\}\mathrm{d}\mathcal{Z}_N(s)$$

Particle table

- Baryons

$N(S=0,I=1/2)$	10
$\Delta(S=0,I=3/2)$	4
$\Lambda(S=-1,I=0)$	6
$\Sigma(S=-1,I=1)$	2
$\Xi(S=-2,I=1/2)$	2

- Mesons

$^1S_0$	π, K, η, η'
$^3S_1$	ρ, K^*, ω, Φ
$^3P_0$	a_0, K_0^*, f_0
$^3P_1$	$a_1, K_1(1280), f_1$
$^3P_2$	a_2, K_2^*, f_2, f_2'
$^1P_1$	$b_1, K_1(1400), b_1, h_1$

Parameters

Nucleon-Nucleon

Temperature parameter: $\boxed{\Theta = 0.3\ GeV}$

→ mean kinetic energy of hadrons in the cluster rest system

Radius parameter: $\boxed{R = 1.7\ fm}$

→ mean multiplicity

Slope parameter: $\boxed{\beta = 3\ GeV^{-2}}$

→ distribution of leading clusters

Momentum cut-off: $\boxed{\overline{Q} = 0.4\ GeV/c}$

→ transverse dimension of phase-space

Suppression factor: $\boxed{\lambda = 0.15}$

→ quarks are sampled according to $u : d : s = 1 : 1 : \lambda$

p + p

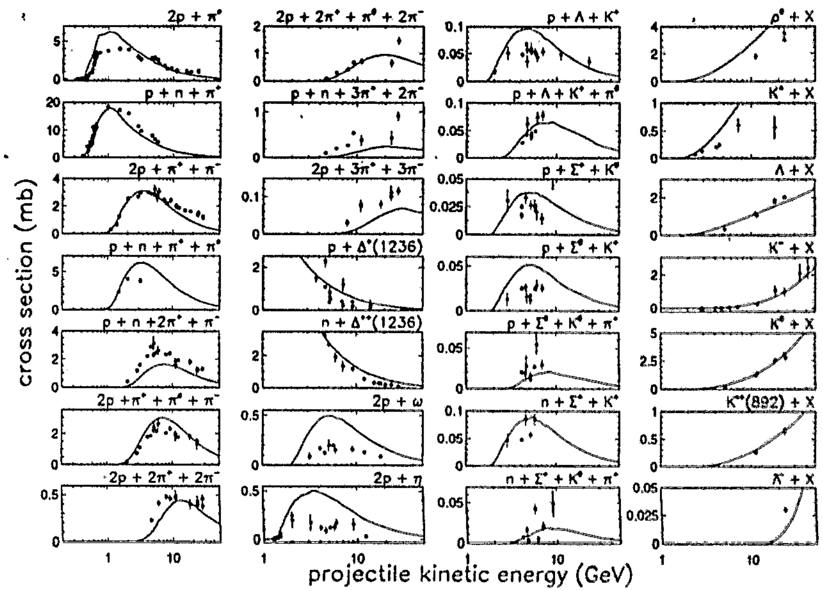

Energy dependence of the cross sections for various particle-production channels in pp collisions. Experimental data (*blue points*) are compared with ROC model results (*red lines*)

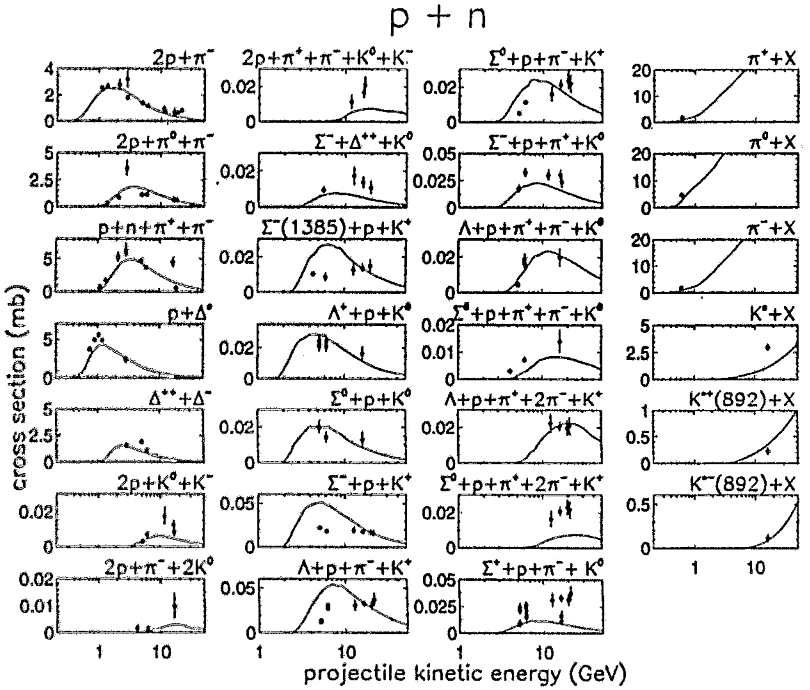

Energy dependence of the cross sections for various particle-production channels in pn collisions. Experimental data (*blue points*) are compared with ROC model results (*red lines*)

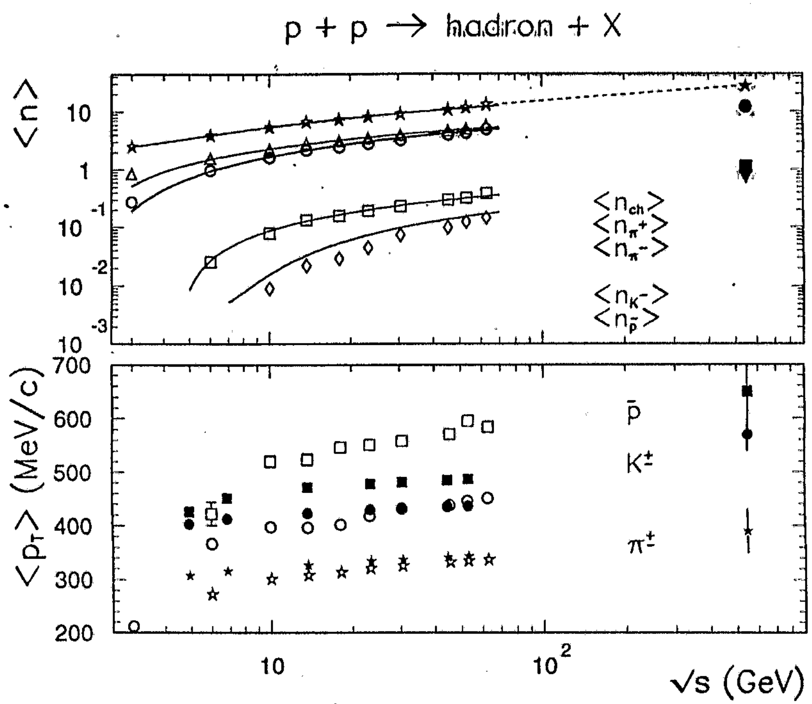

Energy dependence of mean multiplicities and mean transverse momenta. The lines are fits to experimental data. Full symbols are experimental data.

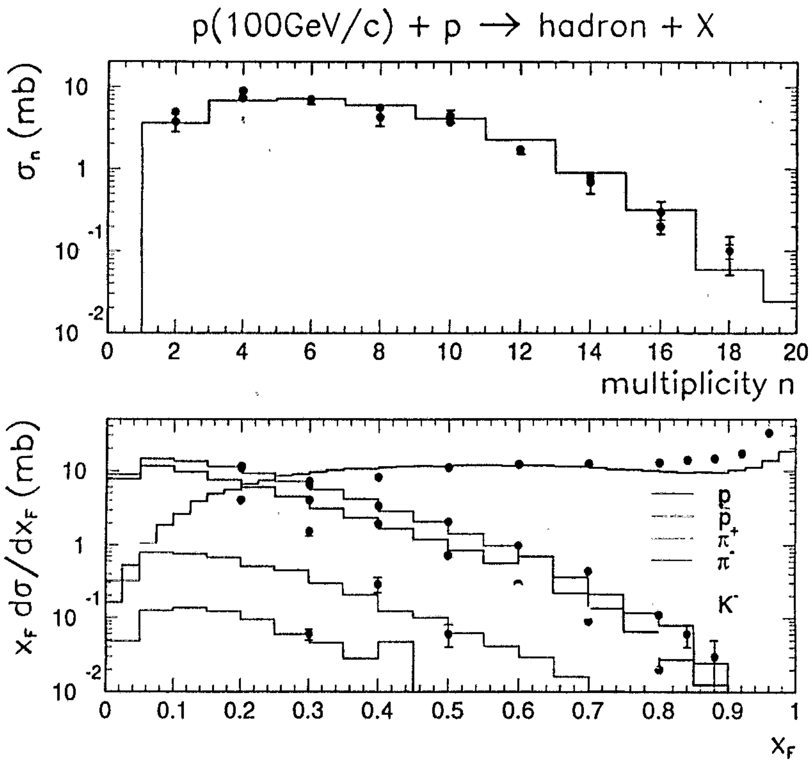

Multiplicity distribution and invariant cross section (integrated over transverse momentum) for hadron production as function of Feynman-x. Points with error bars are experimental data, histograms are ROC model results

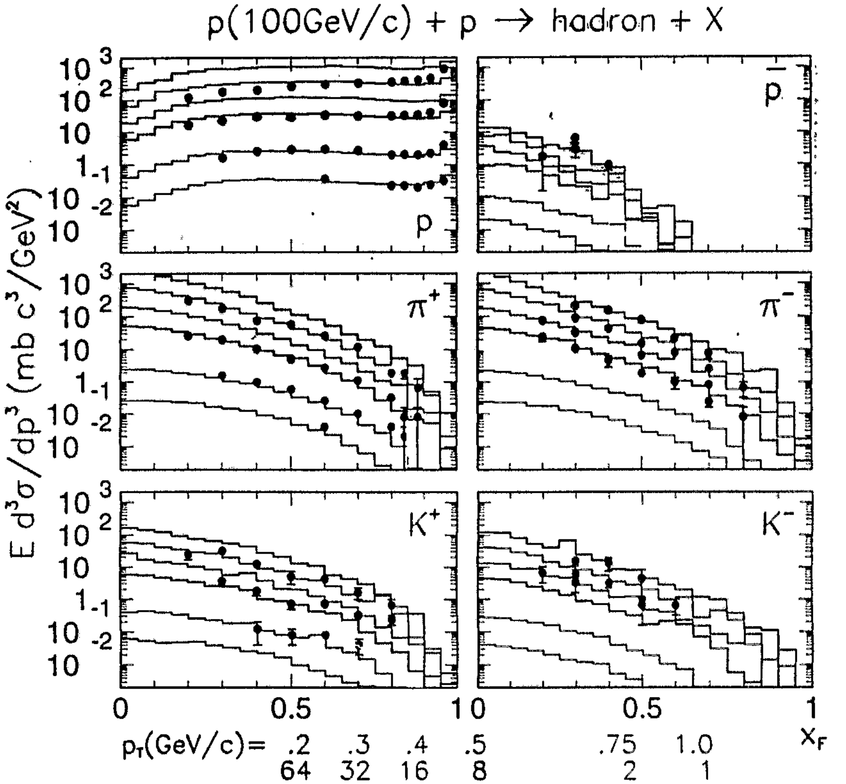

Invariant cross section for hadron production as function of Feynman-x for various p_T values. Points with error bars are experimental data, histograms are ROC model results

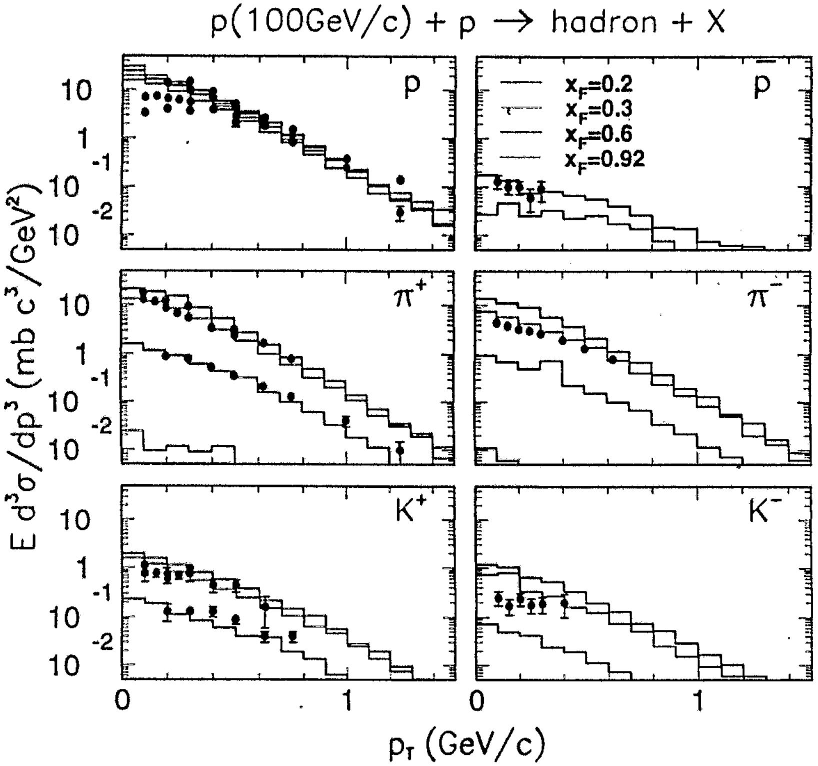

Invariant cross section for hadron production as function of transverse momentum at various x_F values. Points with error bars are experimental data, histograms are ROC model results

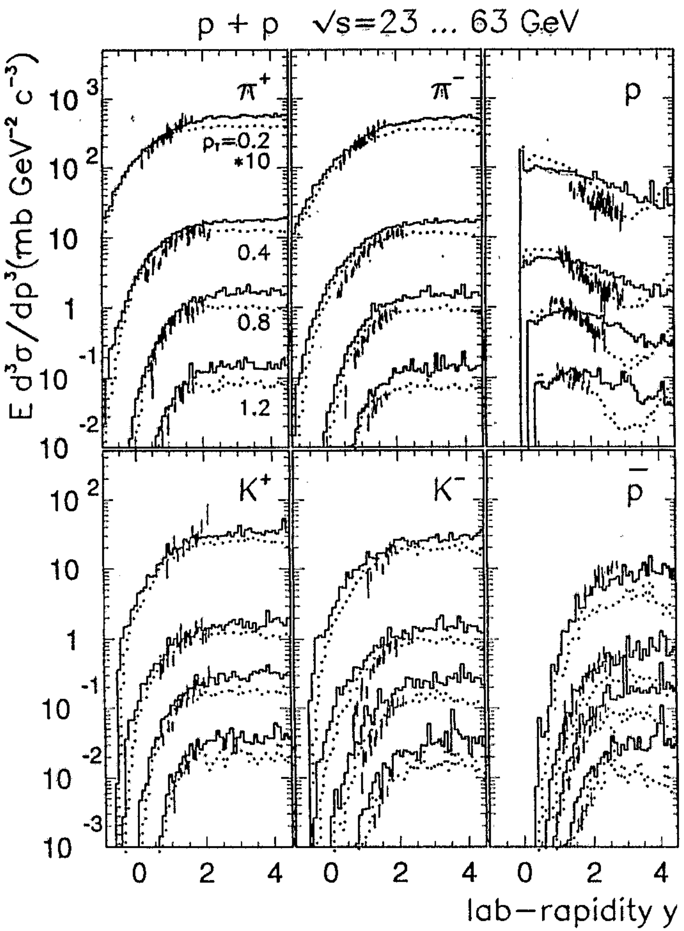

Invariant cross sections for the production of hadrons at different energies and indicated values of transverse momentum as a function of rapidity. Experimental data (*colored points*) are compared with ROC model results (*black histograms: dotted* $\sqrt{s} = 23$ GeV, *full* $\sqrt{s} =$ 63 GeV)

Isospin dependence of K^- meson production in nucleon-nucleon interactions

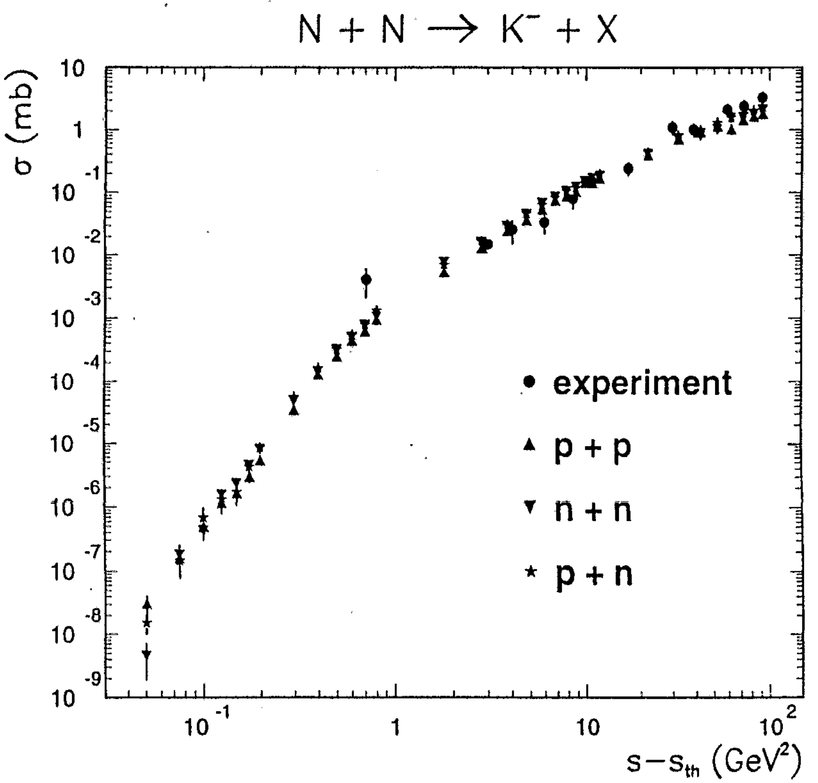

Cross section for inclusive K^- meson production in pp, nn and pn interactions as a function of $s - s_{th}$

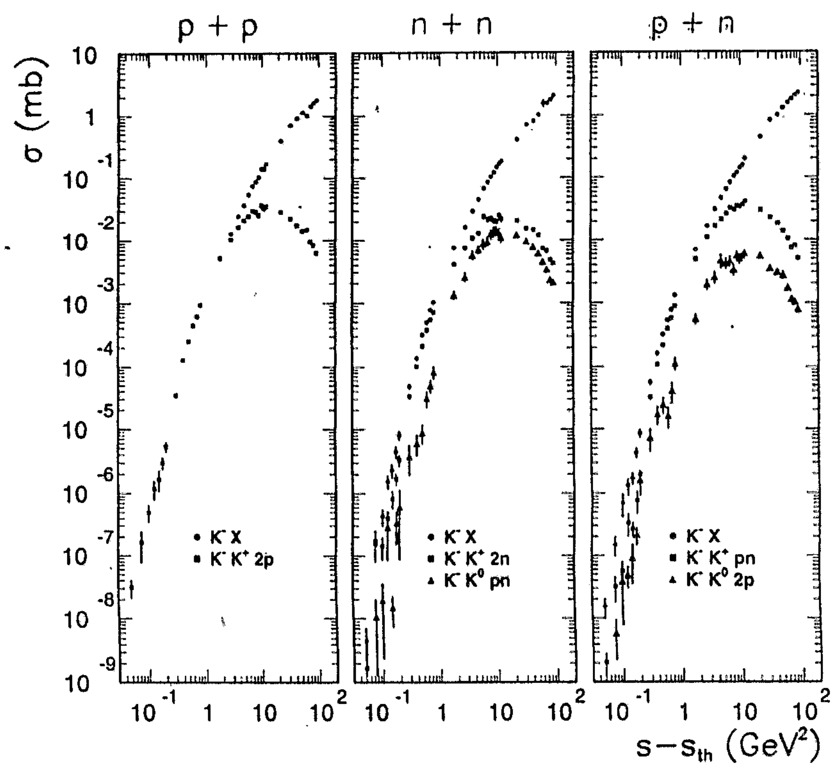

Cross section for inclusive and exclusive K^- meson production in pp, nn and pn interactions as a function of $s - s_{th}$

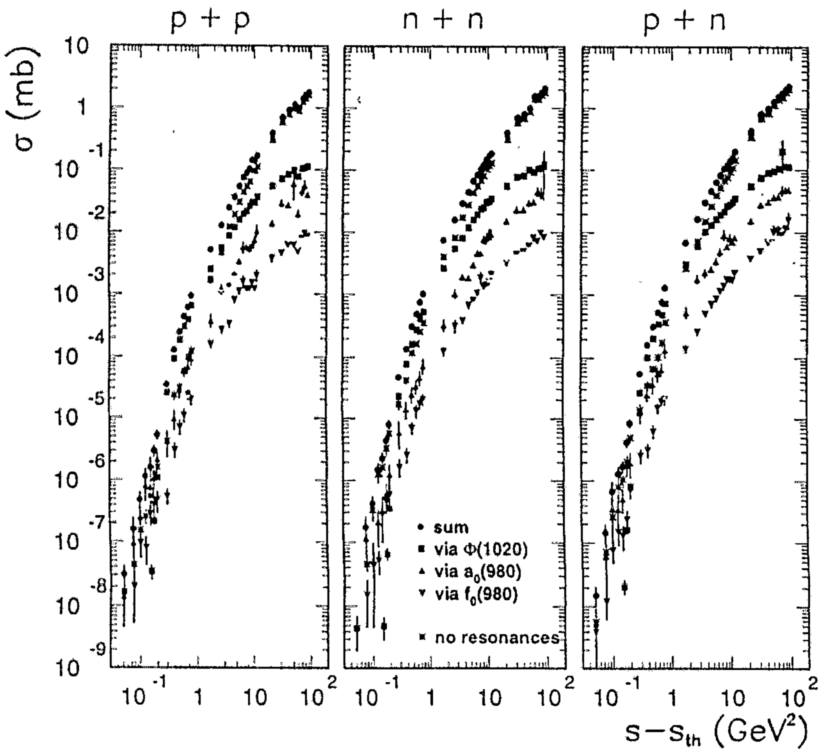

Partial cross section for inclusive K^- meson production in pp, nn and pn interactions via resonances as á function of $s - s_{th}$

ROC model

Summary

- unified description of hadronic and nuclear reactions
- simultaneous description of all reaction channels for
  - any projectile-target combination
  - wide energy region
- implemented as Monte-Carlo generator → complete events
  - comparison with any experimental results
  - event generator for simulation of experiments

P. Michel K^+ data from COSY

"K^+-Daten am COSY-TOF"

Y. Michel

Assoziierte Strangeness-Produktion im p-p-Stoß (#15)
(COSY-TOF-Kollab. Uni Erlangen)

warum? Konsistente Theorie der Baryon-Baryon-WW

$\binom{u}{d}$ $\binom{c}{s}$ $\binom{t}{b}$
$\Downarrow$ N, $\Downarrow$ Y

wie?
- Erzeugungsmechanismus v. Strangeness (Erzeugung im NN-System als Input für Strangenessprod. im N-Kern oder Kern-Kern-system)
- YN-Wechselwirkung als Komponente der Baryon-Baryon-Wechselwirkung (über FSI bei kleinen Relativenergien)

strangeness produktion:

über starke WW (assoziiert)	$p\bar{p} \to \bar{Y}Y$	(Cern)
	$\pi^+ d \to K^+(YN)$	(AF)
	[$pp \to K^+(YN)$]	(Saturne, COSY...)
	($K^- d \to \pi^-(YN)$)	
über elm. WW	$\gamma p \to K^+\Lambda$	
über schwache WW	$dp \to \Lambda pp$	#33 T. Seyfrik

Was geht an COSY? $p_{max} \approx 3.3$ GeV/c

$pp \to K^+(YN)$

Λ uds, $I_z = 0$ | Σ^+ uus, $I_z = +1$ | Σ^0 uds, $I_z = 0$ | Σ^- dds, $I_z = -1$

$\rightsquigarrow pp \to K^+\Lambda p$ — $p_T = 2.339$ GeV/c
$\to K^+\Sigma^+ n$ — $p_T = 2.560$ GeV/c
$\to K^+\Sigma^0 p$ — $p_T = 2.566$ GeV/c

Weltdatenvorrat 1995

- (z.B. Saturn 2.3 – 2.7 GeV inklusive Messungen mit K^+ Nachweis im Magnetspektrometer, keine $\not{Y}$-Inform. über restl. Reaktionsteilchen, $\Lambda, \Sigma^\pm, \Sigma^0$-Kanäle nicht getrennt)

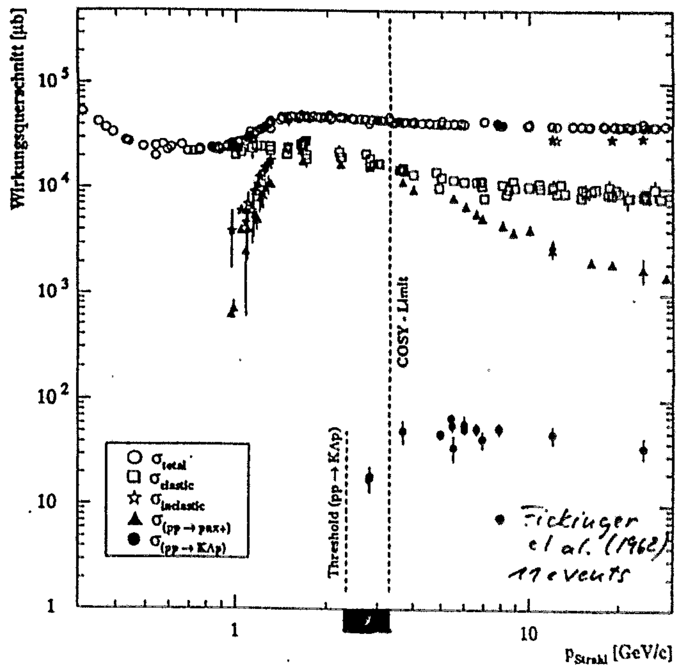

Theoretische Beschreibung

Quark-Gluonen-Modell

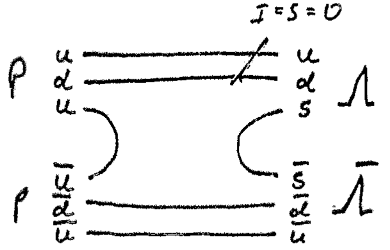

Quarks in rel. S-Zustand
⇝ (ud) koppelt zu S = I = 0
⇝ Spinobservablen des Λ ($\bar{\Lambda}$) auf Spineigenzust. v. s ($\bar{s}$) zurückführbar

⇓

$pp \to K^+ p \Lambda$

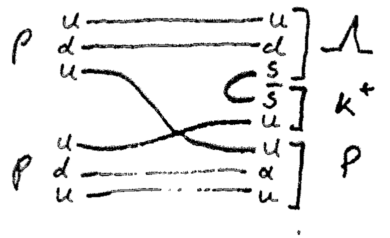

Mesonenaustauschmodell

wichtigste Ordnung:

Kaonenaustausch

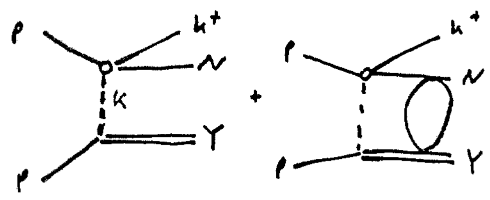

Pionenaustausch

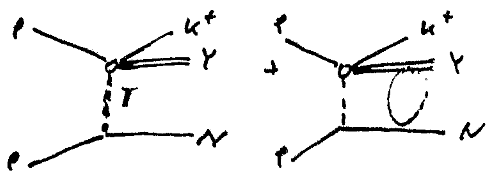

direkte Kaon-Emission

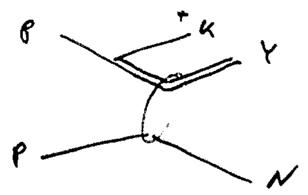

Experiment:

1. Reaktionskinematik $pp \to$?

Kanal	σ/σ_{tot}	sek. Zerfall	$N_{gel.}^{prompt}$	+ $N_{gel.}^{sek.}$ (Signatur!)	Energiebilanz
pp	0.42	–	2	0	
$pn\pi^+$	0.34	$\pi^+ \xrightarrow{c\tau = 7.8\,m} \mu^+\nu_\mu$	2	0	
$pp\pi^0$	0.08	$\pi^0 \xrightarrow{25\,nm} 2\gamma$	2	0	
$pn\pi^+\pi^0$	0.08	⋮	2	0	
$pp\pi^0\pi^0$	0.017		2	0	
$d\pi^+$	0.001		2	0	
$pp\pi^+\pi^-$	0.05	⋮	4	0	
$pn\pi^+\pi^+\pi^-$	0.006		4	0	
$pn\pi^+\pi^0\pi^0$	0.001		4	0	
$pn\pi^+\pi^0\pi^-$	0.004		4	0	
$K^+ p \Lambda$	0.00027	$K^+ \xrightarrow{3.7\,m} \mu^+\nu_\mu$ / $\pi^+\pi^0$ ⋮			
		$\Lambda \xrightarrow{7.9\,cm} p\pi^-$ 64 %	2	2	$E_{inc} = \sum_i E_i^{gem.}$
		$n\pi^0$ 36 %	2	0	
$K^+\Sigma^+ n$		$K^+ \longrightarrow$			
		$\Sigma^+ \xrightarrow{2.4\,cm} p\pi^0$	2	0	
		$n\pi^+$	2	0	
$K^0\Sigma^+ p$		$\Sigma^+ \longrightarrow$ – " –			
		$K_s^0 \xrightarrow{2.7\,cm} \pi^+\pi^-$ / $\pi^0\pi^0$ ⋮	2	2	$E_{inc} = \sum_i E_i^{gem.} + E_n (E_{\pi^0})$
		$K_L^0 \xrightarrow{16\,m}$	2	0	
$K^+\Sigma^0 p$		$K^+ \longrightarrow$			
		$\Sigma^0 \xrightarrow{20\,fm} \gamma\Lambda$	2	2	$E_{inc} = \sum_i E_i^{gem} + E_\gamma$

online Trigger! | off line

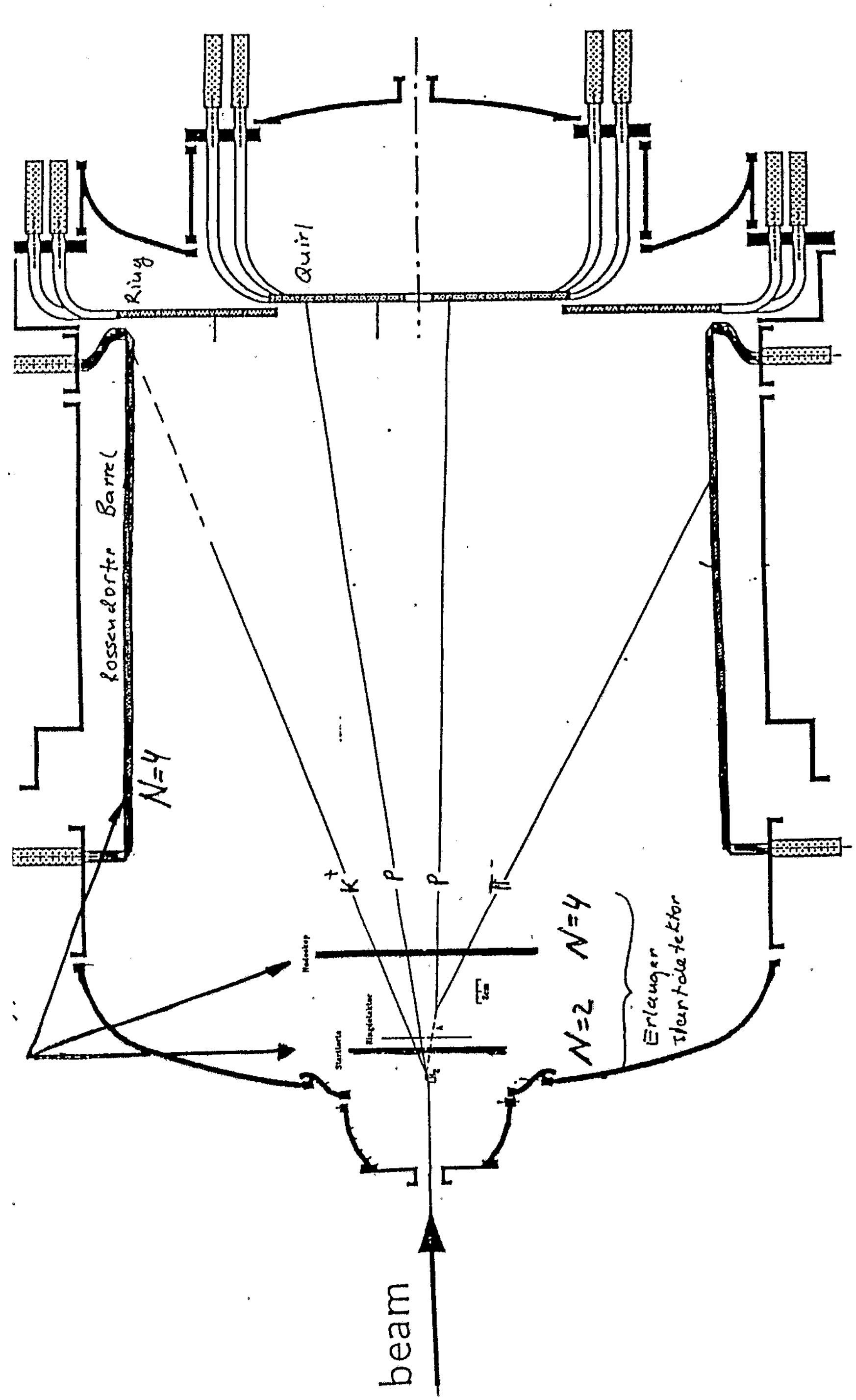

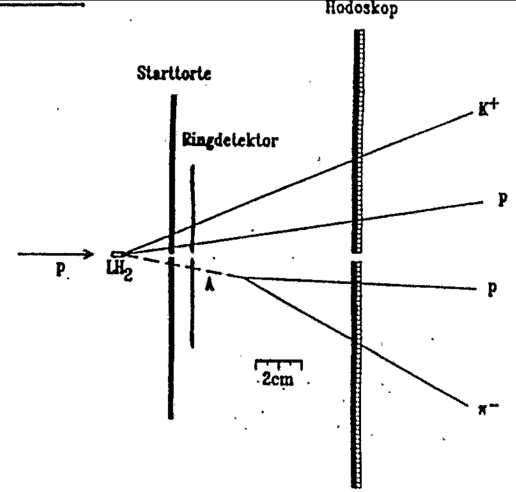

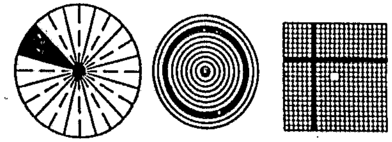

2 Lagen a 12 Segmente Szintillator	100 Ringe Si-μ-Streifen	2 Lagen (x,y) a 96 Streifen Szintillator
1mm NE104	520 μm Si	2×2 mm² BCF12
∅ Innenloch: 2mm	∅ Innenl.: 1.5mm	□ 2mm Loch
Δt ~ 0.3ns (fwhm)	Δϑ ~ 280 μm	Δx,y ~ 2mm
	∅ aktive Zone: 3.1 – 31 mm	

* M
* Δt start
* ρi

* M
* ϑi
* ΔEi

* M
* xi yi → ρi, ϑi
* ΔEi

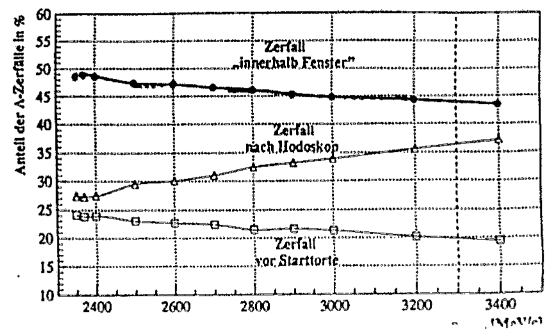

Stopdetektor

Endkappe:

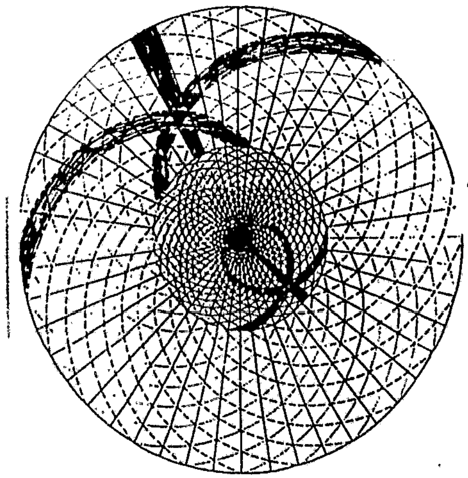

Ring:

96 gerade
48 linke
48 rechte
0.5 mm
$\varnothing$: 116 cm – 300 cm

Quirl:

48 gerade
24 linke
24 rechte

0.5 mm
$\varnothing$ Innenloch: 8 cm

Barrel:

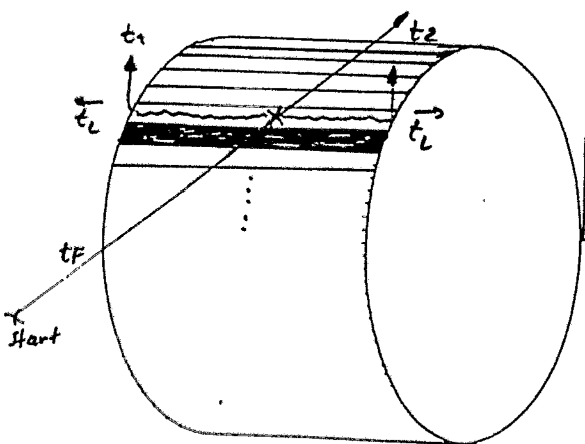

$t_1 = t_F + \overleftarrow{t_L}$
$t_2 = t_F + \overrightarrow{t_L}$

$t_1 - t_2 \sim x$
$t_1 + t_2 \sim t_F$

$t_L = \frac{x}{v_L}$

96 Szintillatoren NE110A (Bicron)

3000 x 100 x 15 mm

* M

* ρ_i

* ϑ_i

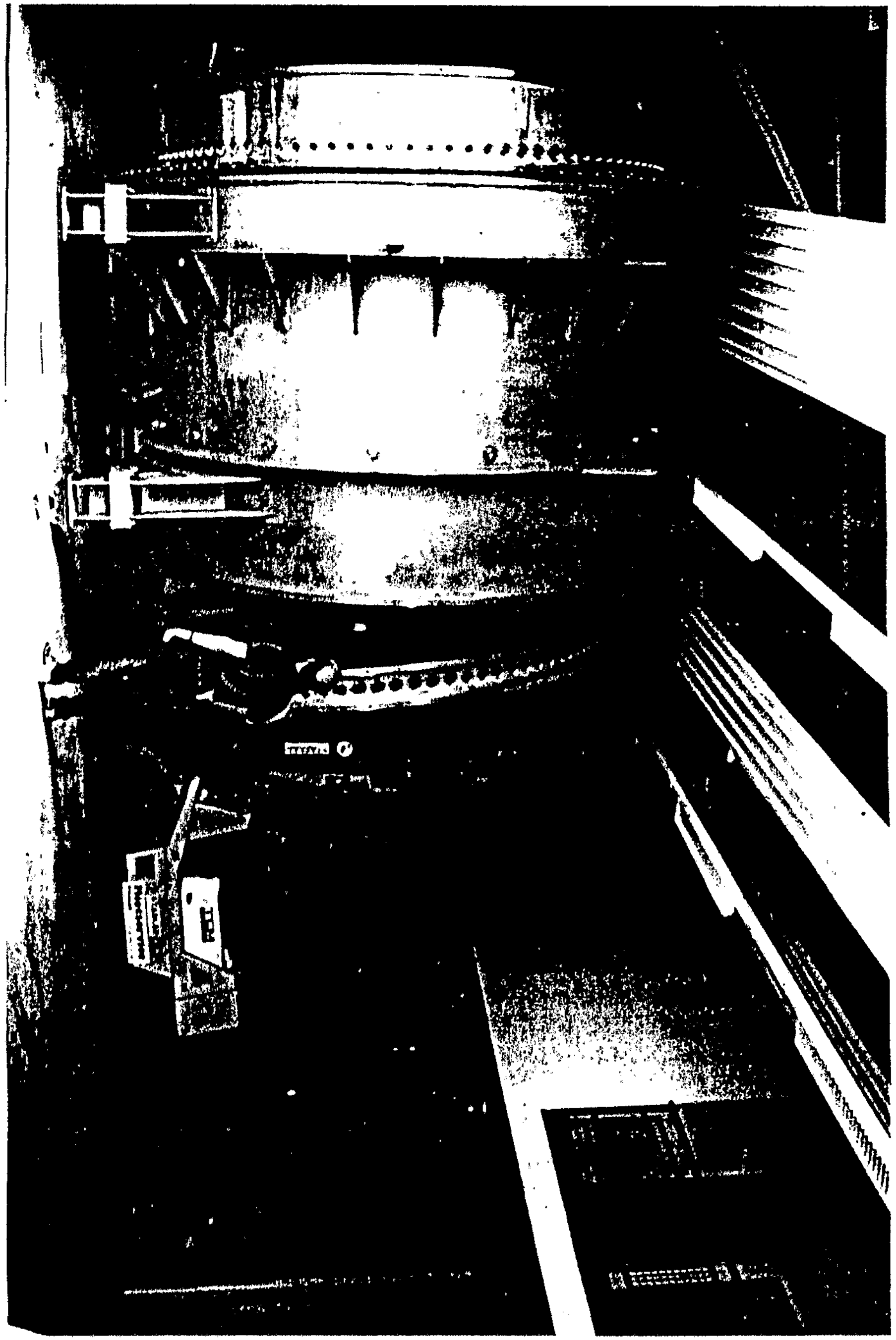

LH_2 - Target

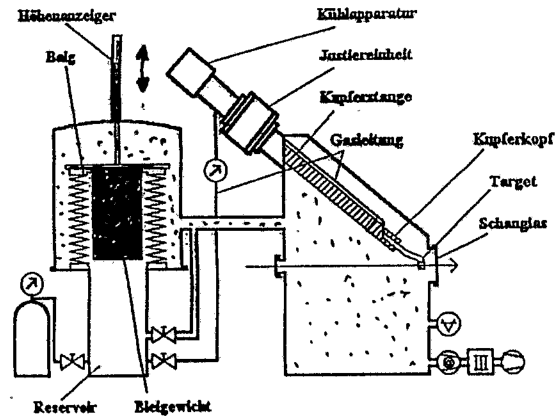

13 - 14 K

$\Delta P = 200$ mbar

Eintritts-Austrittsfolien: 1 µm Hostaphan
Target ø : 6 mm
Targetlänge : 4 mm
ϱ $1.8 \cdot 10^{22}$ p / cm²

Meßergebnisse:

Meßzeiten: 4/96
6/96

2-Spurevent

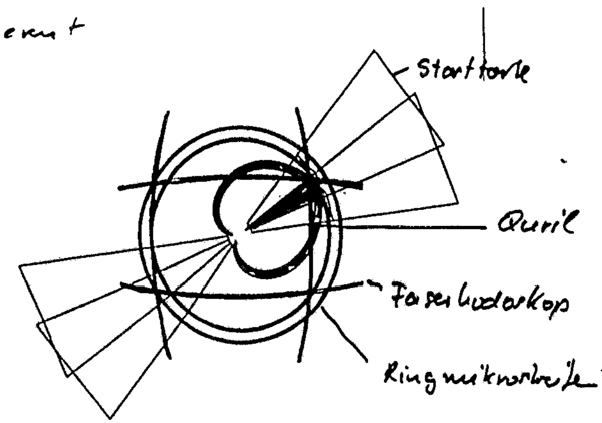

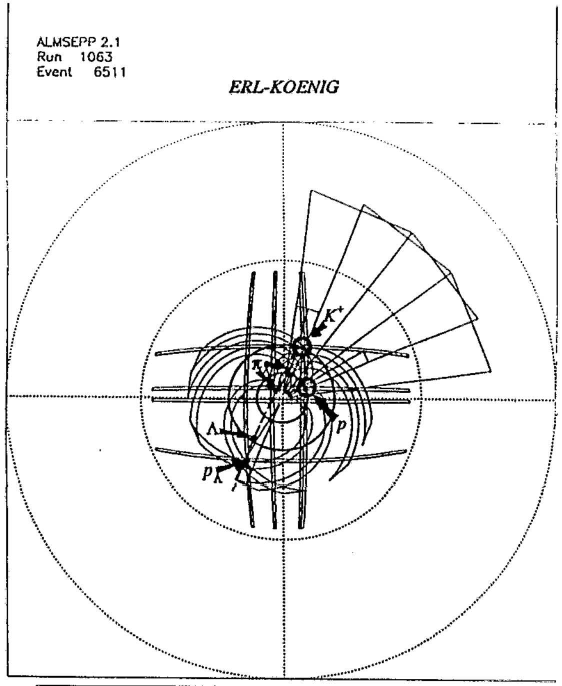

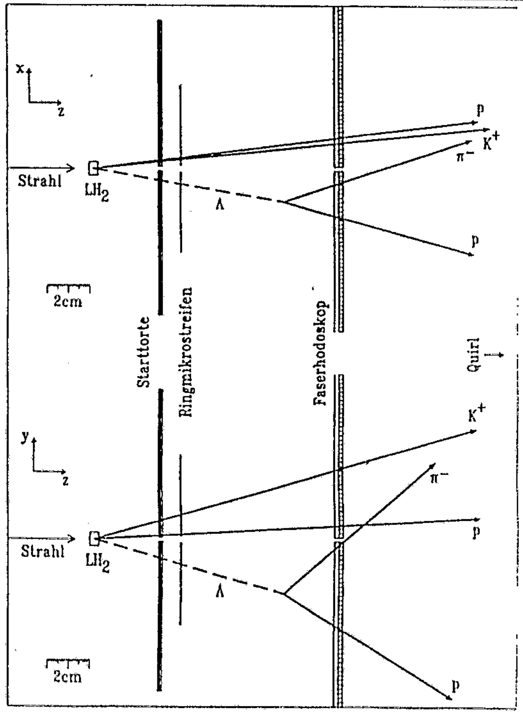

Ereignisrekonstruktion!

1. K^+, p .... Ereignisvertex im Target

K^+, p - Unterscheidung Δt, ΔE

Impulsvektor Λ in Ebene $(\vec{p}_\Lambda, \vec{\pi}^-_\Lambda)$

Test für richtige Zuordnung:

$$m_\Lambda^2 \overset{?}{=} \left(\sqrt{p_{Strahl}^2 + m_p^2} + m_p - E_p - E_K\right)^2 - \left(\vec{p}_{Strahl} - \vec{p}_p - \vec{p}_{K^+}\right)^2$$

$(E, p)_{\perp\Lambda}$ — Messung überbestimmt! 95% Wkt. für richtige Teilchenzuordnung!

2. p_Λ, π^-_Λ

da Messung überbestimmt!

Ereignisrekonstruktion möglich für K^+-Zerfallsevents (47% Ruhepunkt!)

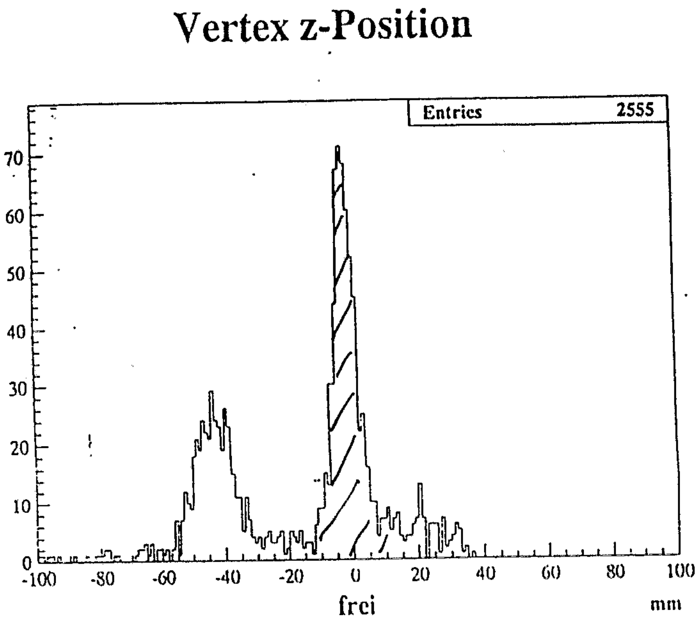

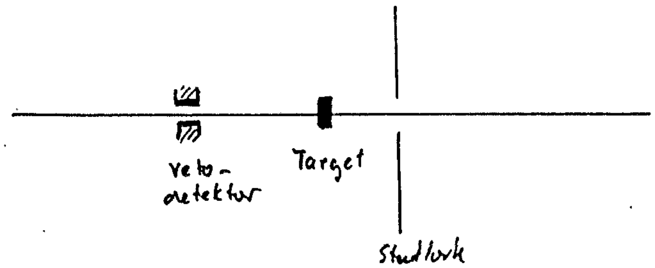

E. Grosse	K^+ experiments at SPES3
E. Grosse	$K^\pm$ experiments at KaoS

Hadrons within the medium

Typical result of an NJL model calculation: (Lutz & Weise, 1992)

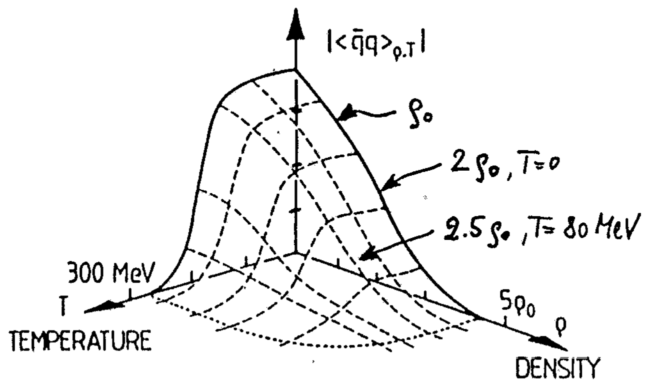

The $<\bar{q}q>$ condensate as a function of density ρ and temperature T.

Chiral symmetry is restored at large ρ (and T)

hadron masses go down: $m_B^{eff}(\rho,T) \propto |\langle\bar{q}q\rangle_{\rho,T}|$

↷ production **near threshold goes up**

[illegible] & Kaplan (198?): $m_K^{eff}(\rho)^2 = m_K^2 - \frac{\Sigma_{KN}}{f_\pi^2}\rho + \dots$ (↑ K-N scattering; ← K decay)

SPES 3 at Saturne

Boivin, Le Bornec, Tatischeff, Willis et al.
(LNS-IPN-collaboration)

$\vartheta_{LAB} = 40°$

$\frac{\Delta p}{p} \cong 10^{-4}$

$\Delta\Omega \cong 10$ msr

$p = \begin{cases} 350 - 800 \\ 500 - 1100 \end{cases}$ MeV/c

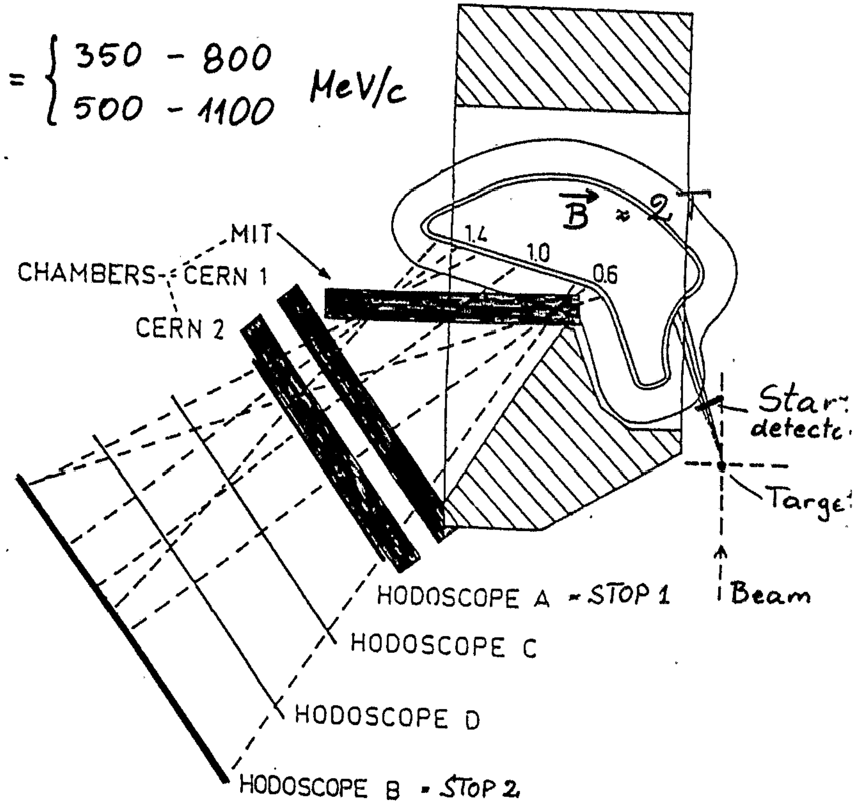

Particle identification: $m = \frac{p}{\beta\cdot\gamma}$ (TOF)

Measured: p, π^+, K^+

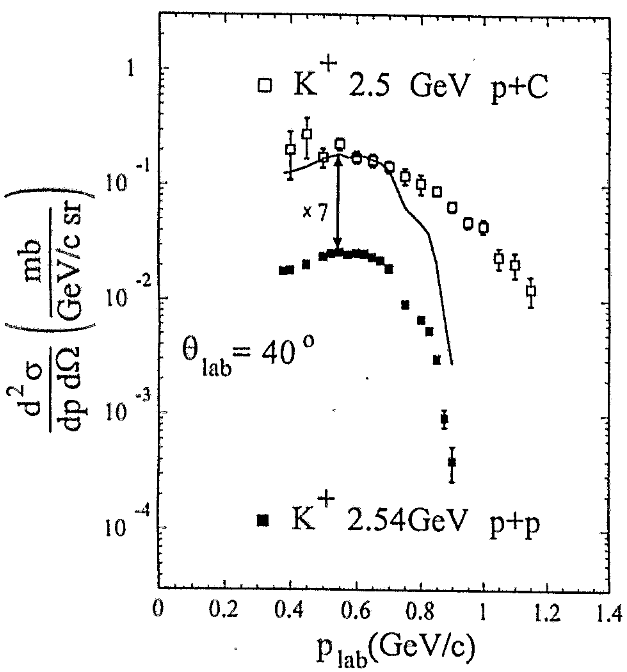

□ Debowski *et al.* (1995)

SPES-3 coll. : GSI + TH Darmstadt, IPN Orsay, LNS Saclay, UJ Cracow

■ Hogan *et al.* Phys. Rev. (1968)

$$\frac{\sigma_C^{inel}}{\sigma_p^{inel}} = 7.0$$

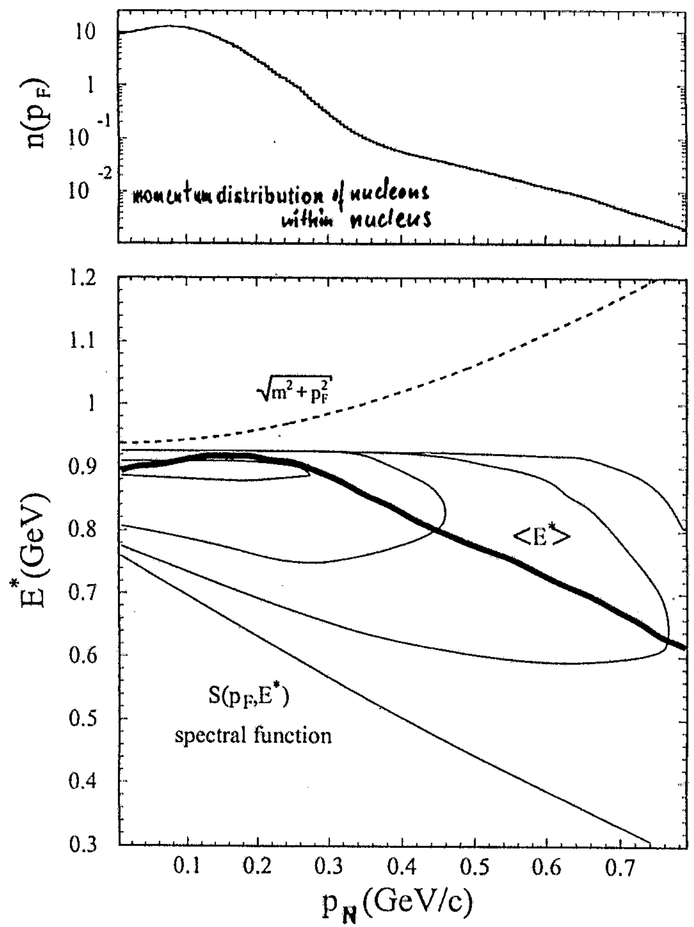

based on quasi-free electron scattering data

I.Sick, S.Fantoni, A.Fabrocini and O.Benhar (1994

folding with elementary cross section $\sigma_{elem}(NN \rightarrow NYK)$

$$\sigma_{pA} = \frac{\sigma_A^{inel}}{\sigma_p^{inel}} \int S(p_N, E^*)\, \sigma_{elem}(s)\; d^3p_N dE^*$$

$$s = (E_p + E^*)^2 - (\vec{p}_p + \vec{p}_N)^2$$

$p + {}^{12}C \rightarrow K^+ + X$

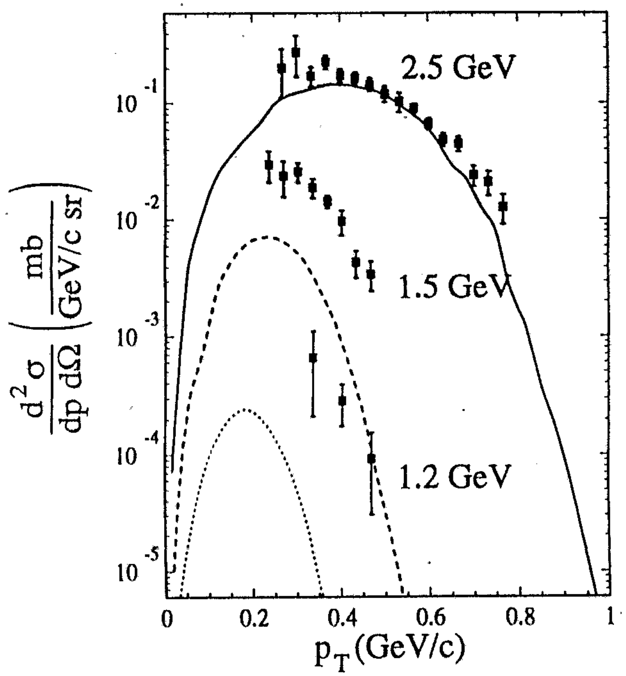

folding with spectral function

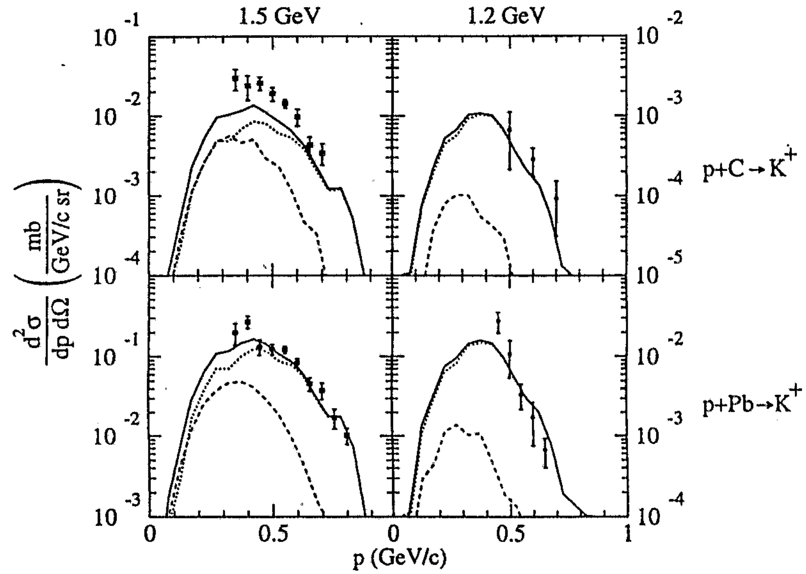

- - - - folding

——— " plus 2-step processes

$pN \rightarrow N\Delta$

$\Delta \rightarrow N\pi$

2nd step: $\pi N \rightarrow K\Lambda$

or: $\Delta N \rightarrow K\Lambda N$

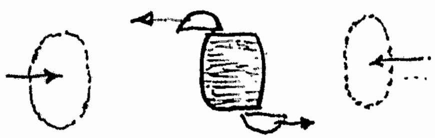

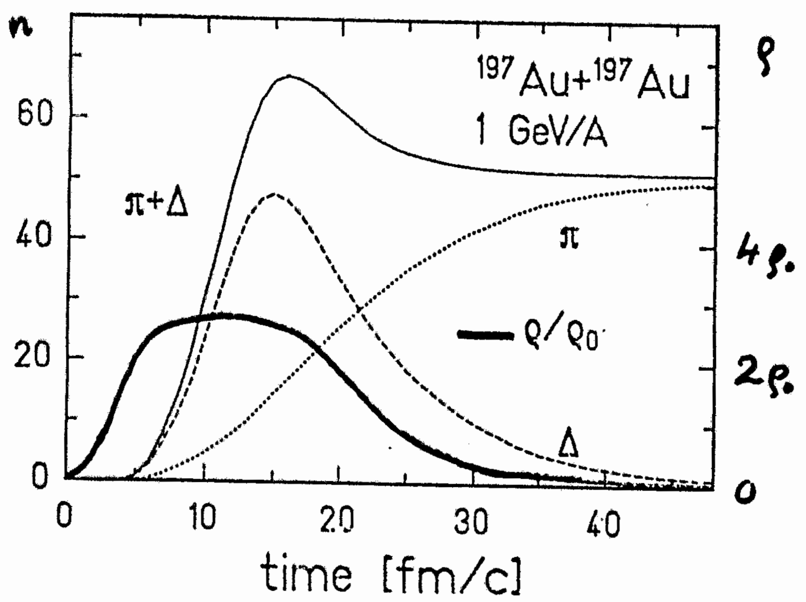

Transport model calculation (BUU) including NN→NΔ ; Gy. Wolf et al. '93
↳πN (Giessen & GSI)

In central collisions the projectile energy is converted into:

- compression → expansion
- heat → thermal motion →
- baryon excitation → meson production

σ (πN → Δ) ~ 200 mb [illegible]

[illegible]

The KaoS Spectrometer at SIS

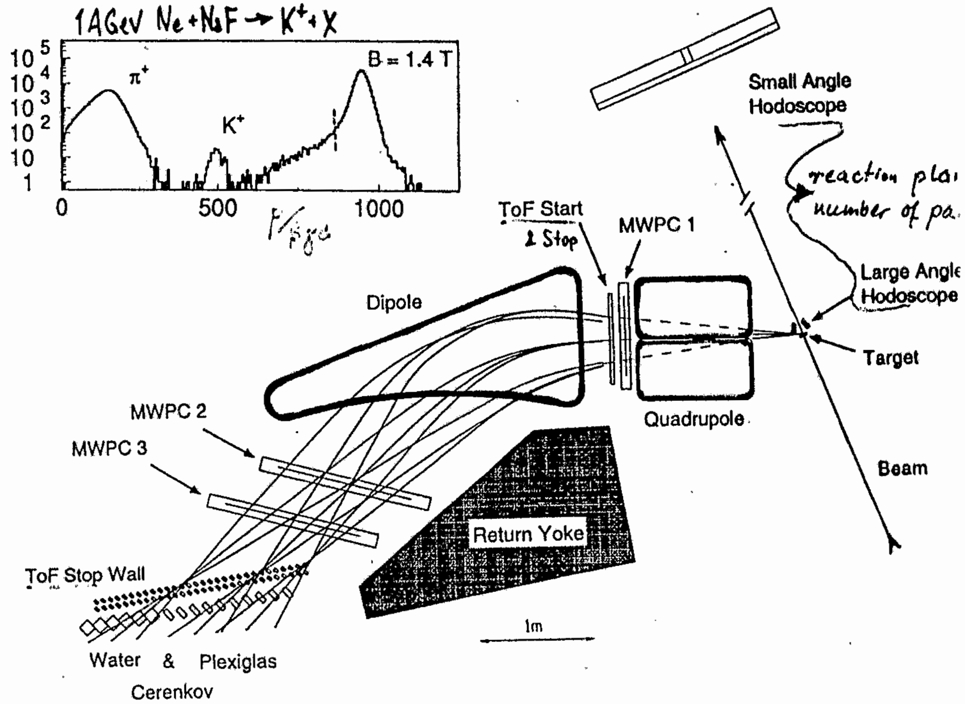

KaoS Collaboration

R. Barth[a], D. Brill[c], M. Cieślak[a], M. Dębowski[a], E. Grosse[a], S. Kabana[a], P. Koczoń[a], B. Kohlmeyer[d], F. Laue[a], M. Mang[a], Ch. Müntz[b], H. Oeschler[b], F. Pühlhofer[d], E. Schwab[a], P. Senger[a], Y. Shin[c], J. Speer[d], R. Stock[c], H. Ströbele[c], Ch. Sturm[b], K. Völkel[d], A. Wagner[b], W. Waluś[e], M. Waters[a], and I. K. Yoo[d]

[a] GSI Darmstadt, [b] TH Darmstadt, [c] Univ. Frankfurt, [d] Univ. Marburg, [e] Univ. Kraków

Event Characterization

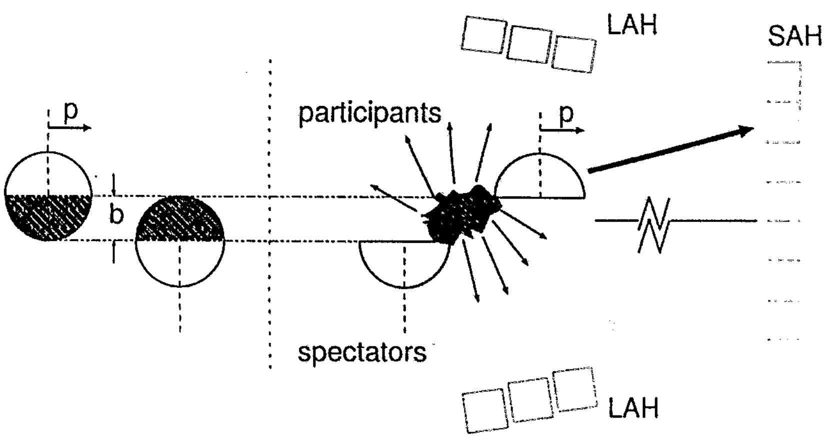

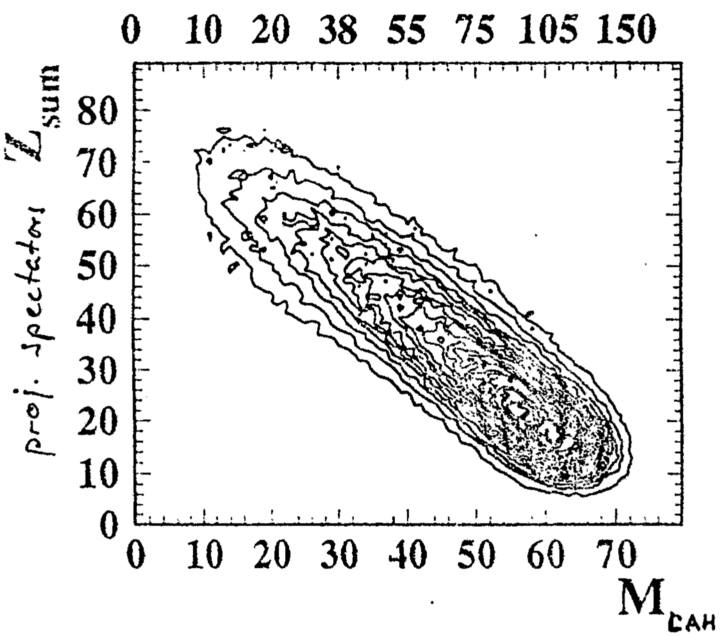

$$A_{PART} = 2 \cdot \frac{A}{Z} \cdot (Z - Z_{SAH}^{SUM})$$

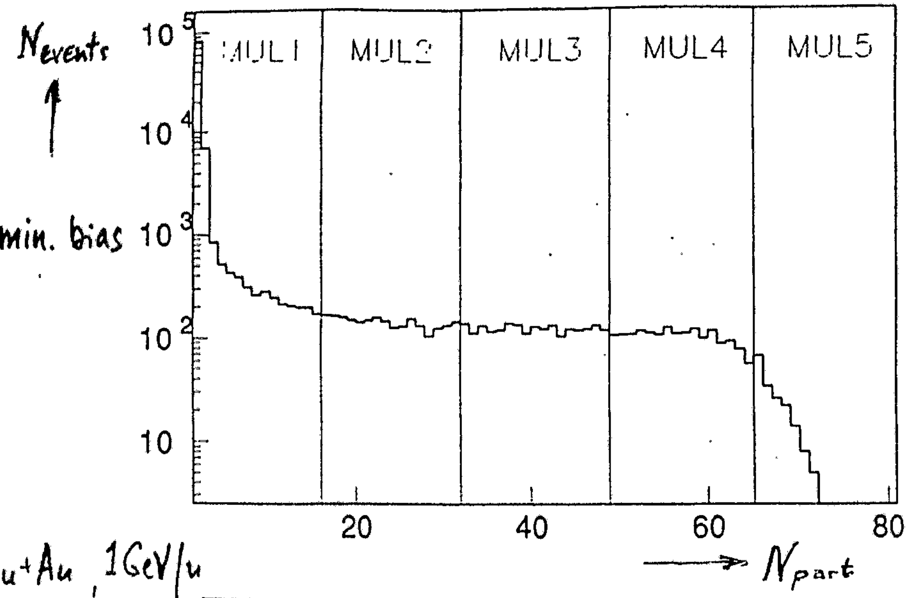

Au+Au, 1GeV/u

with π, K, ..

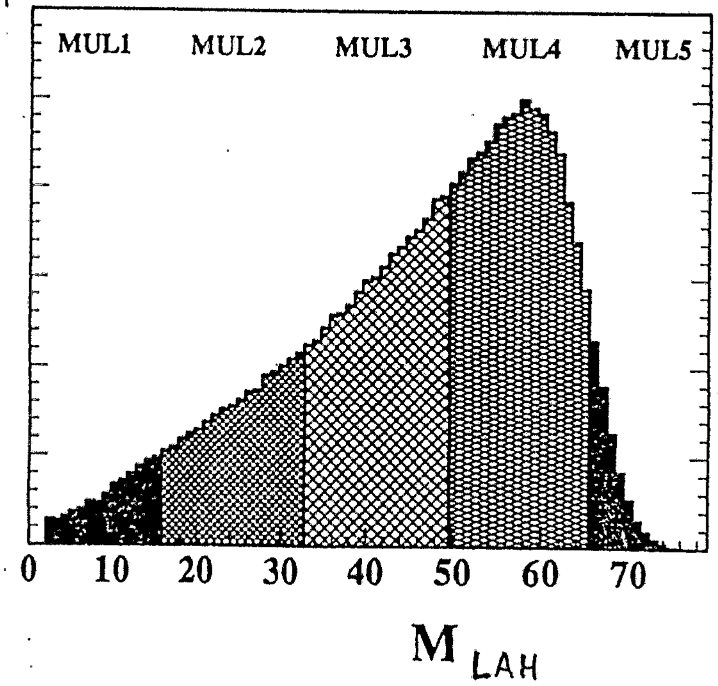

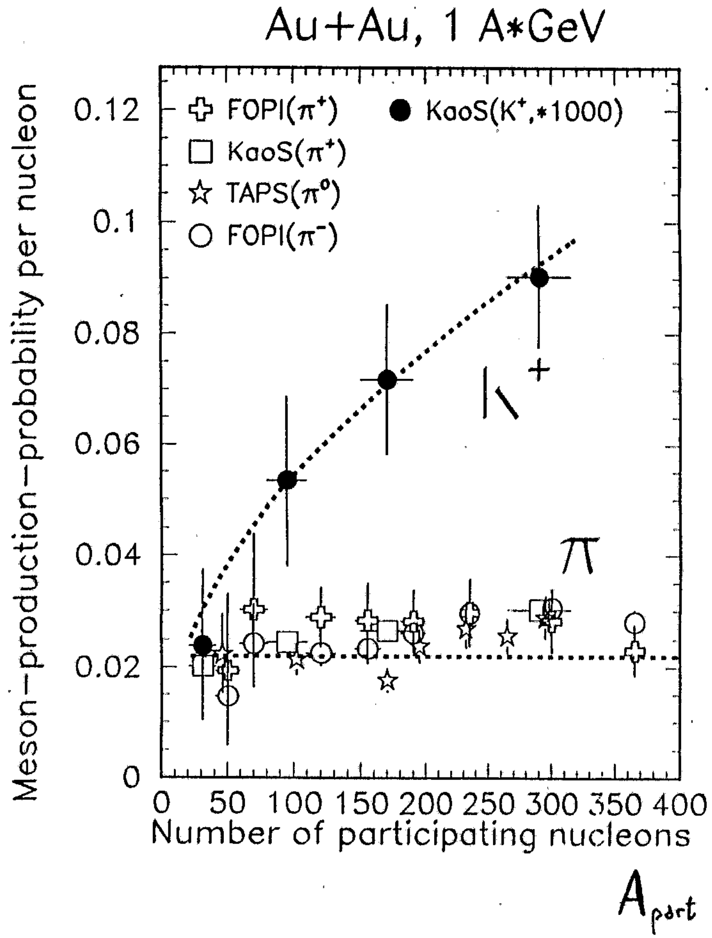

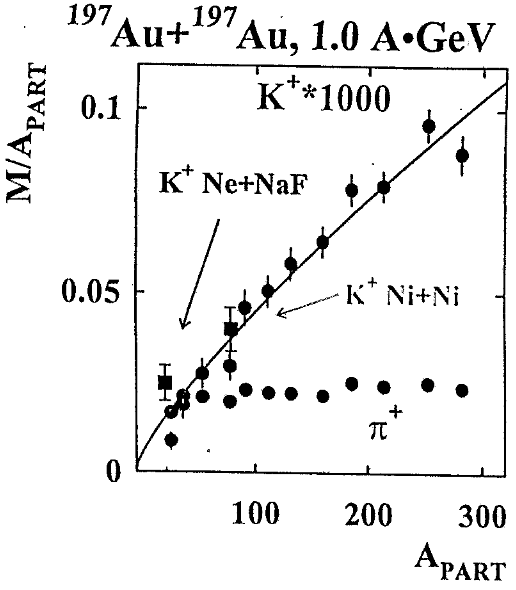

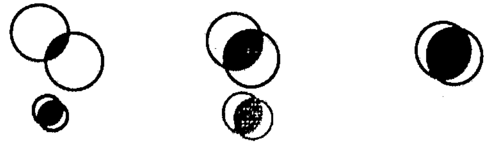

$M^{K^+} = c \cdot A_{part}^{\alpha}$; $\alpha = 1.75 \pm 0.15$

QMD (Hartnack et al., Nucl. Phys. 580 (1994)):

$M^{K^+} = c \cdot A^{\alpha}$; $\alpha = 1.38$ for stiff eos

$\alpha = 1.62$ for soft eos

K$^+$ from Au+Au at 1.0 AGeV for different Θ_{lab}

→ comparison with $d^3\sigma/dp^3 \propto \exp(-E/T)$

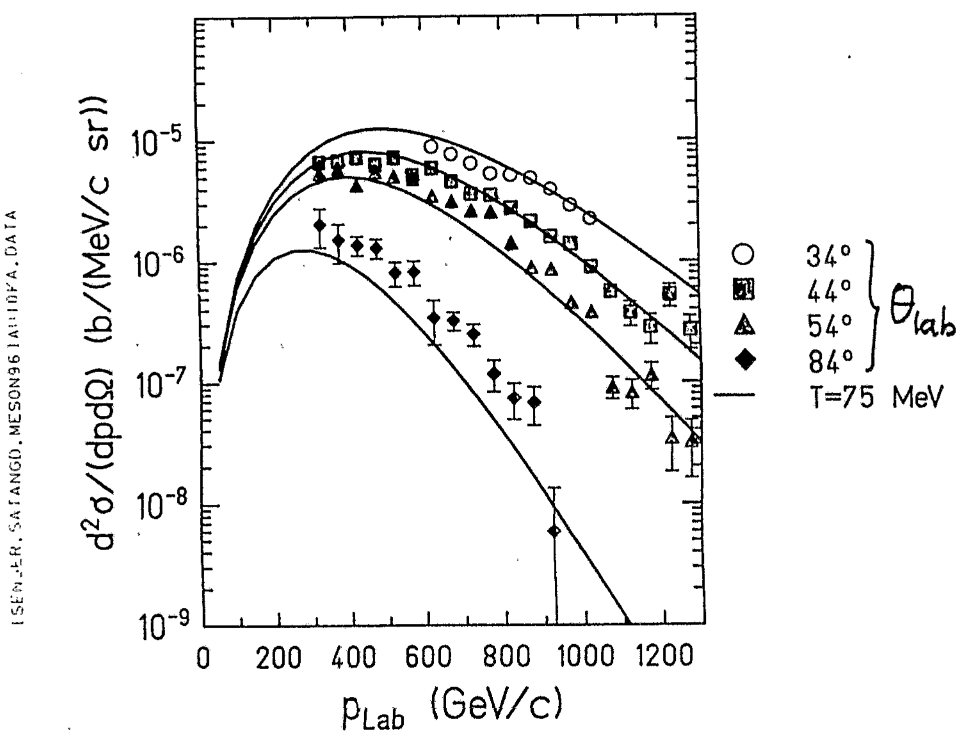

multi-step-processes

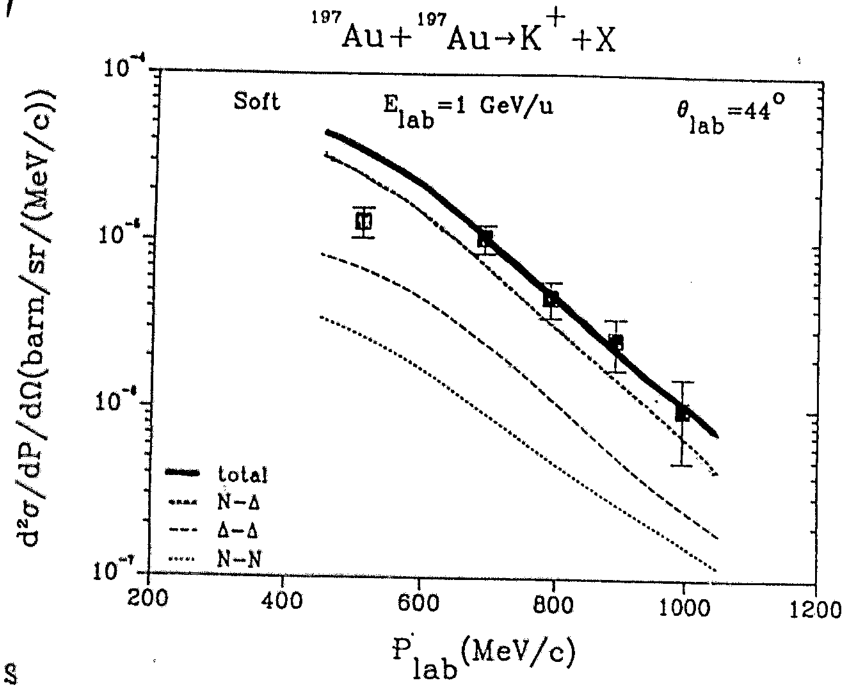

effect of eos

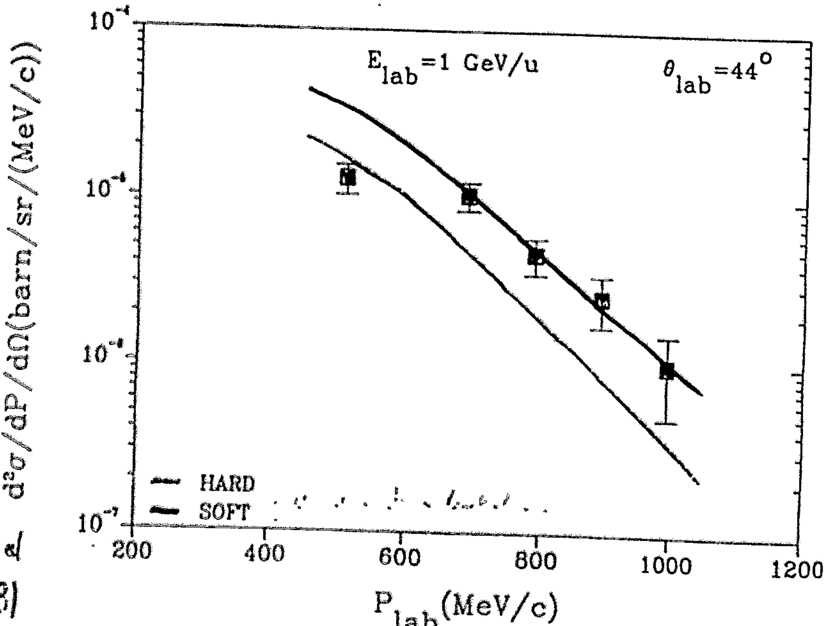

KaoS data

QHD:

Huang, Faessler et al

Phys. Lett. ('93)

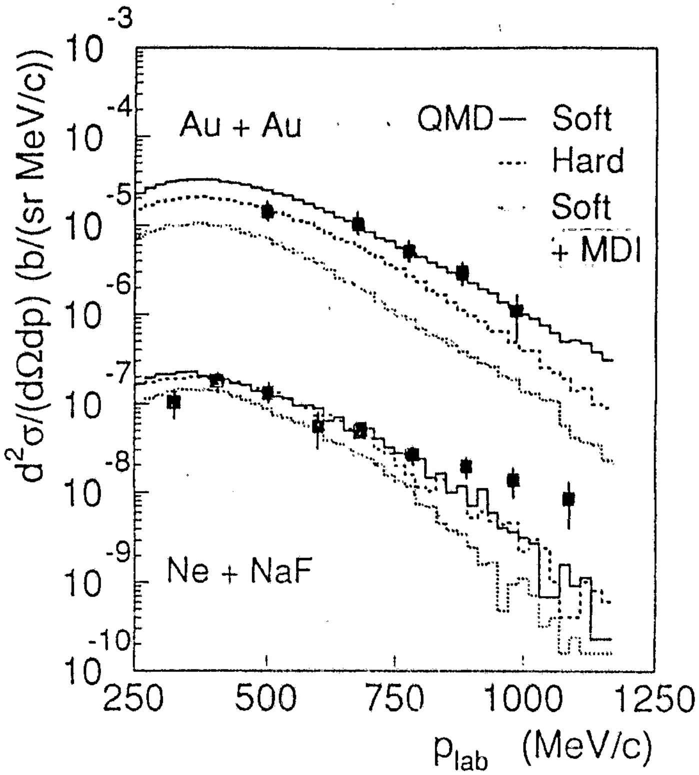

KaoS data

Hartnack & Aichelin ('93)

non-relativistic QMD

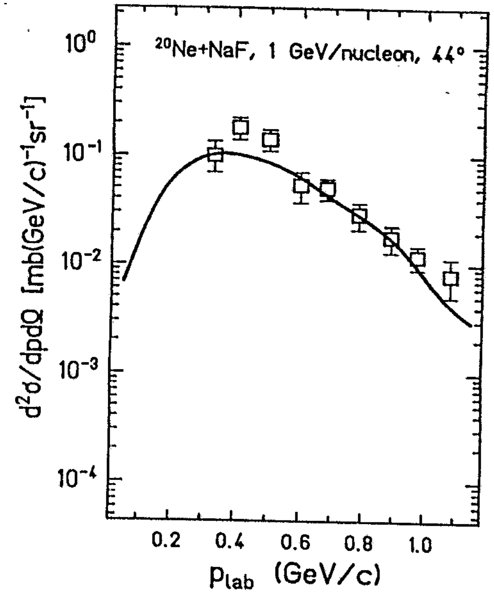

midrapidity
K^+ data
from KaoS
D. Miskowiec et al.

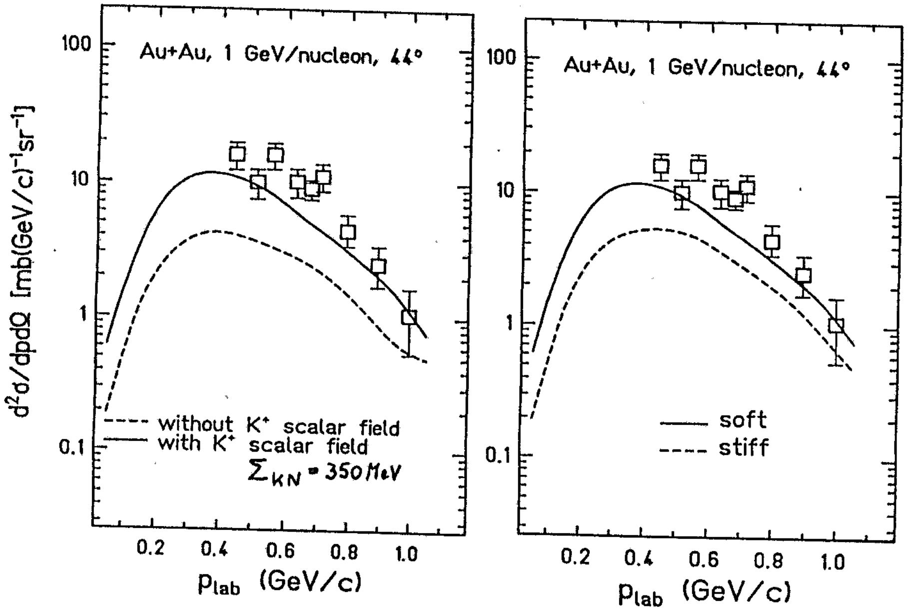

calc. by C.M. Ko, G.Q. Li et al. Phys. Lett. B 349 (1995) 405
Nucl. Phys. A575(1994) 766

In-medium fields acting on hadrons

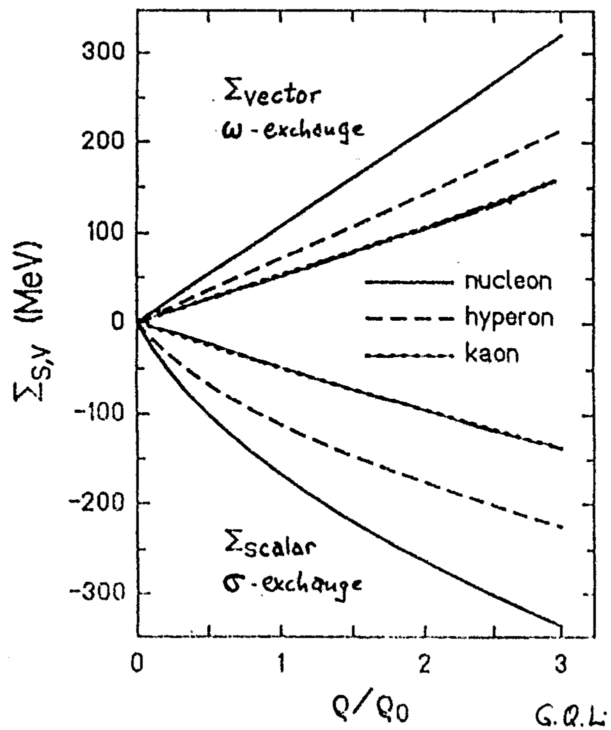

G.Q. Li & C.M. Ko

σ : attractive
ω : repulsive
attractive for antiparticles!

$V_{opt} = \Sigma_s + \Sigma_v \approx -50$ MeV

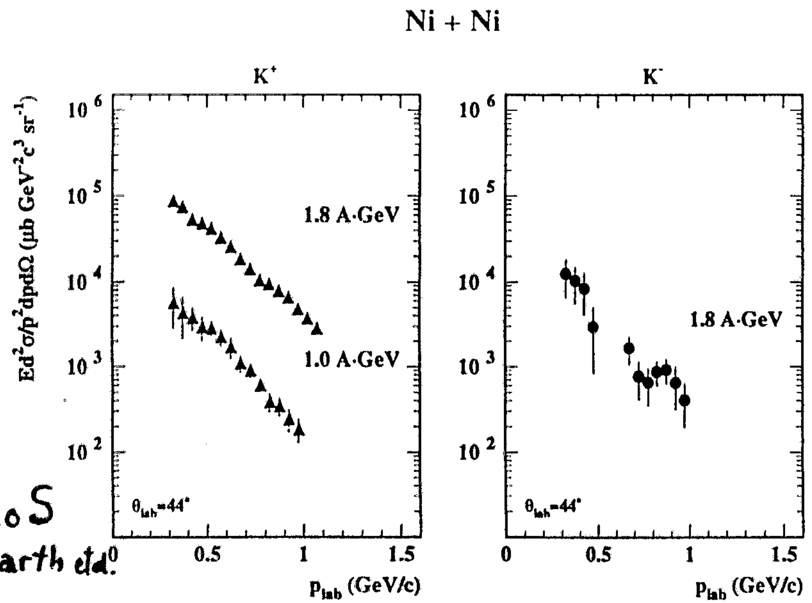

KaoS
R. Barth et al.

TU München - GSI collab.
A. Gillitzer et al.
data taken at SiS-FRS

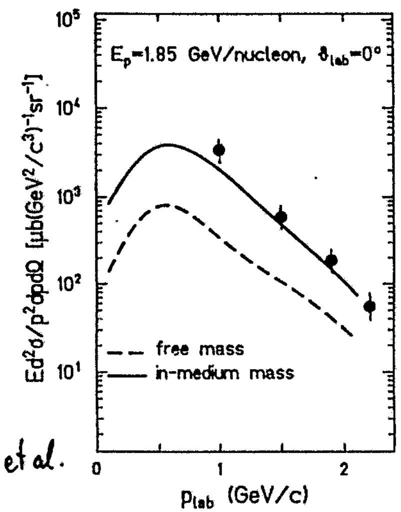

calc. by G.Q.Li, C.M.Ko et al.

FRS-data at 0° (A. Gillitzer et al.)

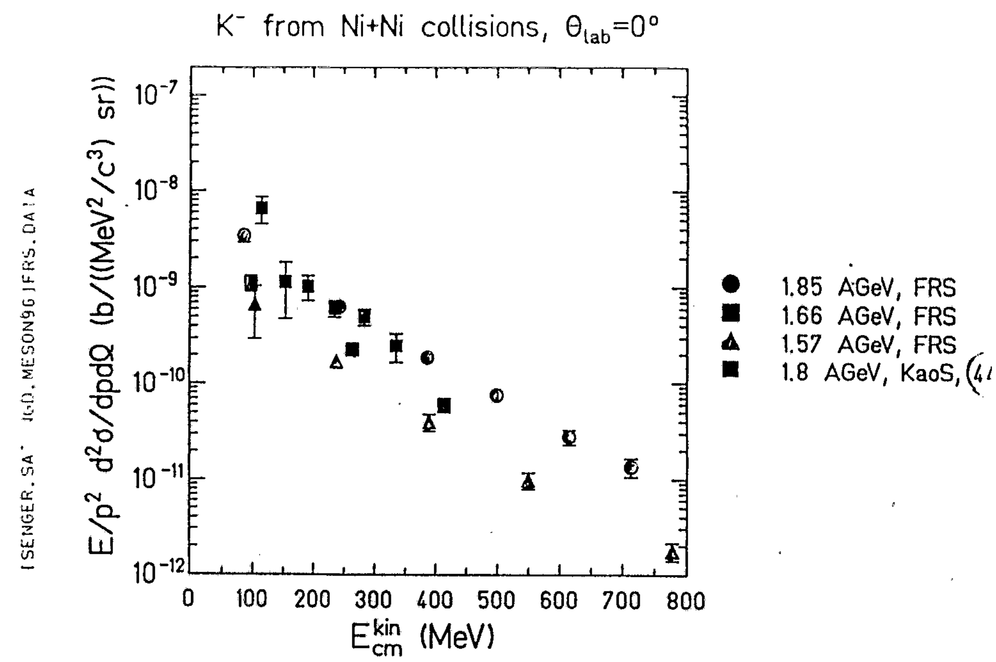

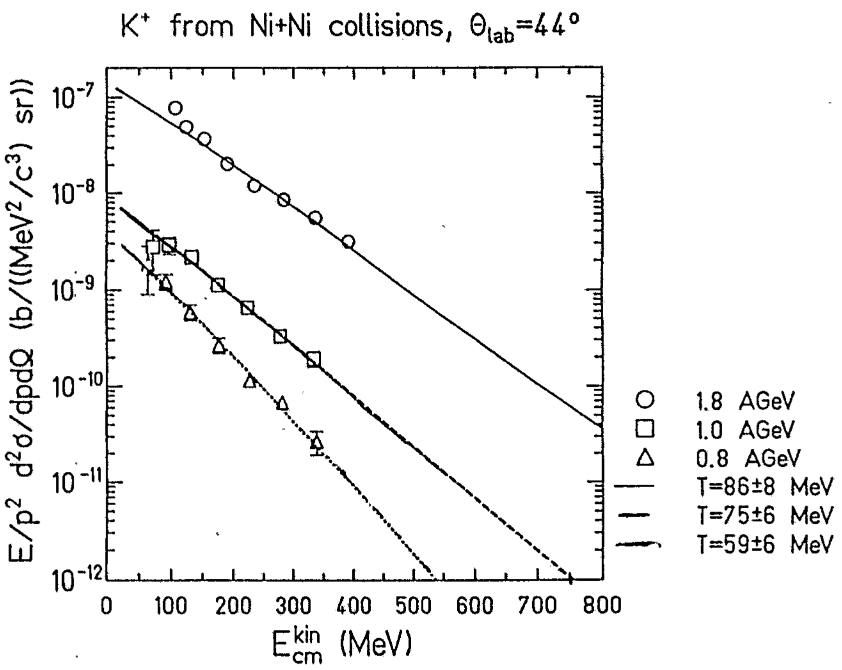

Equivalent energies for K^+ and K^- production

- N+N $\rightarrow$ $K^+\Lambda N$ at 1.0 GeV:

$\sqrt{s} - \sqrt{s}_{thres}$ = 2.32 GeV - 2.55 GeV = -0.23 GeV

- N+N $\rightarrow$ K^+K^-NN at 1.8 GeV:

$\sqrt{s} - \sqrt{s}_{thres}$ = 2.63 GeV - 2.86 GeV = -0.23 GeV

R. Kotte $K^{\pm}, \Lambda$ experiments at FOPI

Study of Hot and Dense Hadronic Matter at SIS Energies (0.1-2A GeV)

Outline and Conclusion:

DATA: FOPI, FRS, KaoS, TAPS

Hadronic matter at $\rho<3\rho_0$, T<100MeV

Particle Production
($\pi,\eta,K,\Delta,\Lambda,\bar{p},\Phi$)

Flow
- sideward
- expansion
  - radial
  - transverse
  - longitudinal

chemical composition

stopping
dynamics
kinetic equilibrium

Large Flow Effects

Consistent Picture not achieved yet (strangeness)

Interesting Measurable Speculations
(chiral symmetry)

Kernmaterie - Phasendiagramm

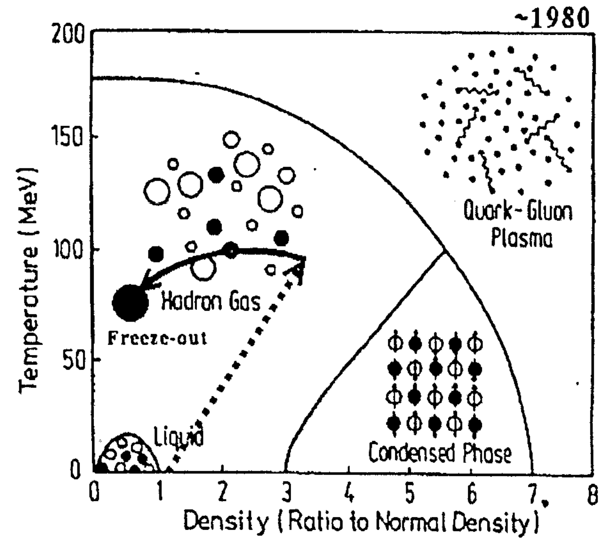

Hadronengas:

$p,n,\Delta,N^*,\Lambda,\pi,K,\rho,\omega,\Phi,\ldots$

! nicht perturbativer Bereich der QCD

Auswirkungen grundlegender Symmetrien?
Gleichgewichtskonzepte anwendbar?

Endzustand aller
(ultra)relativistischen Schwerionenreaktionen

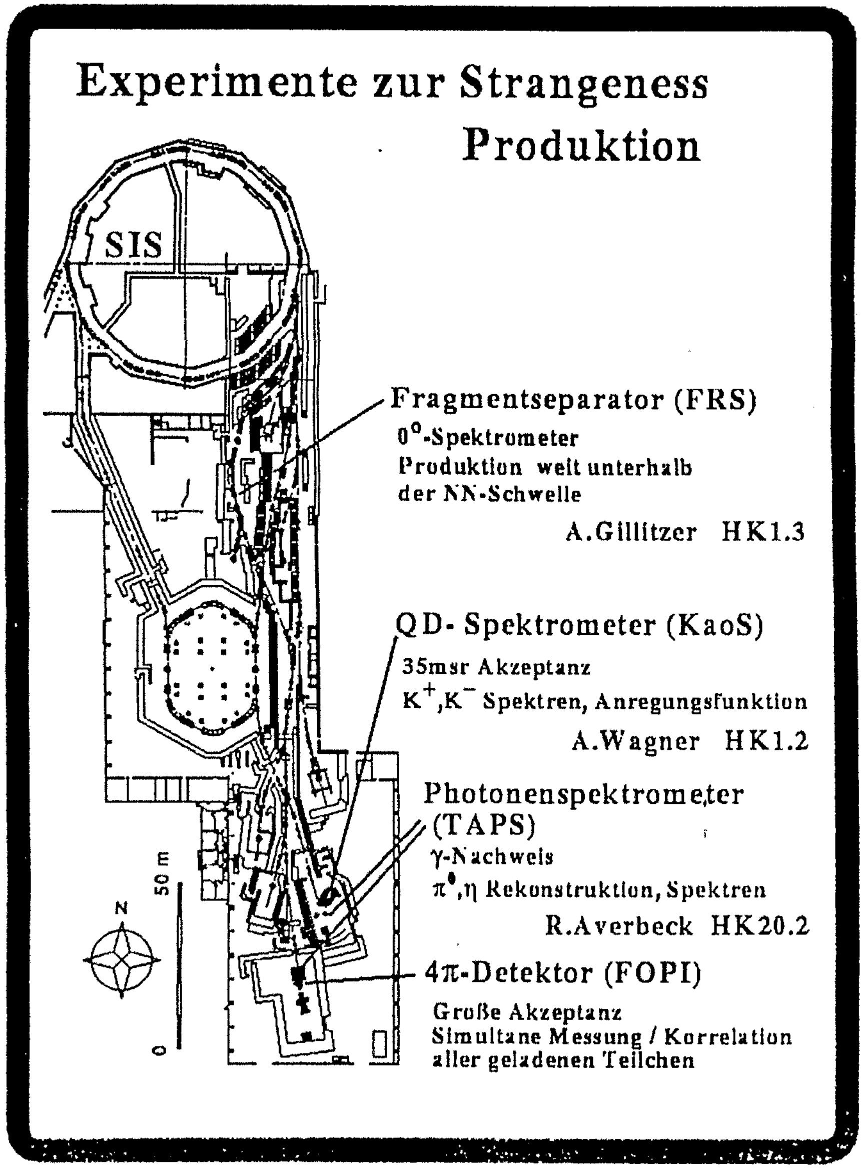

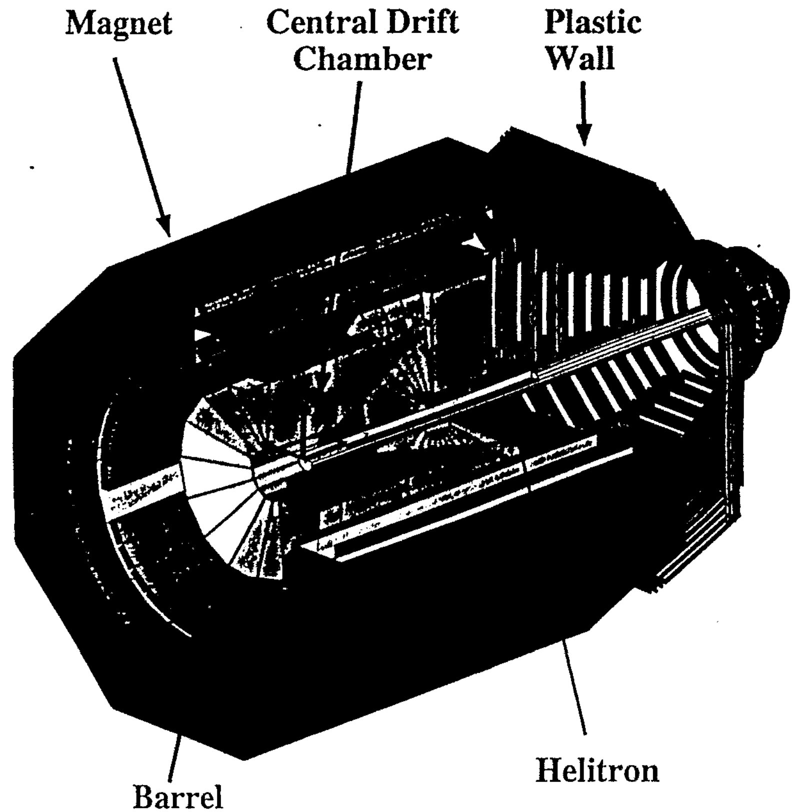

Figure 1: The 4π detector FOPI at GSI. For reference, the 3 arrows at the coordinate system origin are 50 cm long.

Akzeptanz

Häufigkeitsverteilung von Z=1 Teilchen im Geschwindigkeitsraum

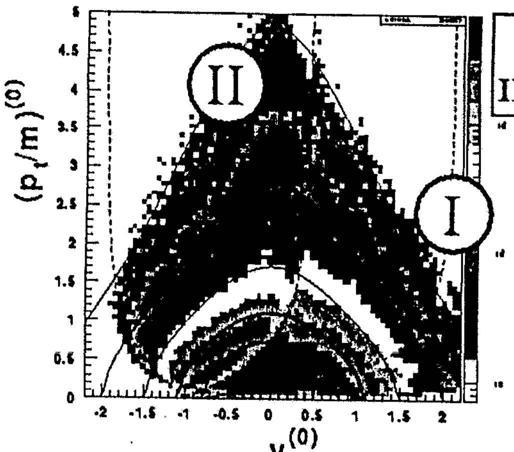

I: ΔE vs. TOF
II: ΔE vs.p vs. TOF

$$y = \tanh^{-1}\beta_{\|}$$
$$p_t/m = \gamma\beta_t$$

$$X^{(0)} := X/X_{projectil} \text{ im CMS}$$

vollständige azimutale Abdeckung!

Bestimmung des Stoßparametervektors (Reaktionsebene):

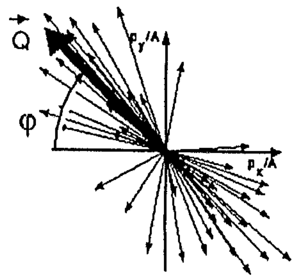

$$\vec{Q} = \sum_i^M \vec{p}_t(i)\,\omega(i)$$
$$\omega(i) = 1 \quad Y_i > Y_{cm}$$
$$\omega(i) = -1 \quad Y_i < Y_{cm}$$

mass determination is restricted only by the finite detector resolution.

After a linearization of the momentum versus velocity data was performed for $Z = \pm 1$ particles with $P_{LAB} \leq 0.6$ GeV/c, the mass spectra shown in Fig. 1 were produced. For the positively charged particles a large peak is located near 0.5 GeV/c^2 which is associated to the K^+ meson. At high momenta this peak vanishes below the background which is due to the finite detector resolution, whereas at lower momenta the background is dominated by mismatched Barrel and CDC data. The mass spectrum of negatively charged particles ($P_{lab} < 0.6$ GeV/c) reveals, in addition to the π^- contribution, an intriguing structure near 0.5 GeV/c^2 albeit with low statistics. Not only are the location and width of this structure in agreement with the expected values for antikaon production, the yield relative to the K^+ is comparable to previous measurements near this energy [4].

The acceptance for kaons in the transverse momentum versus laboratory rapidity plane is shown in Fig. 2. The data analyzed here are within the horizontally hashed region displayed for the Barrel, but with a further restriction imposed that the maximum laboratory momentum be 0.5 GeV/c. For reference, the arrow marks mid-rapidity for a colliding system at 1.93 A·GeV. The kaon yield is concentrated mostly in the range of rapidity between the target and mid-rapidity. At 1.93 A·GeV K^+ mesons can be produced in first chance nucleon-nucleon collisions with a maximum momentum up to the kinematic limit ($P^{k.l.}_{1.93GeV} = 0.32$ GeV/c) which is denoted by the dot-dashed curve. Since almost the full detector acceptance is beyond this limit, even at beam energies slightly above the free nucleon-nucleon threshold FOPI is primarily sensitive to kaons produced by collective production processes.

The reaction channel to produce a K^+ with the lowest threshold (1.6 GeV) includes a hyperon in order to conserve strangeness:

$$N + P \rightarrow N + \Lambda + K^+.$$

Since the Λ is neutral and decays with a lifetime $c \cdot \tau_0 = 7.9$ cm it can not be directly measured by FOPI. However, the products of its main decay channel ($\Lambda \rightarrow p\pi^-$, branching ratio 64%) can be readily detected by the CDC. The Λ is identified by calculating the invariant mass (M_{inv}) of all $p\pi^-$ pairs that intersect to form a secondary vertex away from the main event vertex as shown by the open points in Fig. 3. In this figure a very pronounced peak from the Λ is visible above the mixed event background which is marked by the dashed histogram.

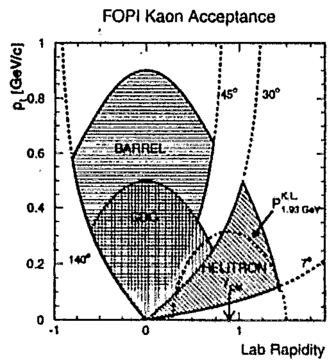

Figure 2. Kaon acceptance of the FOPI detector system. The data evaluated here are from within the horizontally hashed area marked for the Barrel. For reference, mid-rapidity of systems at 1.93 A·GeV is denoted by the arrow.

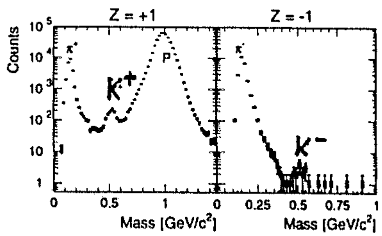

Figure 1. Reconstructed mass using the matched CDC-Barrel data for $P_{lab} < 0.6$ GeV/c for (left) positively charged particles and (right) negatively charged particles.

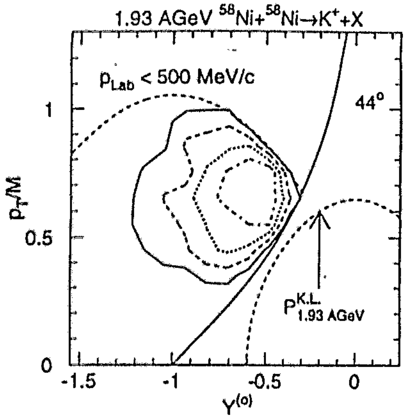

Figure 4. Transverse momentum p_T versus scaled rapidity $Y^{(0)}=Y/Y_{CM}$-1 for K^+ particles measured in Ni+Ni collisions at 1.93 AGeV.

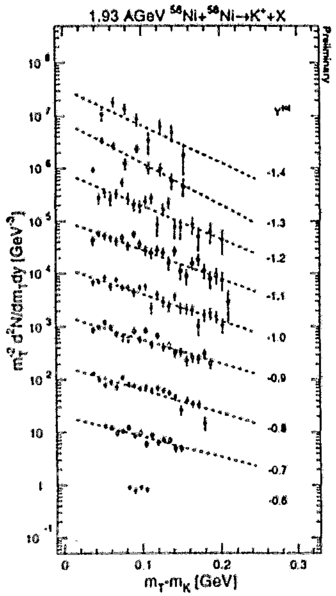

Figure 5. Measured K^+ m_T spectra for various slices in normalized rapidity.

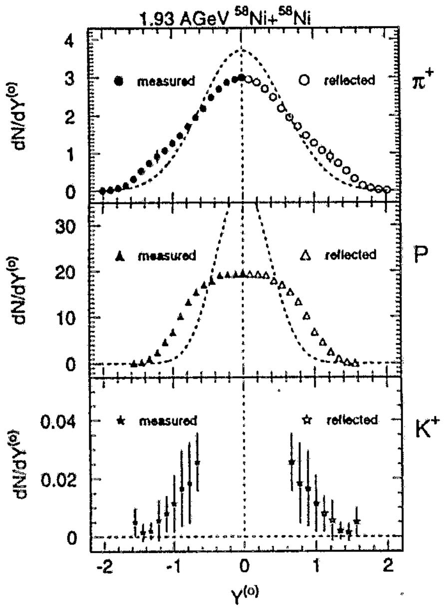

Figure 6. Measured yields of K^+, proton and π^+ as functions of normalized rapidity.

Teilchen Identifizierung

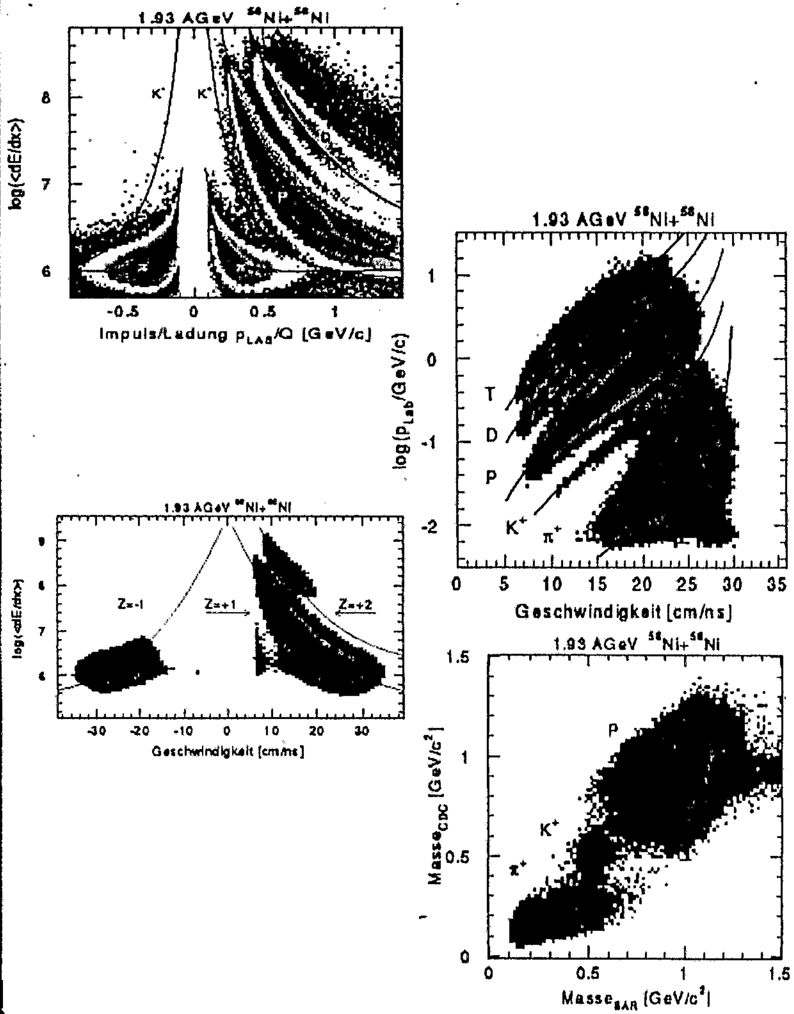

Rekonstruktion seltsamer Teilchen

$$M_{inv} = \sqrt{(\sqrt{p_1^2 + m_1^2} + \sqrt{p_2^2 + m_2^2})^2 - (\vec{p_1} + \vec{p_2})^2}$$

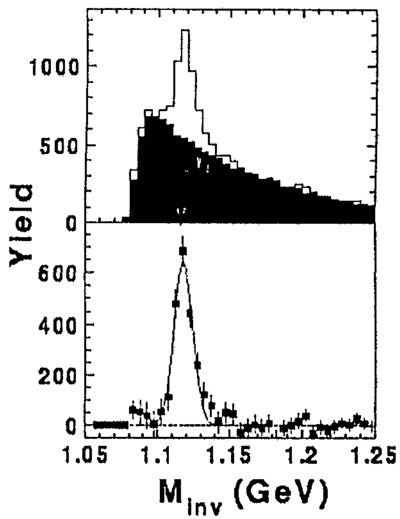

$\Lambda \to \pi^- p$ (64.2%)
m=1116MeV
$c\tau$=7.89cm

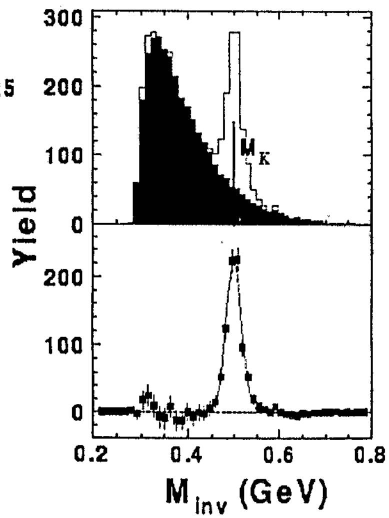

$K^0_S \to \pi^+\pi^-$ (68.6%)
m=498 MeV
$c\tau$=2.68cm

Transverse Mass Spectra (all)

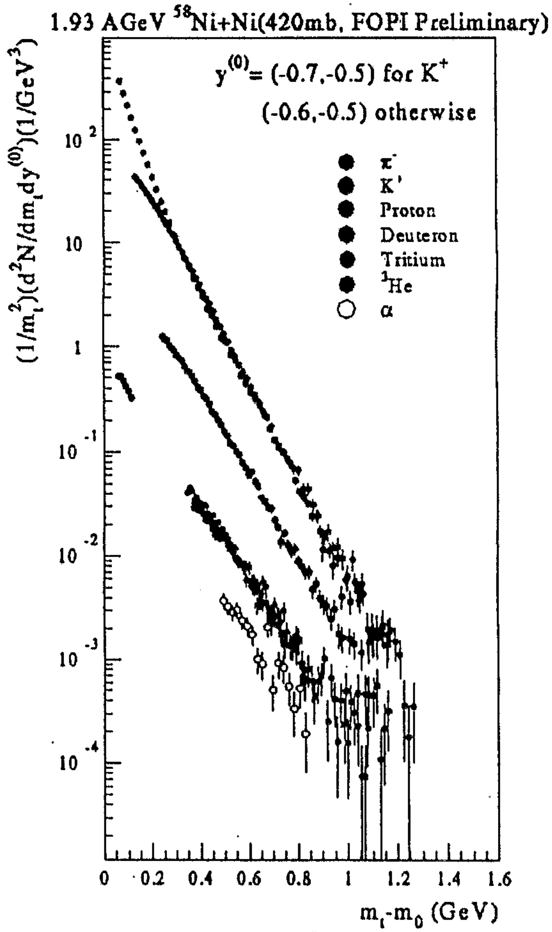

Spektren (π, K^+)

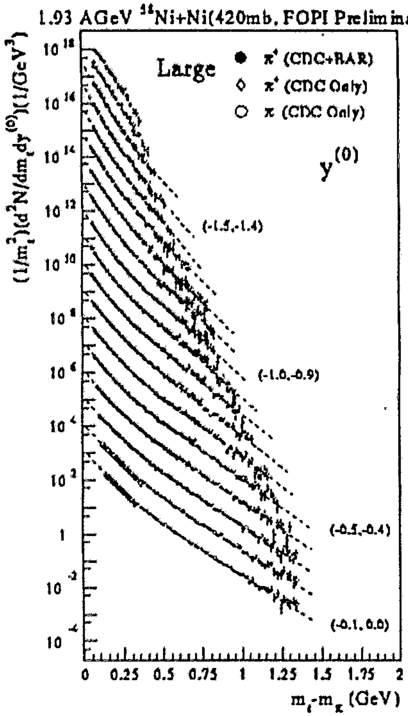

Transversale Masse

$m_T = \sqrt{p_T^2 + m^2}$

Boltzmann Spektrum

$d^3N/dp^3 \propto m_T^{-2} d^2N/dm_T dy$

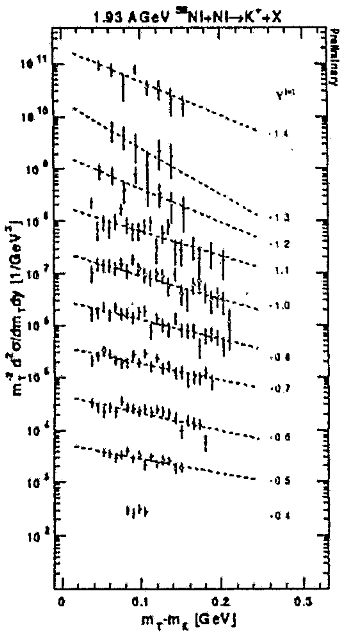

Pionen: zwei Komponenten

$\pi^+ = \pi^-$

Kaons: einfach exponentiell

Relativistische Kinematik

$E = m_t cosh(y)$ — totale Energie

$Ed^3\sigma/dp^3 = \frac{1}{2\pi m_t} d^2\sigma/dm_t dy$ — invarianter W.-Querschnittt

$d^3\sigma/dp^3 \propto e^{-E/T}$ — Boltzmann Verteilung

$= \frac{1}{2\pi cosh(y)} \frac{1}{m_t^2} e^{-m_t cosh(y)/T}$

$\propto \frac{1}{m_t^2} e^{-m_t/T_B}$

$\rightarrow T_B = \frac{T}{cosh(y)}$ — Abfallparameter

keine Zentralitäts-abhängigkeit!

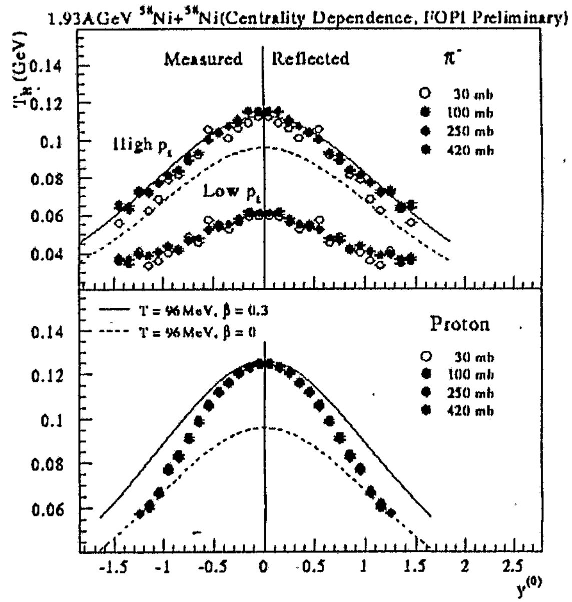

Vergleich der Abfallparameter

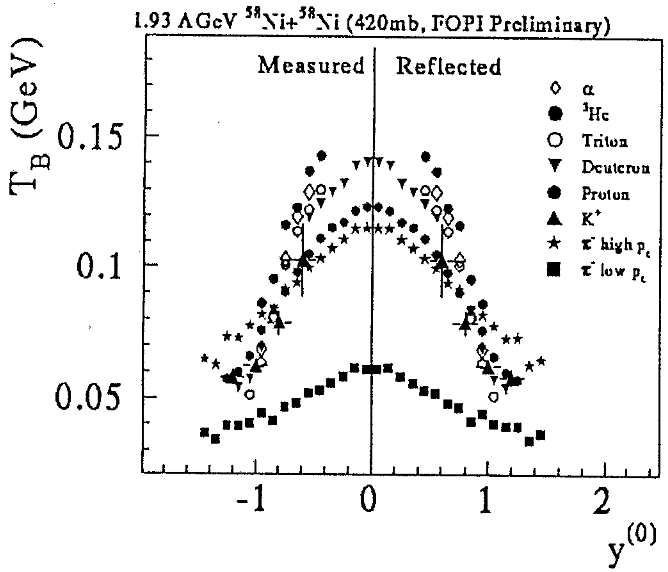

Exponentielle Spektren

Systematische Variation mit der Rapidität

Abfallparameter für Kaonen und Protonen sind ähnlich

Bei $y^{(0)}=0$: Ordnung nach der Ejektilmasse

Rapiditätsdichteverteilungen

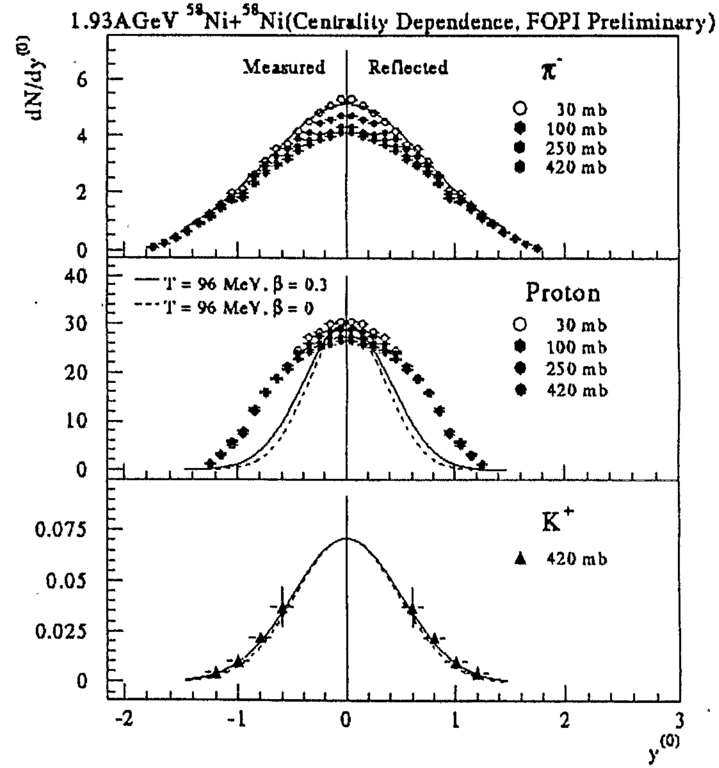

Protonendaten zeigen anisotropes Verhalten (prolat)

Rapiditätsdichteverteilungen der Mesonen sind durch eine isotrope Emissionsverteilung parametrisierbar

Gerichteter K^+ - Fluß

eine Sonde für das Kaon-Potential in Kernmaterie ?

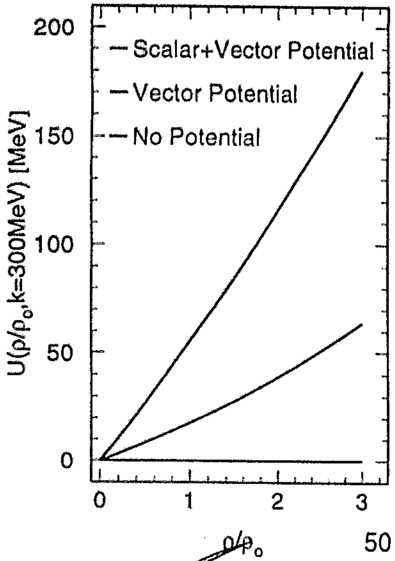

G.Q.Li, C.M.Ko, B.Li,
PRL 74 (1995) 235
NPA 594 (1995) 460

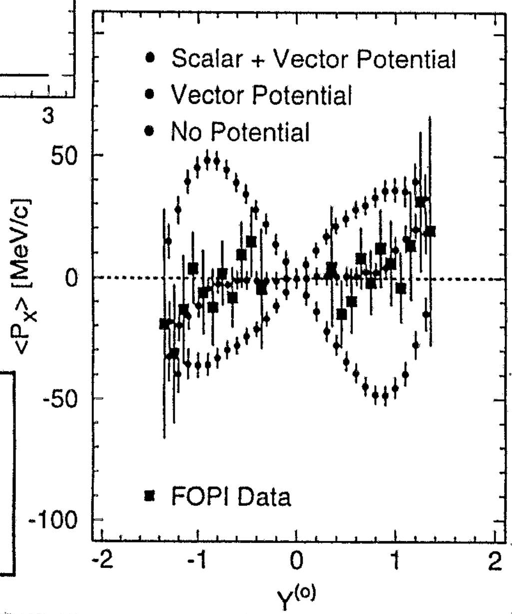

Kaonen bewegen sich in einem Potential

Skalares Potential ist zur Beschreibung der Daten notwendig

meson-production probability (V.Metag)

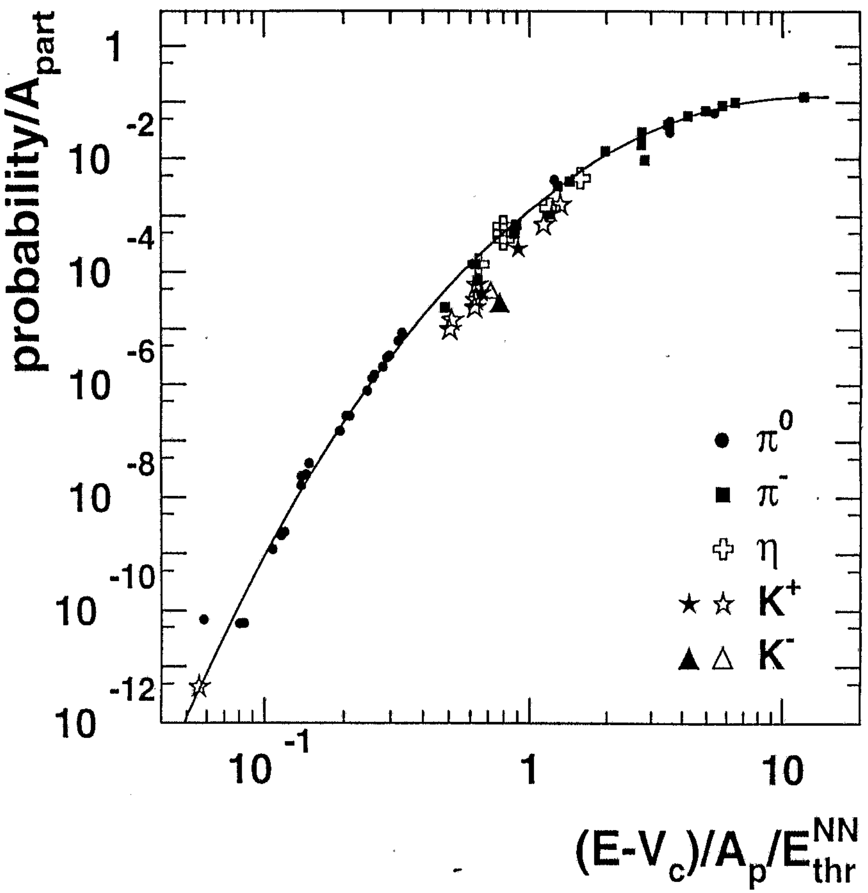

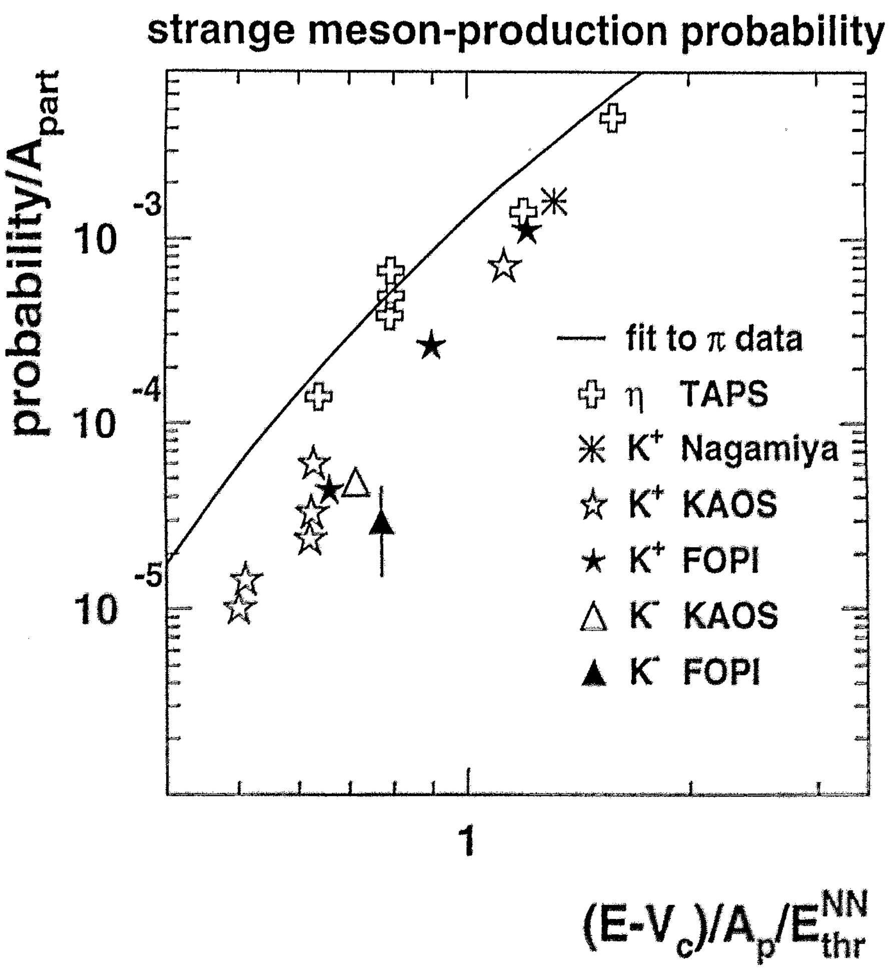

strange meson-production probability
probability/A$_{part}$
10^{-3}
10^{-4}
10^{-5}
1
(E-V$_c$)/A$_p$/E$_{thr}^{NN}$
fit to π data
η TAPS
K$^+$ Nagamiya
K$^+$ KAOS
K$^+$ FOPI
K$^-$ KAOS
K$^-$ FOPI

COSY-Proposals mit Strangeness-"Content"

COSY-Energiebereich: **40 MeV - 2.5 GeV** **(p = 270 MeV/c - 3.3 GeV/c)**

Proposal Nr.	Thema
1	Spectroscopy of Light Hyper-Nuclei with BIG KARL (Ernst, Bonn)
2	Λ-Production at Rest by Means of the $^4He(p,{}^4HeK^+)\Lambda$ Reaction at 1 GeV (Ernst, Bonn)
6	A Precision Study of Near Threshold Two Meson Production via the Reaction $p+d \rightarrow {}^3He+\pi^++\pi^-$ and $p+d \rightarrow {}^3He+K^++K^-$ (Jahn, Bonn)
11	Threshold Meson Production at the Internal COSY-Beam in the Range of Scalar Mesons involving Strangeness (Oelert, Jülich)
12	Study of η and η' Production and Interaction (Roderburg, Jülich)
13	Production of Very Heavy Λ-Hypernuclei at Energies Below the Nucleon-Nucleon Threshold (Schult, Jülich)
15	Associated Strangeness Production in pp-Reactions (Eyrich, Erlangen)
18	Study of the Subthreshold K^+ Production with a 0°-Facility at TP2 in COSY (Sistemich, Jülich)
21	Study of subthreshold K^--production (Müller, Rossendorf)
32	Measurement of the lifetime of the Hypertriton $^3_\Lambda H$ (Nann, Indiana Univ.)

COSY-Proposal 6:

A Precision Study of Near Threshold Two Meson Production Via the Reaktion $p+d \rightarrow {}^3He+\pi^++\pi^-$ and $p+d \rightarrow {}^3He+K^++K^-$

Detektor: BIG KARL, MOMO

Physikalische Motivation:

- $p+d \rightarrow {}^3He+\pi^++\pi^-$ (E_p=432-510MeV)
- $p+d \rightarrow {}^3He+K^++K^-$ (E_p=1.73 - 1.83 GeV)
- precision data on low energy (T<50MeV) meson-meson interaction (Phase behaviour, resonances in meson-meson-scattering)
- ABC-effect, $K\bar{K}$ molecules?
- radiative Φ(1020) decay? → strange quark content of f_0 (975)
- glueball in the 1 GeV missing mass region? (determination of the $K^+K^-/\pi^+\pi^-$ ratio)

Experimentaufbau:

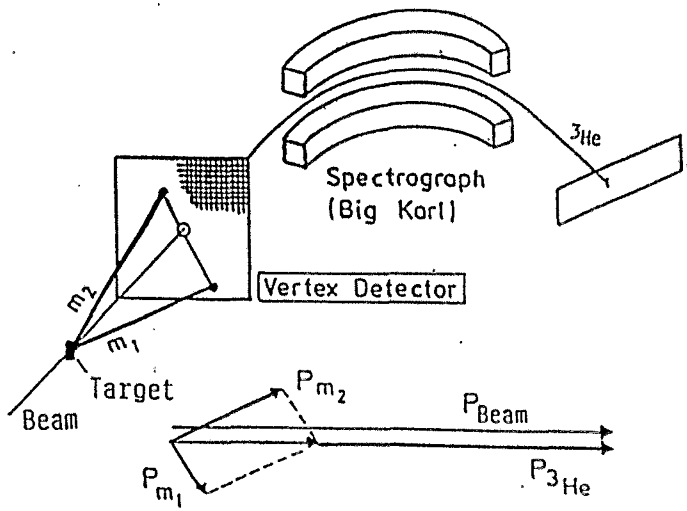

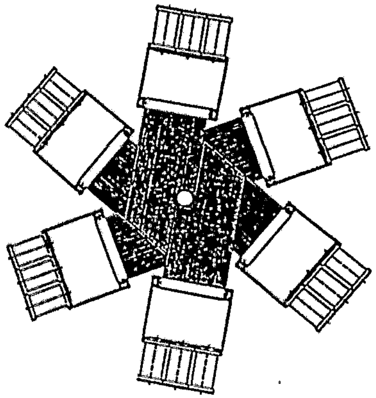

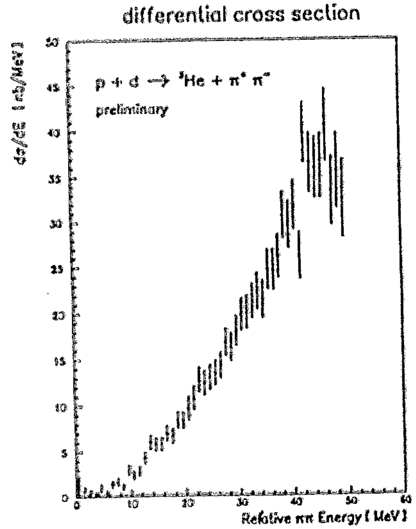

Fig. 4: Relative energy spectrum of two - pion events from the reaction pd → ^{3}He $\pi^+\pi^-$ at 1150 MeV/c incident proton beam momentum

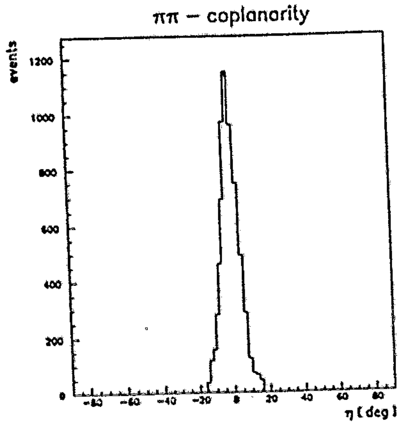

Fig. 3: Coplanarity of the $\pi^+\pi^-$ - events

COSY-Proposal 12:

Study of η and η' Production and Interaction

Detektor: **TOF**

Physikalische Motivation:

- measurement of cross section of $pp \to pp\eta$
- measurement of cross section of $pp \to pp\eta'$
- $pd \to ppK\Lambda$, $3pKK$, $^3He\eta$, $^3He\eta'$
  → constraints on the quark and gluonic content of η and η'
-

$$\eta = \eta_8 \cdot \cos\theta_p - \eta_1 \cdot \sin\theta_p$$
$$\eta' = \eta_8 \cdot \sin\theta_p + \eta_1 \cdot \cos\theta_p$$

$$\eta + \eta' = 2 \cdot K \qquad (1506 \leftrightarrow 995)\ (MeV/c^2)$$
$$\phi + \omega = 2 \cdot K^* \qquad (1801 \leftrightarrow 1784)\ (MeV/c^2)$$

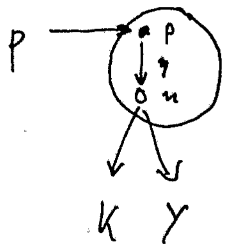

1.) $pp \to pp\eta(')$

2.) $\eta(') + n \to KY$
$kk̄N$

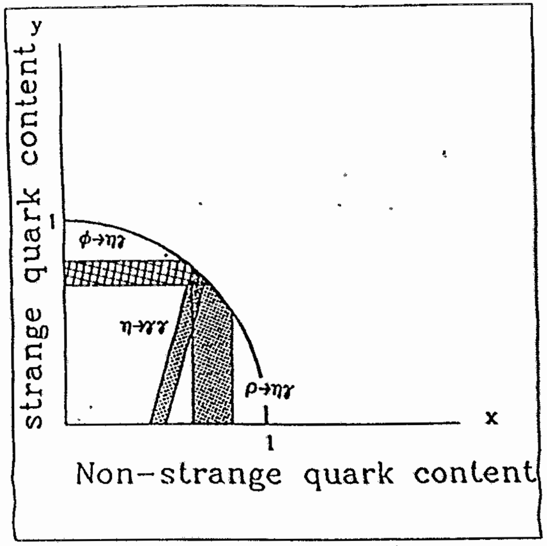

Fig. 1 η quark content [4]. x and y are defined in the formula:
$|\eta\rangle = x \cdot 1/\sqrt{2}\ |u\bar{u}+d\bar{d}\rangle + y \cdot |s\bar{s}\rangle$

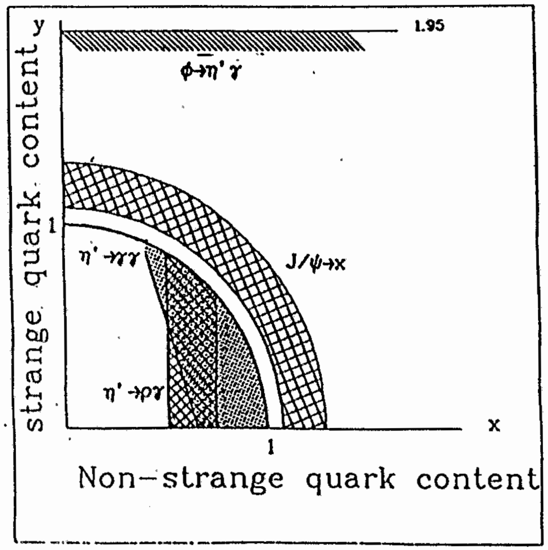

Fig. 2 η' quark content [4]. (Updated for Φ->η'γ [5] and for J/Ψ -> vector + pseudoscalar meson [6])

Reaction	pp->ppη	pp->ppη'	pd->3pKK̄	pd->ppKΛ	pd->3He η	pd->3He η'
Threshold (GeV/c)	1.986	3.208	2.521	1.850	1.573	2.434
Momentum of scattered protons (3He) (GeV/c) at threshold	0.77	1.06	0.62	0.50	1.32	1.18
at threshold +50 MeV/c	.61-.98	.94-1.23	.42-.86	.31-.72	1.19-1.52	1.63-2.18
at threshold +100 MeV/c	.55-1.08	.81-1.40	.35-.97	.24-.83	1.15-1.62	1.56-2.18
Maximum lab.-angle of scattered protons (3He) at threshold + 50 MeV/c	10.5	7.6	16.7	21.0	6.3	5.7
at threshold + 100 MeV/c	14.7	10.2	23.7	30.0	8.9	8.0

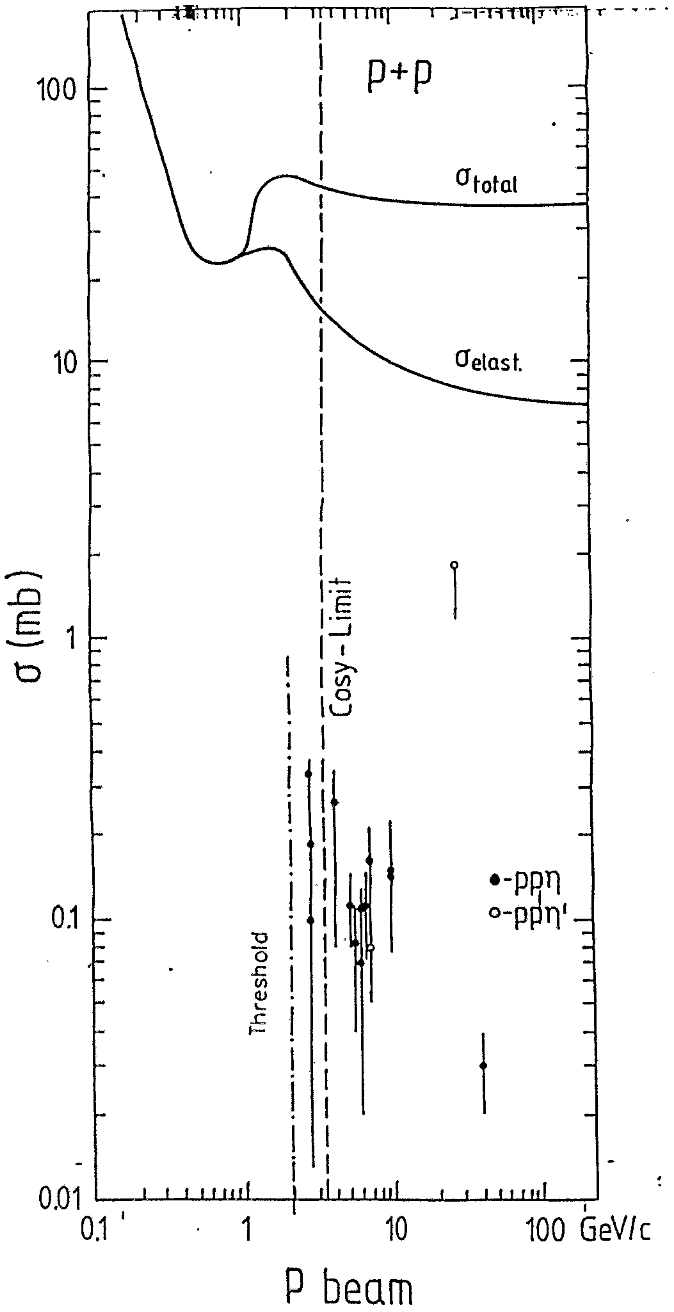

Fig. 6 Cross-section pp-> ppη in comparison to the total cross-section :

Mögliche Prozesse zur Strangeness-Untersuchung an COSY-TOF

Reaktion	Schwellenenergie $\sqrt{s}$ in GeV	Impuls GeV/c	kinetische Energie GeV
$pp \rightarrow K^+\Lambda p$	2.548	2.339	1.582
$K^+\Sigma^+ n$	2.622	2.560	1.789
$K^+\Sigma^0 p$	2.624	2.566	1.793
$K^0\Sigma^+ p$	2.625	2.569	1.796
$pd \rightarrow K^+\Lambda d$	3.485	1.839	1.127
$p^4He \rightarrow K^+\Lambda\, ^4He$	5.338	1.581	0.900
$p^{12}C \rightarrow K^+\Lambda\, ^{12}C$	12.787	1.400	0.747
$pp \rightarrow K_s K_s pp$	2.875	3.327	2.518

Tabelle 2.1: Schwellenimpulse für die protoninduzierten Reaktionskanäle der assoziierten Strangeness-Produktion am Proton und an leichten Kernen im Impulsbereich von COSY

$pp \rightarrow \Sigma^+ K_s p$

$pp \rightarrow K^+ K^- pp$

$pp \rightarrow K_s K_s pp$

Decomposition of phase-space Nucleus-Nucleus

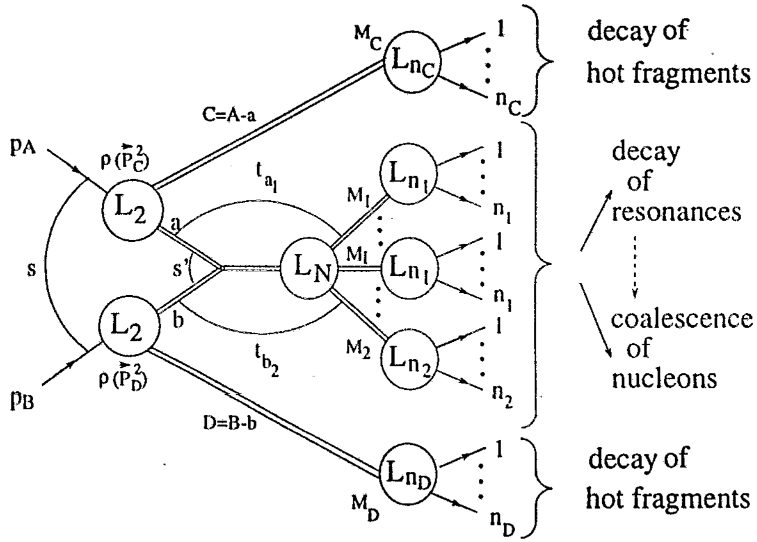

Nucleus-Nucleus

- Differential cross section

$$d\sigma_{AB}(s;\vec{\alpha}) = \sum_a \sum_{z_a} \sum_b \sum_{z_b} \sigma_{az_abz_b} \frac{dW_{az_abz_b}(s;\vec{\alpha}_N)}{\sum_{\vec{\alpha}} \int dW_{az_abz_b}(s;\vec{\alpha}_N)}$$

$\sigma_{az_abz_b}$: Glauber

- Probability of populating channel

$$\vec{\alpha}_N = (\alpha_1, \ldots, \alpha_N, \alpha_C, \alpha_D)$$

$$dW(s;\vec{\alpha}_N) \propto d\mathcal{Z}_C(\alpha_C) d\mathcal{Z}_D(\alpha_D) \left\{ \prod_{i=1}^{N} d\mathcal{Z}_I(\alpha_I) \right\} d\mathcal{Z}_N(s')$$

- Number of final states in α_J $(J = C, D)$

$$d\mathcal{Z}_J(\alpha_J) = dM_J^2 \frac{d^3P_J}{E_J} \rho(\vec{P}_J^2) \left(\frac{V_J}{(2\pi)^3} \right)^{n_J - 1} \left\{ \prod_{i=1}^{n_J} (2\sigma_i + 1) 2m_i dm_i F_i(m_i) \right\} \left(\frac{M_J}{\Theta_J} \right) K_1 \left(\frac{M_J}{\Theta_J} \right) dL_{n_J}(M_J;\alpha_J)$$

ρ: Internal momentum distribution

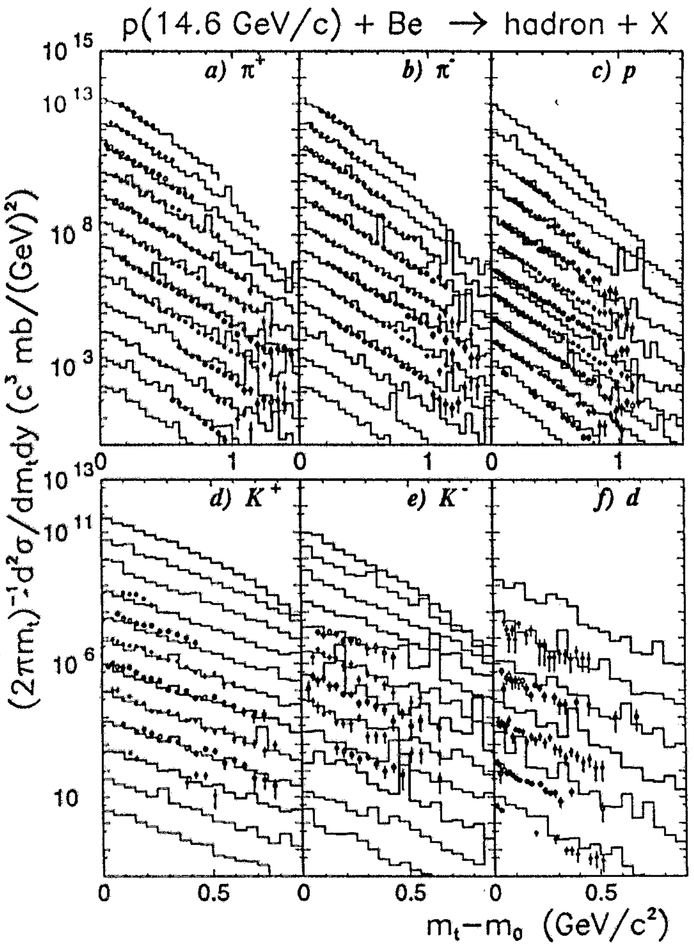

Invariant cross sections in the rapidity interval $0.4 < y < 2.8$ as a function of $m_t - m_0$ with $m_t^2 = m_0^2 + p_t^2$. Spectra are multiplied by powers of 10. Data (points) from E802 collaboration [T. Abott et al., Phys. Rev. D **45** (1992) 3096] are compared with ROC calculations (histograms)

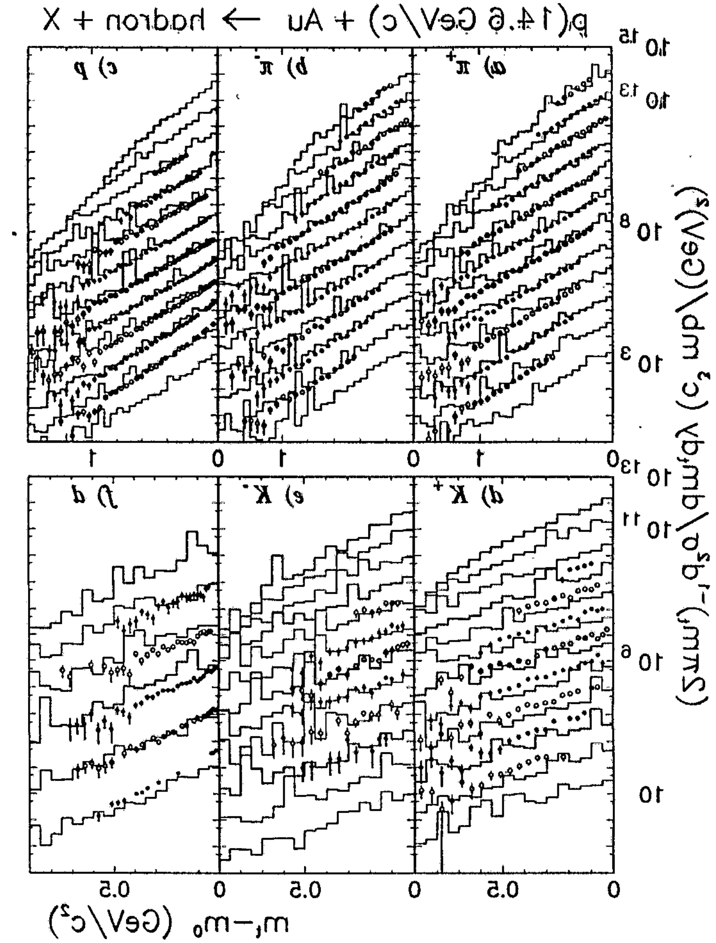

Invariant cross sections in the rapidity interval $0.4 < y < 2.8$ as a function of $m_t - m_0$ with $m_t^2 = m_0^2 + p_t^2$. Spectra are multiplied by powers of 10. Data (points) from E802 collaboration [T. Abott et al., Phys. Rev. D **45** (1992) 3096] are compared with ROC calculations (histograms)

Rapidity distributions

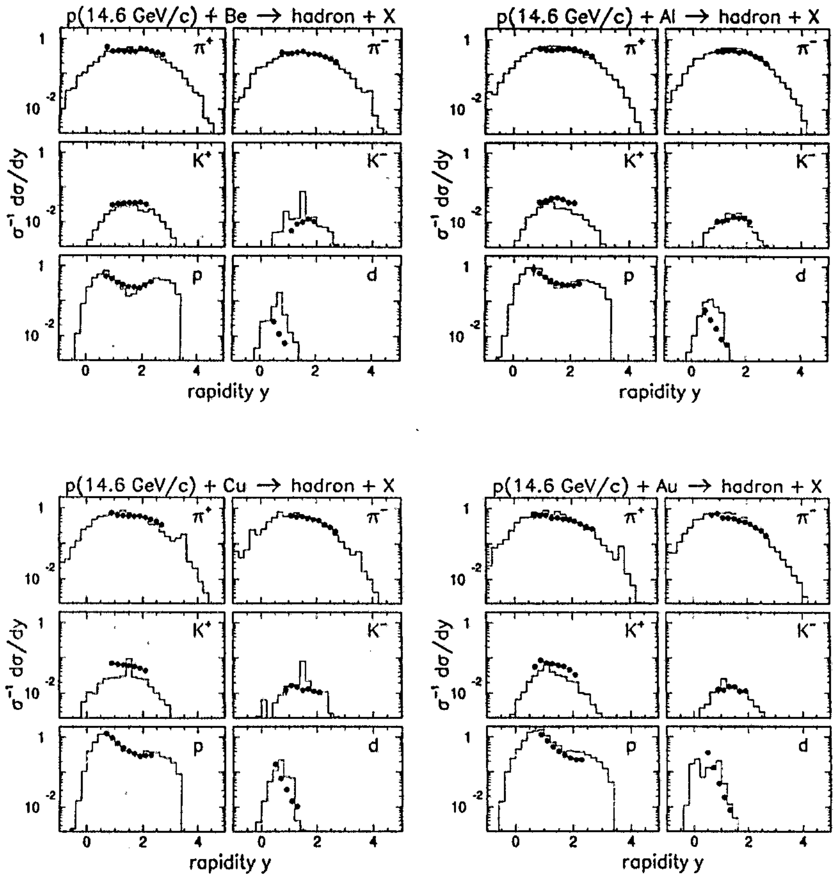

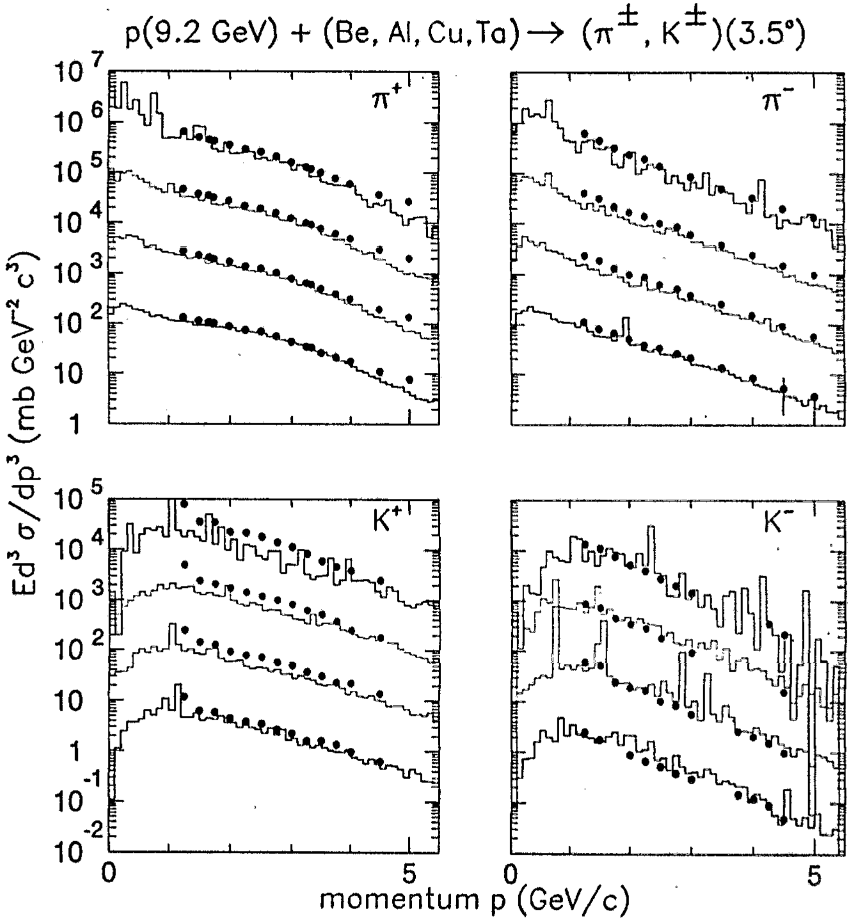

Data (blue points) from E802 collaboration [T. Abott et al., Phys. Rev. Lett. **66** (1991) 1567, Phys. Rev. D **45** (1992) 3096] are compared with ROC calculations (red histograms).

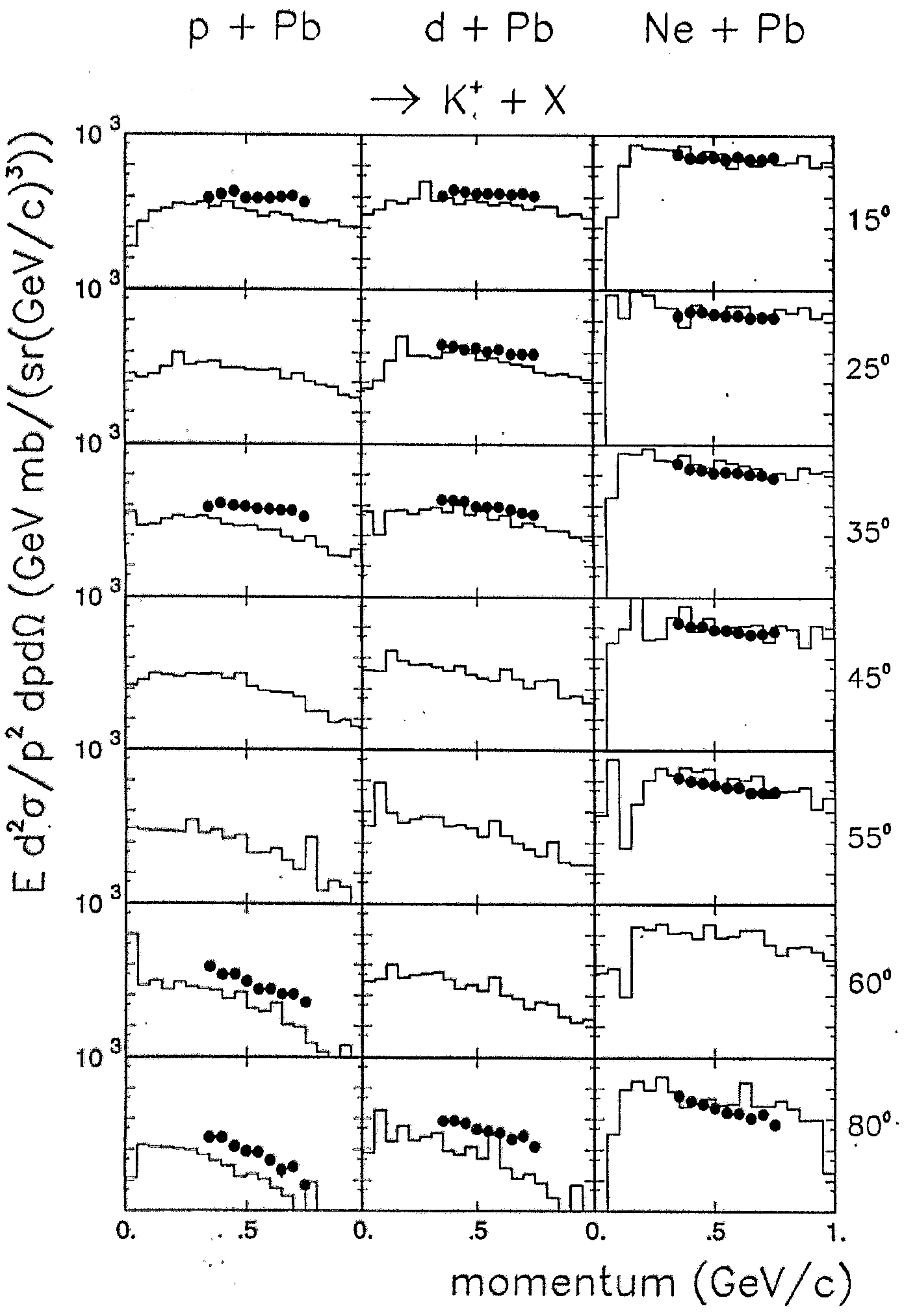
p + Pb
d + Pb
Ne + Pb
→ K+ + X
E d²σ/p² dpdΩ (GeV mb/(sr(GeV/c)³))
15°
25°
35°
45°
55°
60°
80°
momentum (GeV/c)

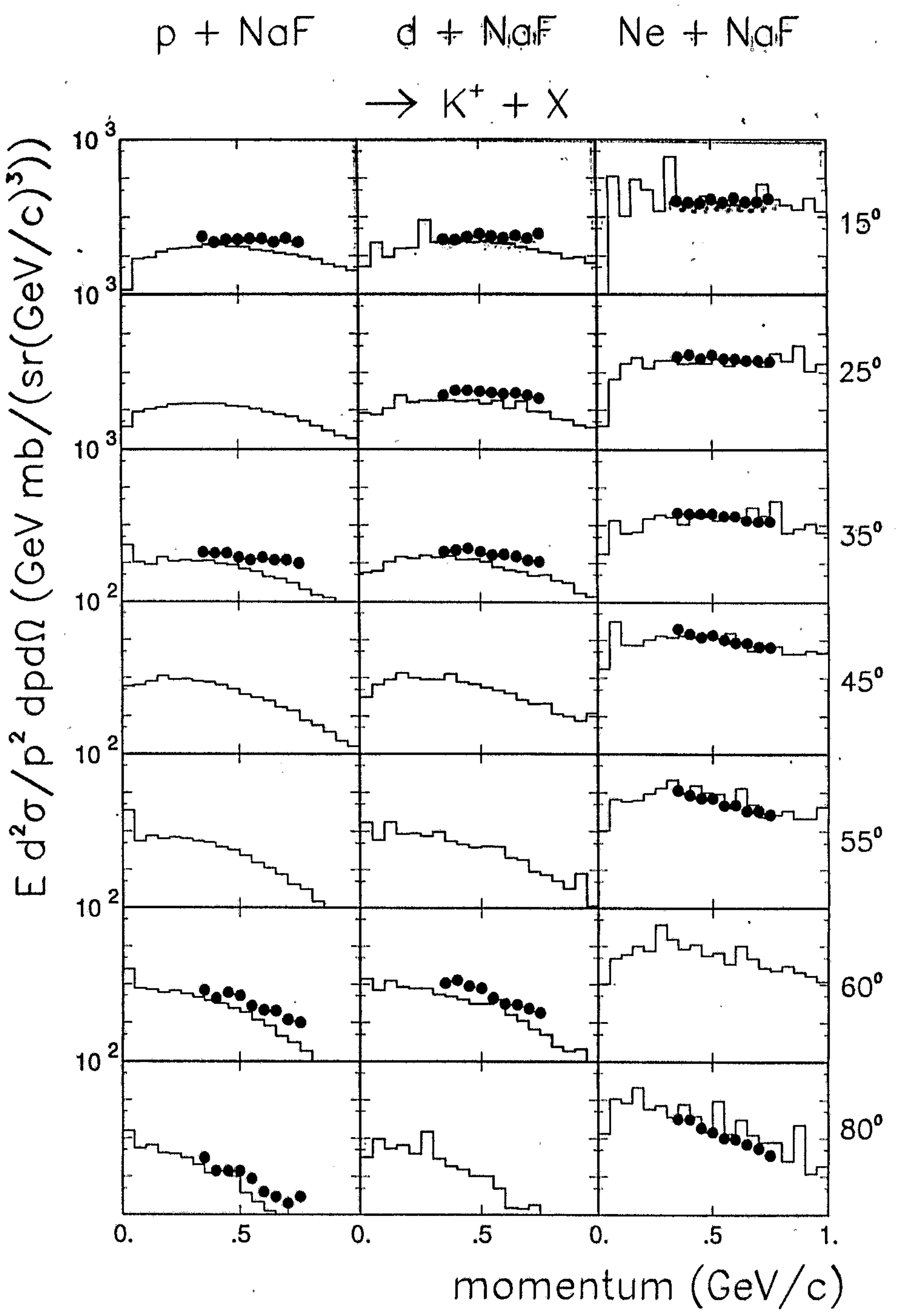
p + NaF
d + NaF
Ne + NaF
→ K+ + X
E d²σ/p² dpdΩ (GeV mb/(sr(GeV/c)³))
15°
25°
35°
45°
55°
60°
80°
momentum (GeV/c)

$p + {}^{12}C \rightarrow h(40^o) + X$

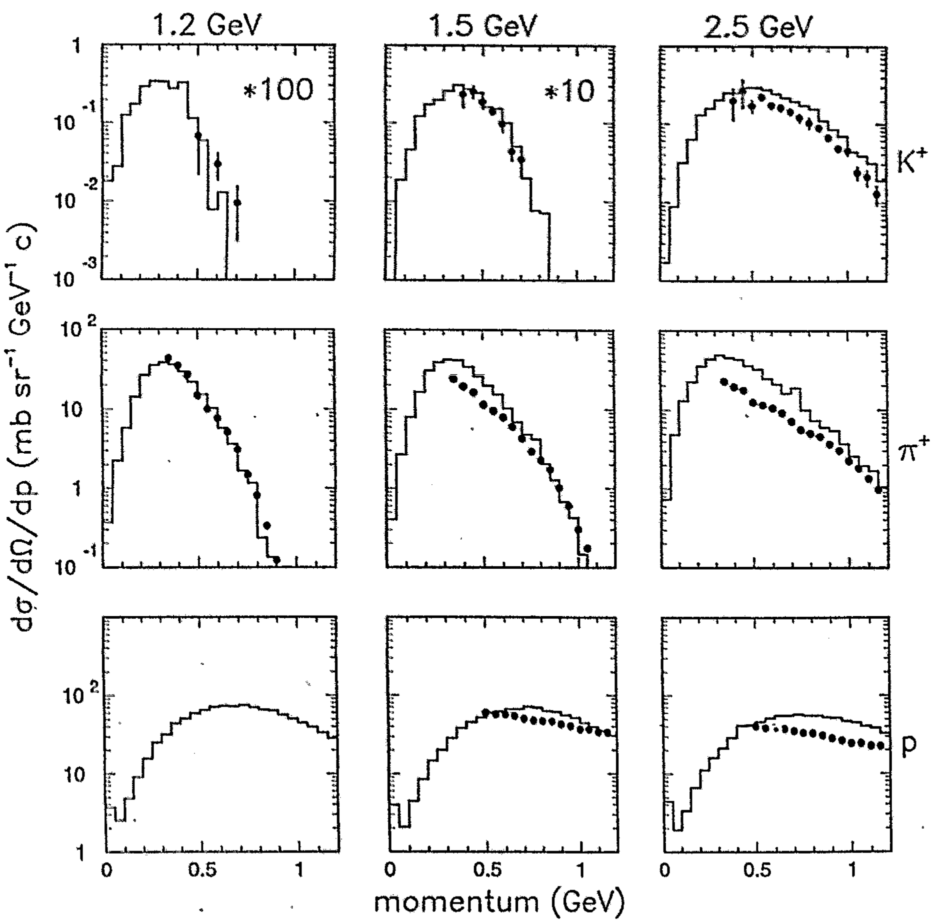

Study of subthreshold K^- production

1 Introduction

2 Model calculations

2.1 Total cross sections and inclusive spectra

2.2 Correlations

2.2.1 Background

2.2.2 Momentum spectra

2.2.3 Invariant-mass spectra

2.2.4 Missing-mass spectra

2.2.5 Ratio of kaon- to pion-pair production

3 Experimental set-up

3.1 General layout

3.2 Momentum and angular acceptance

3.3 Particle identification

3.4 Resolution

3.5 Counting rates

4 Proposed measurements

Near- and sub-threshold strangeness production

$ep \to e' \Lambda K^+$ CEBAF	$ep \to e' p\, \phi$ CEBAF
$pp \to K^+ Y N$ COSY-15	$pp \to K^+ K^- pp$ COSY-11
$pA \to K^+ X$ COSY-18	$pA \to K^+ K^- X$ COSY-21 (hopefully)
$AA \to K^+ X$ SIS	$AA \to K^+ K^- X$ SIS

Data

subthreshold K^- production

- available

C + C
Si + Si
Ca + Ca

1.0 ... 2.1 GeV per nucleon

Ne + NaF
Ne + Cu
Ne + Sn
Ne + Bi
Ni + Ni

1.6 ... 2.0 GeV per nucleon

- not available

data from hadron-nucleus

K^- production

1. **direct**

$$N+N \to N+N+u\bar{u}+s\bar{s} \to N+N+K^+ +K^-$$

2. via mesonic **resonances**

$$N+N \to N+N+q\bar{q} \to N+N+meson \to N+N+K^+ +K^-$$

- well established:

$\phi(1020)$ $\Gamma = 4.2$ MeV

- structure under discussion:

$a_0(980)$ $\Gamma = 50 \ldots 300$ MeV

$f_0(980)$ $\Gamma = 40 \ldots 400$ MeV

3. via baryonic $\Lambda(1520)$ **resonance** $\Gamma = 15.6$ MeV

$$p+N \to p+N+s\bar{s} \to N+\Lambda(1520)+K^+ \to N+p+K^- +K^+$$

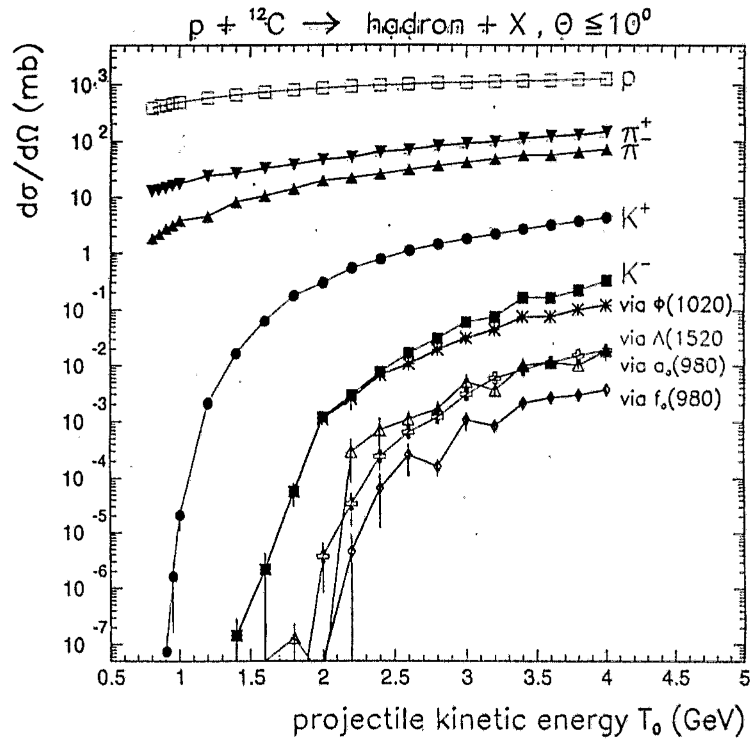

Energy dependence of differential cross sections calculated with the ROC model. In case of K^- production the contributions from intermediate resonances are indicated

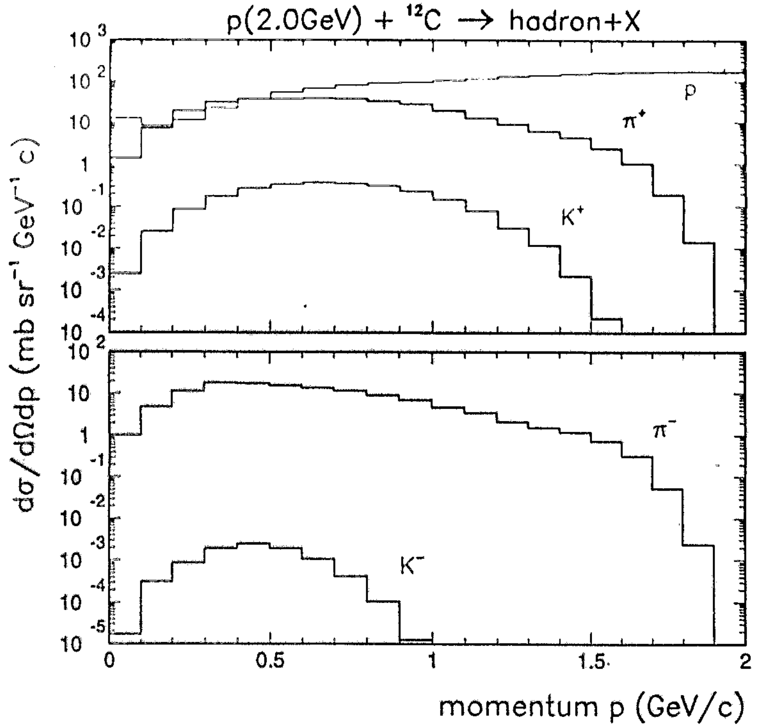

Calculated momentum spectra of positively and negatively charged particles produced in p^{12}C interactions at angles $\Theta \leq 10°$

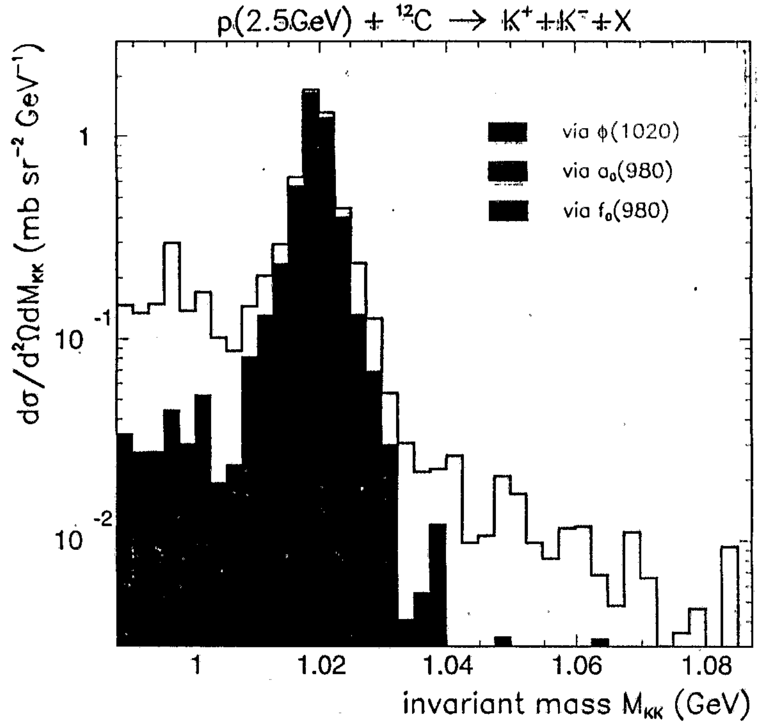

Calculated K^+K^- invariant-mass spectrum for emission angles $\theta \leq 10°$

- strength of $\phi(1020)$ production
- propagation of $\phi(1020)$, K^+ and K^- through nuclear matter

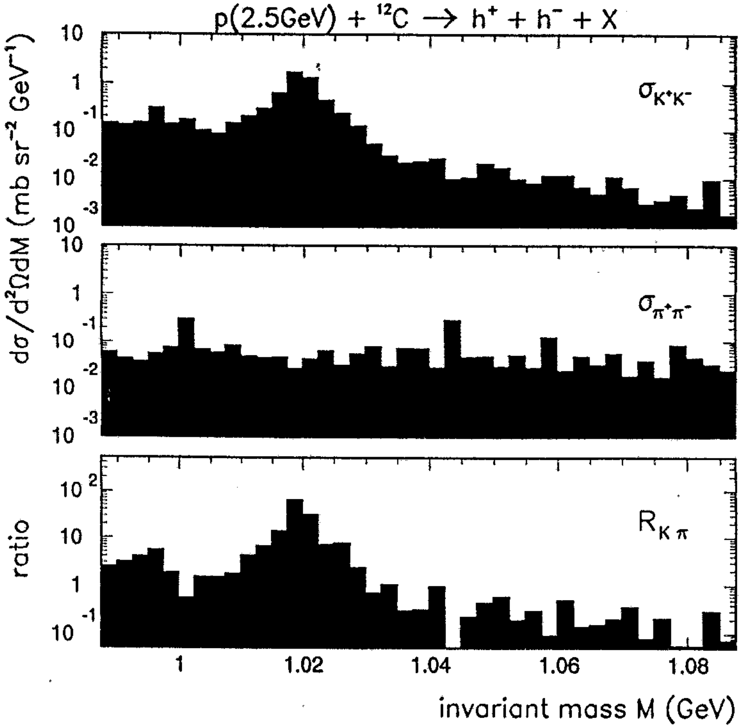

Calculated invariant mass spectra of kaon ($\sigma_{K^+K^-}$) and pion pairs ($\sigma_{\pi^+\pi^-}$) and the ratio $R_{K\pi} = \sigma_{K^+K^-}/\sigma_{\pi^+\pi^-}$ for p^{12}C interactions at 2.5 GeV

- enhanced strangeness production due to locally heated nuclear matter?
- admixture of $s\bar{s}$ component to the wave function of nucleons???

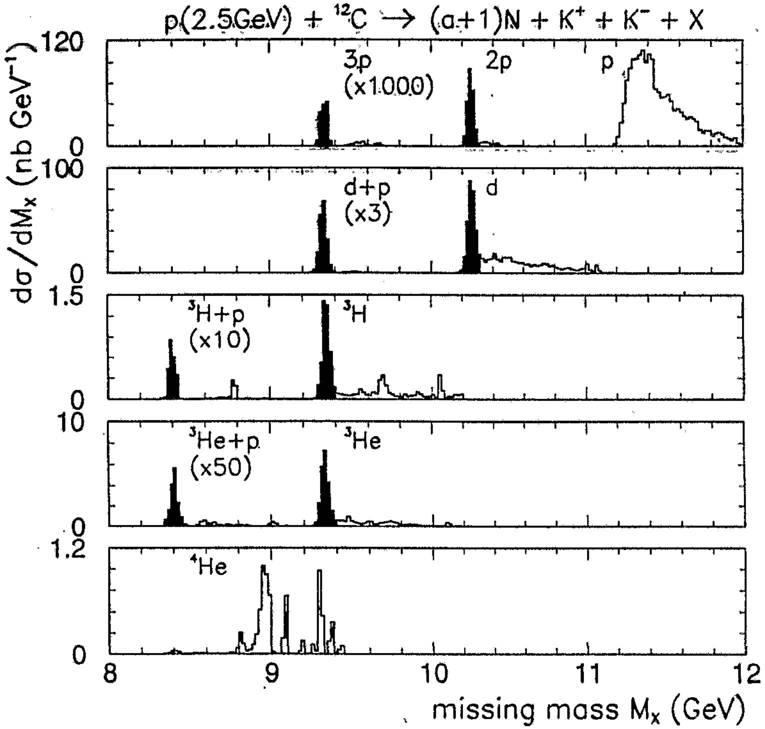

Calculated missing mass spectra from p^{12}C interactions at 2.5 GeV for the production of K^+/K^- pairs accompanied by $(a+1)$ nucleons with a being the number of participants according to

$$p + [aN] \to (a+1)N + K^+ + K^-$$
$$(a = 1 \ldots A)$$

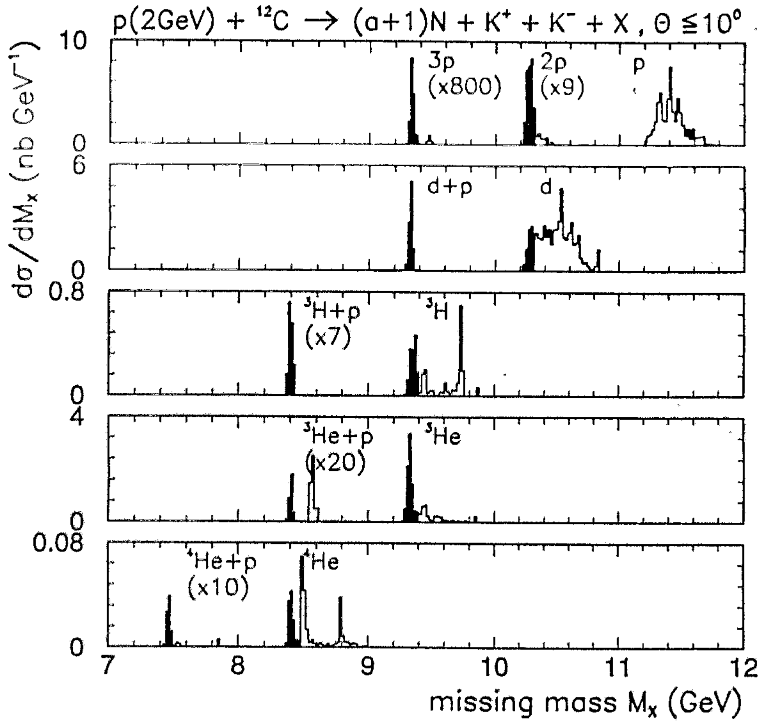

Calculated missing mass spectra from p^{12}C interactions at 2.0 GeV for the production of K^+/K^- pairs accompanied by $(a+1)$ nucleons with a being the number of participants according to

$$p + [aN] \rightarrow (a+1)N + K^+ + K^- \quad (a = 1 \ldots A)$$

Counting rates

Decay-in-flight and detection efficiencies of 40% for K^+, 80% for K^- and 90% for all other particles have been taken into account. Counting rates smaller than 1 h^{-1} have been omitted (except for K^+K^- at 1.5 GeV)

Energy/GeV	2.5	2.0	1.5
Luminosity/cm^{-2}s^{-1}	$4 \cdot 10^{32}$	$3 \cdot 10^{32}$	$2 \cdot 10^{32}$
Detected particles	counts/h		
K^+K^-	2300	140	0.05
$\pi^+\pi^-(M_{\pi\pi} \geq 0.98\text{GeV})$	3000	300	5
$K^+K^-\ 2p$	50	—	—
$K^+K^-\ d$	200	20	—
$K^+K^-\ dp$	20	2	—
$K^+K^-\ {}^3He$	5	3	—
$K^+K^-\ {}^3H$	2	1	—

Proposed measurements

Energy and target mass number
dependence of

1. invariant-mass spectra $\boxed{K^+K^-}$

   → strength of $\phi(1020)$ production

   → propagation of $\phi(1020)$, K^+ and K^- through matter

2. ratio of $\boxed{K^+/K^- \text{ to } \pi^+/\pi^-}$ pair production

   → production of strange and non-strange particles at the same transferred four-momentum

3. missing-mass spectra

$$\boxed{\begin{array}{c} K^+K^-\,d \\ K^+K^-\,{}^3H \\ K^+K^-\,{}^3He \\ K^+K^-\,2\,p \\ K^+K^-\,p\,d \\ \vdots \end{array}}$$

   → determination of number of participants

   → key for the understanding of the reaction mechanism

C. Schneider K^+ experiments at ANKE

Besonderheit der K^+-Missing Mass-Messung

$$p + [aN] \rightarrow aN + K^+ + \Lambda$$
$$\hookrightarrow \pi^- + p$$
$$\hookrightarrow \pi^o + n$$

$$M_{Sp}^2 = p_{Sp}^2 = (p_{init} - p_{K^+} - p_{p_\Lambda} - p_{\pi^-_\Lambda} - \sum_{i=1}^{a'} p_i)^2$$

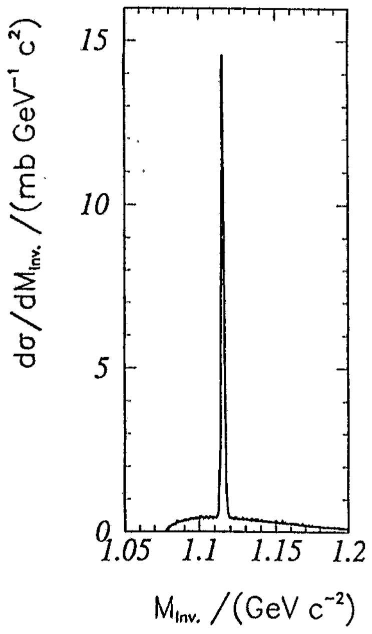

4π-Geometrie

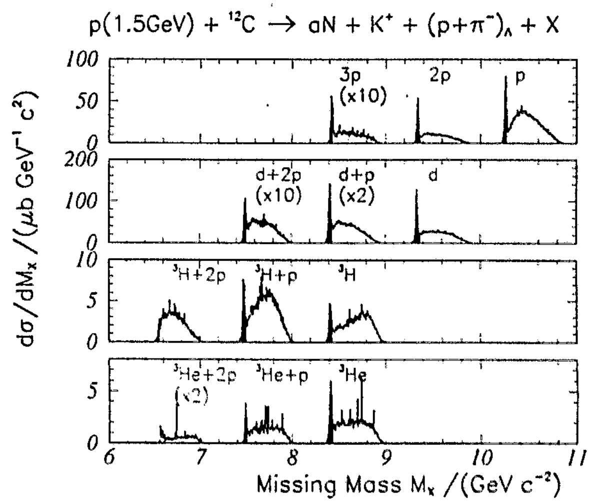

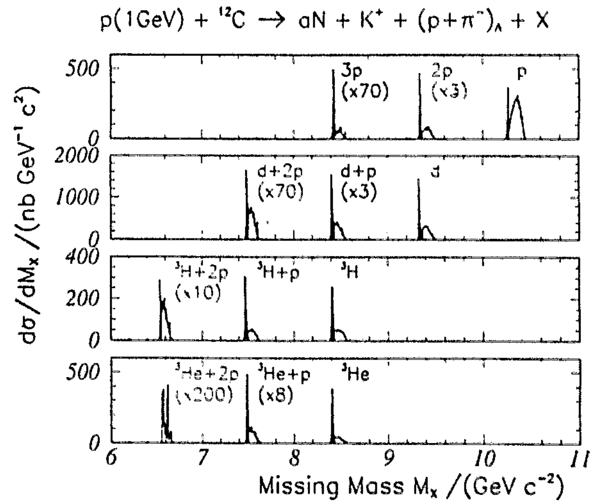

Impulsauflösung an ANKE

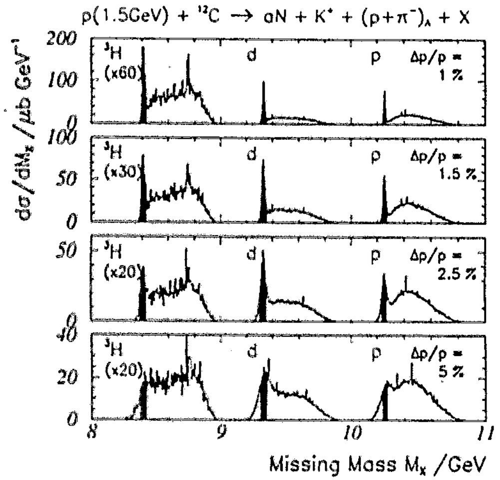

Auflösung mit 4π-Pionen-Detektor

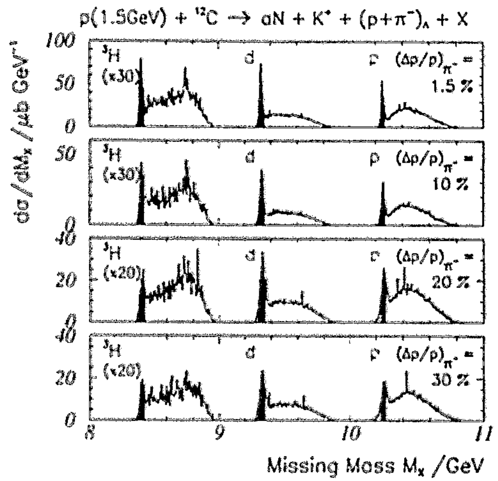

Winkel-Impuls-Korrelationen

Projektilenergie 1,5 GeV

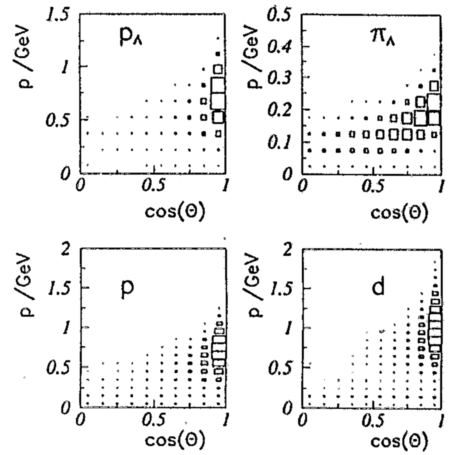

Projektilenergie 1,0 GeV

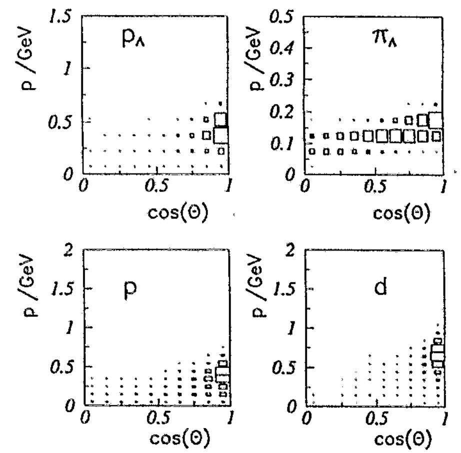

Raten am ANKE-Spektrometer

Energie T_N /GeV	1,5	1,0
Luminosität/$cm^{-2}s^{-1}$	$3 \cdot 10^{32}$	$3 \cdot 10^{32}$
Gemessene Teilchen	Teilchen/h	
$K^+\pi^-\ p\ p$	930	0,0015
$K^+\pi^-\ p\ p\ p$	–	–
$K^+\pi^-\ p\ d$	60	0,3
$K^+\pi^-\ p\ {}^3H$	–	–

Raten mit 4π-Pionen-Detektor

Energie T_N / GeV	1,5	1,0
Luminosität/$cm^{-2}s^{-1}$	$3 \cdot 10^{32}$	$3 \cdot 10^{32}$
Gemessene Teilchen	Teilchen/h	
$K^+\pi^-\ p\ p$	23000	3
$K^+\pi^-\ p\ p\ p$	36	–
$K^+\pi^-\ p\ d$	2040	39
$K^+\pi^-\ p\ {}^3H$	18	2

H.W. Barz   Calculations of $K^{\pm}$ spectra

CASIMIR (1980-85)

64. Jwe + HW

Dubna : INC
Cugnon : π, N

$E/A = 2 \cdots 4$ GeV

Teilchen: $N^{+} \Delta^{\cdots} \quad \langle N^* \rangle_{T=1/2}$
$\pi^{\pm 0} (\rho = 2\pi)$
$\Lambda, \Sigma^{\pm 0}, K^{\pm}, \bar{K}^0$

Reaktionen:

$\rightarrow \pi + \Delta \equiv \rho + N$

$N + N \rightleftarrows \Delta, N^* \cdots \rightarrow 0 \cdots 3\pi$
$(N,\Delta,N^*) + (N,\Delta,N^*) \rightarrow N + N + K + \bar{K}$
$\pi + (\Lambda, \Sigma) \rightleftarrows N + \bar{K}$
$(N\Delta N^*) + (N\Delta N^*) \rightarrow N + K + (\Lambda\Sigma)$

Querschnitte: Fit; $\Delta N^* \rightleftarrows$
(Randrup + Ko)
Isospininvarianz, Isotropie

kein Potential

Mehrstufenprozesse

$\sigma \sim A^{4/3} \cdot A^{1/3 \cdot n}$
$\sigma_\pi \sim A^{5/3}$ (Volumen)
$\sigma_{K^+} \sim A^{6/3}$
$\sigma_{K^-} \sim \begin{cases} A^{7/3} \\ A^{6/3} \end{cases}$

$\pi + \Lambda$
$N + N \rightarrow K^-$

Beispiele:

1) C + Ta $\quad E/A - 3.36$ GeV

2) Si + Si, $\quad E/A - 2.1$ GeV

$\rightarrow K^-$, zu wenig Isotropie

a) $\pi + \Lambda \rightarrow K^- N$ $\quad$ 75%
b) $N + N \rightarrow N + N + K^+ + K^-$ $\quad$ 25%

Vergleich: PL (1994)

Li & Fang & Ko: $\quad \pi + \Lambda \rightarrow K^- N$ (25%) neglected

$N + N \rightarrow K^- K^+ N N$
in medium

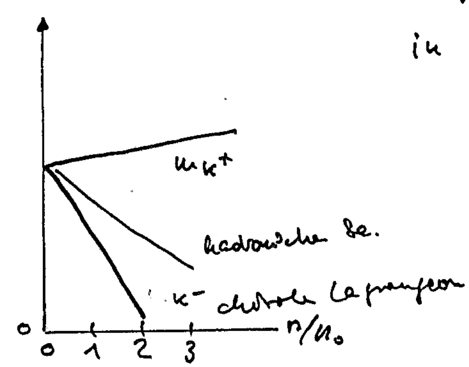

$\sigma_{chir.} = 3 \times \sigma_0$

TABLE 1

Comparison between calculated and measured partial cross section and mean multiplicities

Type	Cascade calculation σ_i[mb]	Cascade calculation $\langle n_i \rangle$	Experiment [a]) σ_i[mb]	Experiment [a]) $\langle n_i \rangle$
incl.	3 200		3445 ± 140	
π^-	15 000	4.8	11 800	3.4 ± 0.2
π^0	14 400	4.6	12 800	3.7 ± 0.3
π^+	11 800	3.8		
K^0_s	94	0.028	86 ± 21 [b])	0.025 ± 0.006
K^+	150	0.046		
Λ	141	0.043		
Σ	186	0.057		
$\Lambda+\Sigma^0$	216	0.066	217 ± 35 [b])	0.063 ± 0.01
K^-	8.4	0.0026		

[a]) Ref. [4]). [b]) Ref. [5]).

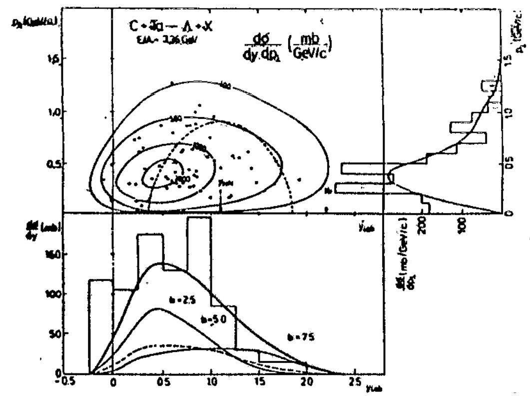

Fig. 12. Contour plots in the rapidity plane of the calculated differential cross section $d\sigma/dy\,dp_\perp$ for Λ-production. The full circles represent the 65 Λ-particles detected in the reaction C+Ta at E_{lab}/A = 3.36 GeV [ref. [3]]. The dashed line shows the kinematical limit of the reaction NN → NΛK. The arrows indicate the position of the NN system and projectile on the y-axis, respectively. The histograms are experimental results. The different curves in the rapidity spectra (labelled by the impact parameters b) show how the effect of slowing down the Λ-particles increases with decreasing impact parameter.

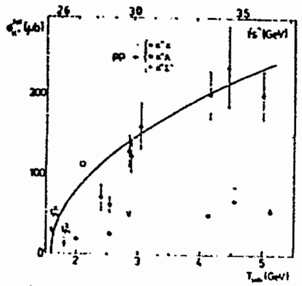

Fig. 3. Inclusive and partial cross sections for K^+ production in pp collisions. The full line indicates the fit used in CASIMIR

where $R_{\Sigma\Lambda}$ is their relative weight depending on energy. The only absolute weights of the different channels known at present stem from the experiment [33]) mentioned above: $\sigma_{K^+\Lambda p}:\sigma_{K^+\Sigma^+ n}:\sigma_{K^+\Sigma^0 p} = 51:47:13$. In addition, at two other energies the relative weights are known from best fits in the phase-space model to experimental data [34]). This information is summarized in our fit

$$R_{\Sigma\Lambda} = 4.35(T - 1.87)\exp(-4(T - 2.1)) + 1\,. \tag{2.16}$$

... can be obtained by isospin reflection while for

$$\sigma^{K^+} = 125\ \mu b \left(\frac{T}{GeV} - 1.585\right)^{0.51}$$

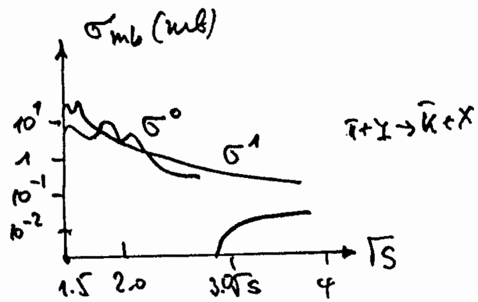

B. Kämpfer   Current studies of strange particle production

Let's Make Strangeness

II. Heavy-Ion Collisions

Present Theoretical Activities in Rossendorf

1. $\sqrt{s} = 200$ - 5500 AGeV: RHIC - LHC B.K./Pavlenko (1996)

uds democracy → charm becomes interesting

2. $E_{lab} = 158$ AGeV: SPS B.K. (1996)

kaons + Lambdas flow as anything else (protons, pions)

3. $E_{lab} = 1$ - 2 AGeV: SIS Kolomeitsev/Voskresensky/B.K. (1996)

explorative study of in-medium effects

Hard QCD Processes at RHIC - LHC

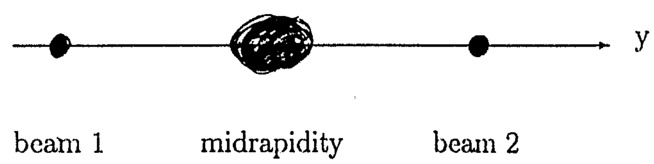

large-angle scattering → large t → perturbative QCD processes

u,d,s are treated on equal footing → no exceptional rôle of strangeness

(unless soft processes become important)

dominant production by gluons:

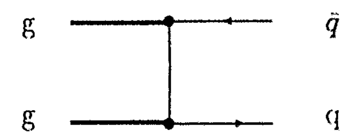

destructive interferences → no liberation of u,d,s towards midrapidity

charm becomes interesting: c = lightest of heavy quarks

attacked problems:

- primordial vs. thermal c production
- open charm decay: c $\bar{c}$ → D, $\bar{D}$

  D, $\bar{D} \to \mu^{\pm}$ + anything → uncorrelated lepton pairs

  → huge combinatorical background for dileptons

  → give up the hope for a thermal signal?

nuclear
gluon
shadowing
→ depletion

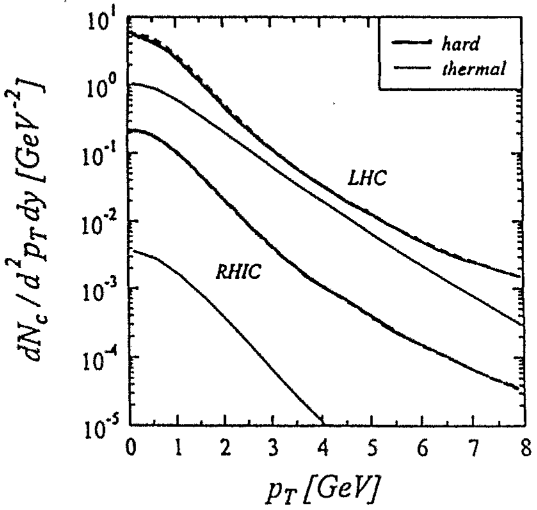

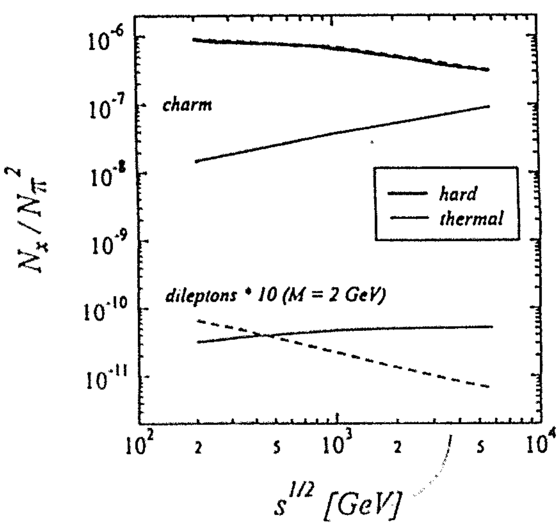

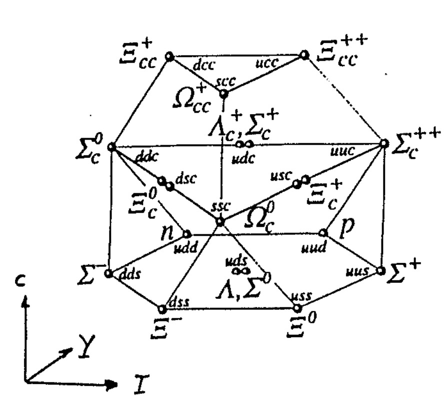

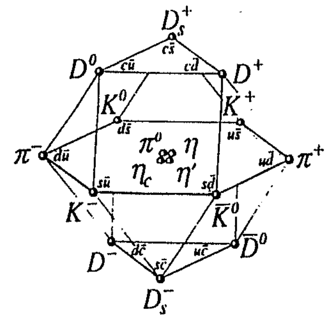

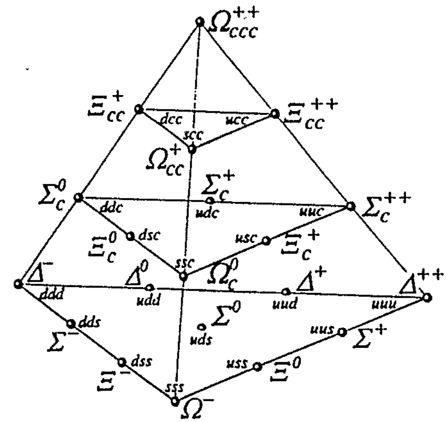

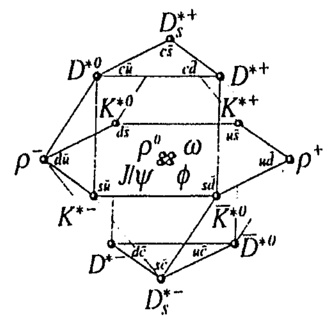

Kaons flow as anything else in Pb + Pb at 158 AGeV

thermal model: $T, \mu \rightarrow$ local momentum distribution

hydro model: $u_\mu \rightarrow$ flow

+ long. boost invariant flow (axisymmetry)
+ linear transverse flow profile
+ Cooper-Frye formalism with unique freeze-out time

$$\frac{dN^i}{m_\perp\, dm_\perp\, dy} = \mathcal{N}_i \int_0^1 d\xi\, \xi\, m_\perp I_0\left(\frac{p_\perp \mathrm{sh}(\rho)}{T}\right) K_1\left(\frac{m_\perp \mathrm{ch}(\rho)}{T}\right),$$

$$\rho = \mathrm{arcth}(v_\perp(\xi)), \quad v_\perp(\xi) = \frac{3}{2} v_\perp^{aver}\, \xi,$$

$$\mathcal{N}_i = g_i R_{f.o.}^2 \tau_{f.o.} \lambda_i \exp\{\frac{\mu_i}{T}\}/\pi(\hbar c)^3$$

NA 49 normalized

NA 44 unnormalized, wider $p_\perp$ ranges

$T = 120$ MeV

$\langle v_\perp \rangle = 0.43\ c$

NA 49 preliminary data

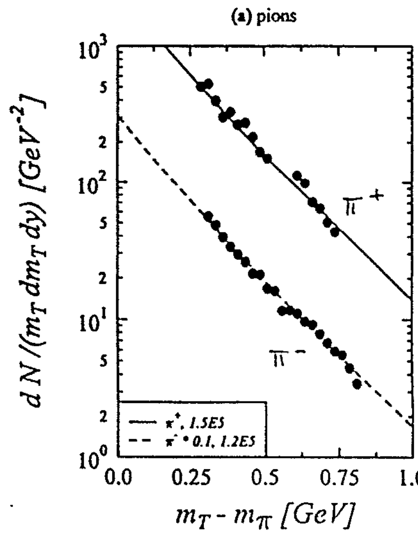

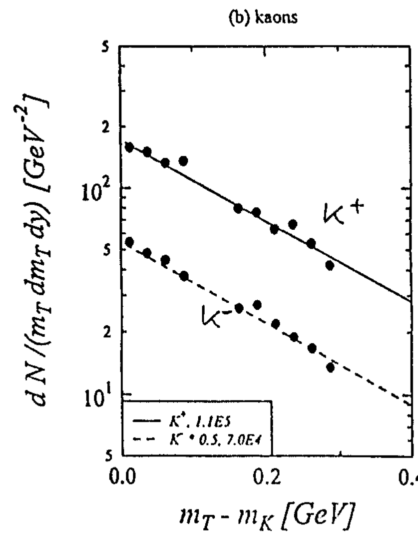

(c) K^0_s

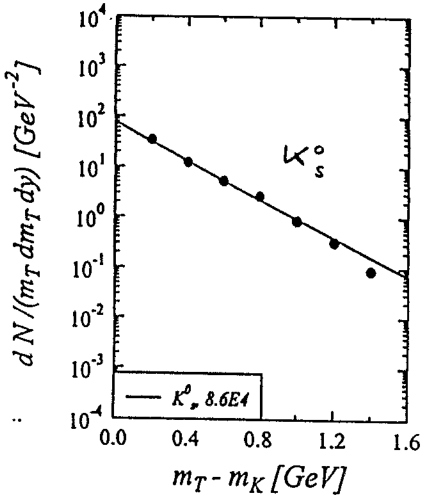

(d) protons

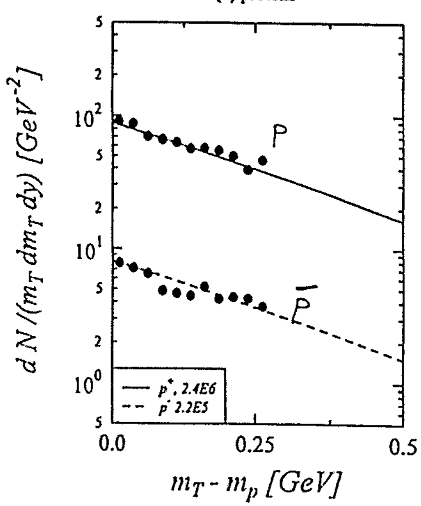

(e) Lambdas

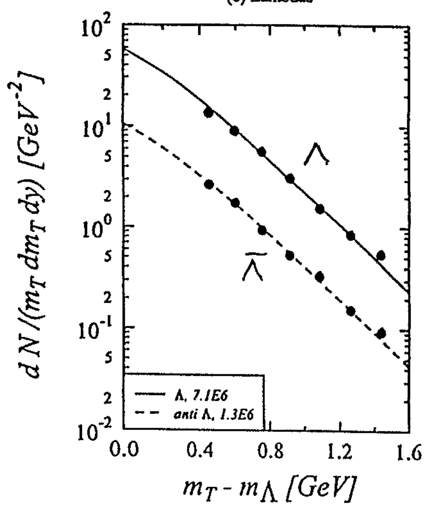

K^- Spectra in HICs at BEVALAC/SIS Energies

studies of in-medium effects:

Brown/Ko/Wu/Xia (1991) $M^*(T,\rho) \rightarrow \sigma(T,\rho)$

Li/Ko (1996) $\omega_\pi(k;T,\rho) \rightarrow \sigma(T,\rho)$

→ Kolomeitsev/Voskresensky/B.K. (1995) K^- quasiparticle excitations

↑ Weise et al (1994/96)

↑

extended studies by Brown/Rho ... Muto ... Yabu ... Kobodera since 1992

↓

K condensation

└ new: 2^{nd} branch with $K^- = \Lambda\ p^{-1}$

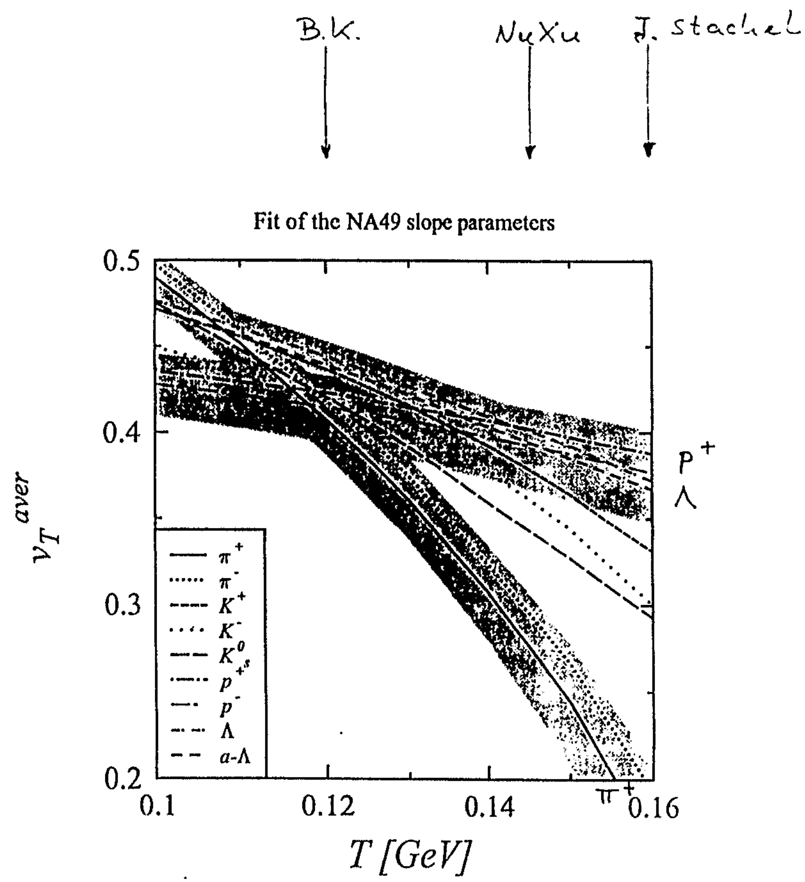

explorative study of K^- freeze-out:

1. fireball model:

   (a) thermal + chemical equilibration

   (b) simplified dynamics

   (c) allows complicated dispersion relation

   $\rightarrow T(t), \rho(t)$

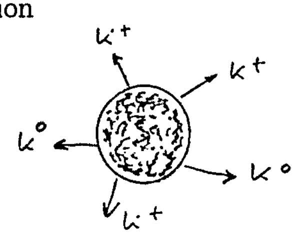

2. leakage of K^+: $\lambda_{K^+} \gg \lambda_{K^-}$

   $\rightarrow$ strangeness destillation

3. adjust μ_{K^+} from $S = 0$ and $N_{K^+}^{exp}$

   $\rightarrow$ s sits mainly in Λ, Σ

   $\rightarrow \sigma_{K^+}$ is needed

	E_{lab} [AGeV]	σ_{K^+} [mb]	
Ne + NaF	2.1	23 ± 8	Schnetzer et al. (1989)
-"-	1.0	0.3± 0.1	Grosse (1993) KaoS
Au + Au	1.0	41 ± 7	Miskovic et al. (1994) KaoS

used for interpolations

4. procedure for hopping on shell: time scale arguments $\rightarrow$

   - upper branch: frozen-in spectrum
   - lower branch: change to vacuum spectrum

5. results for

	E_{lab} [AGeV]	
Si + Si	2.10	Barsch et al. (1985)
Ne + NaF	2.10	Shor et al. (1989)
Ni + Ni	1.85	Schröter et al. (1994) FSR
Si + Si	1.65	Carrol et al. (1988)
Si + Si	1.40	Shor et al. (1989,'92)
Si + Si	1.16	-"-

Ni+Ni 1.8 KaoS under consideration

dispersion relation occupation factors

K^-

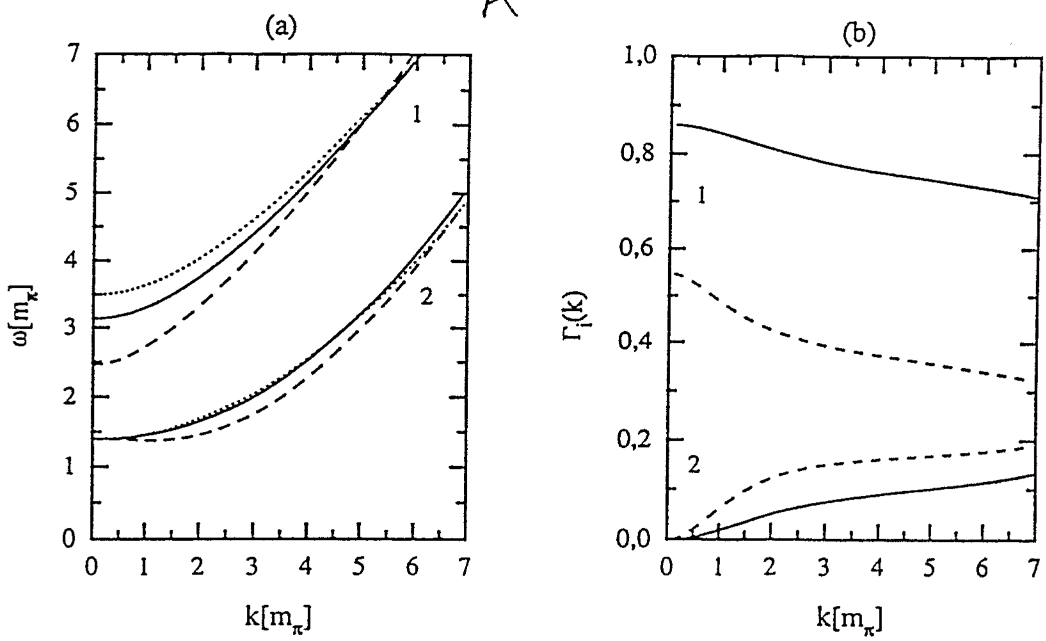

m_1^*: weeker density dependence than Weise et al. (1996)

— $0.6\,\rho_0$
- - - $3\,\rho_0$
······ $\rho_0 \to 0$

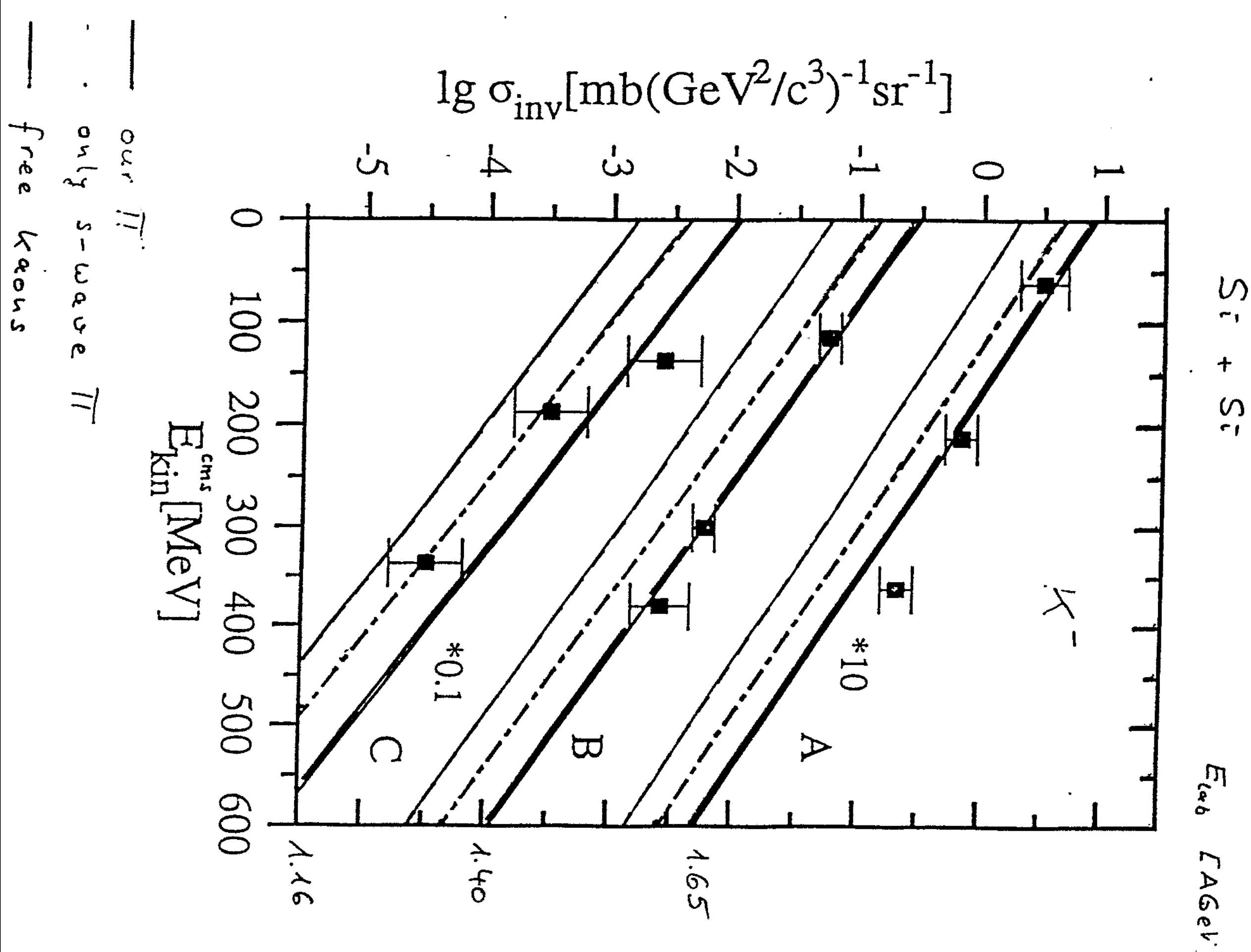

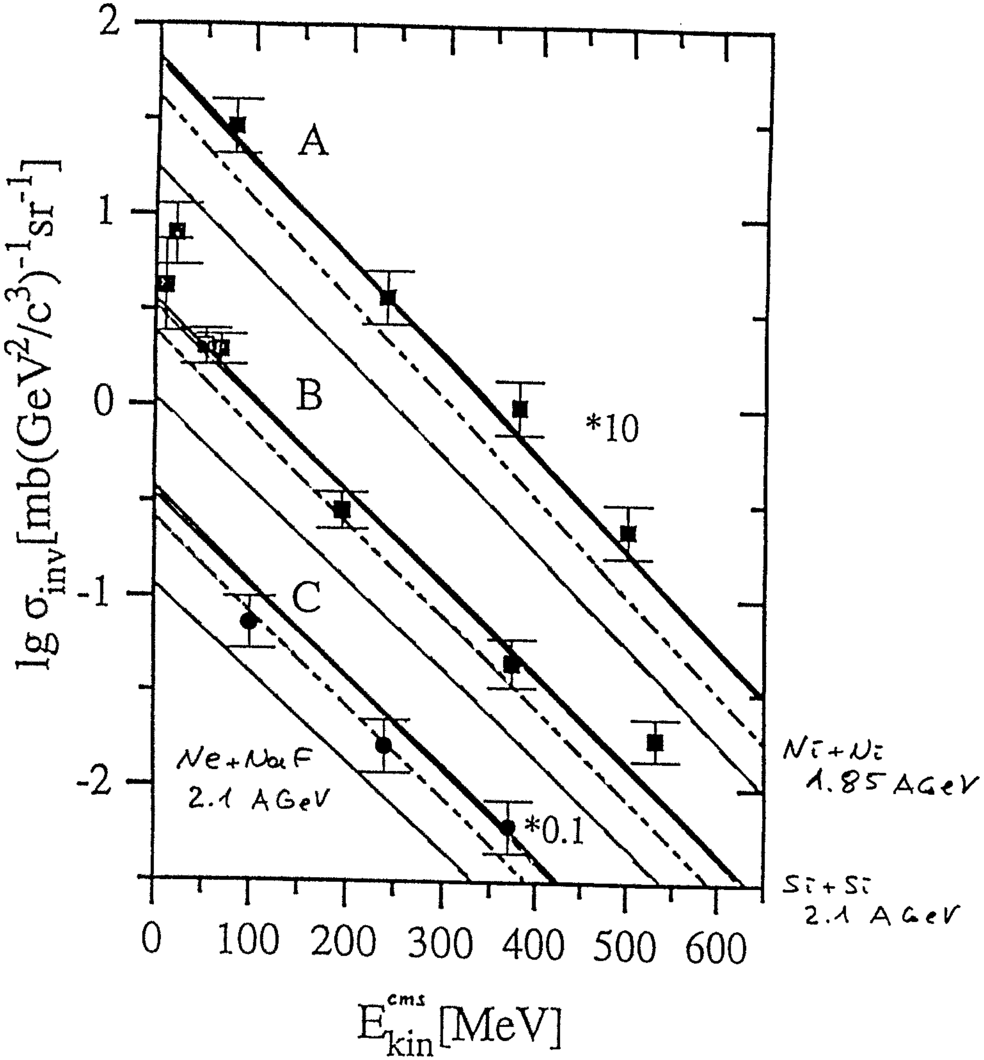

lg σinv[mb(GeV2/c3)-1sr-1]
Ekin cms [MeV]
A
B
C
*10
*0.1
Ne+NaF
2.1 AGeV
Ni+Ni
1.85 AGeV
Si+Si
2.1 AGeV

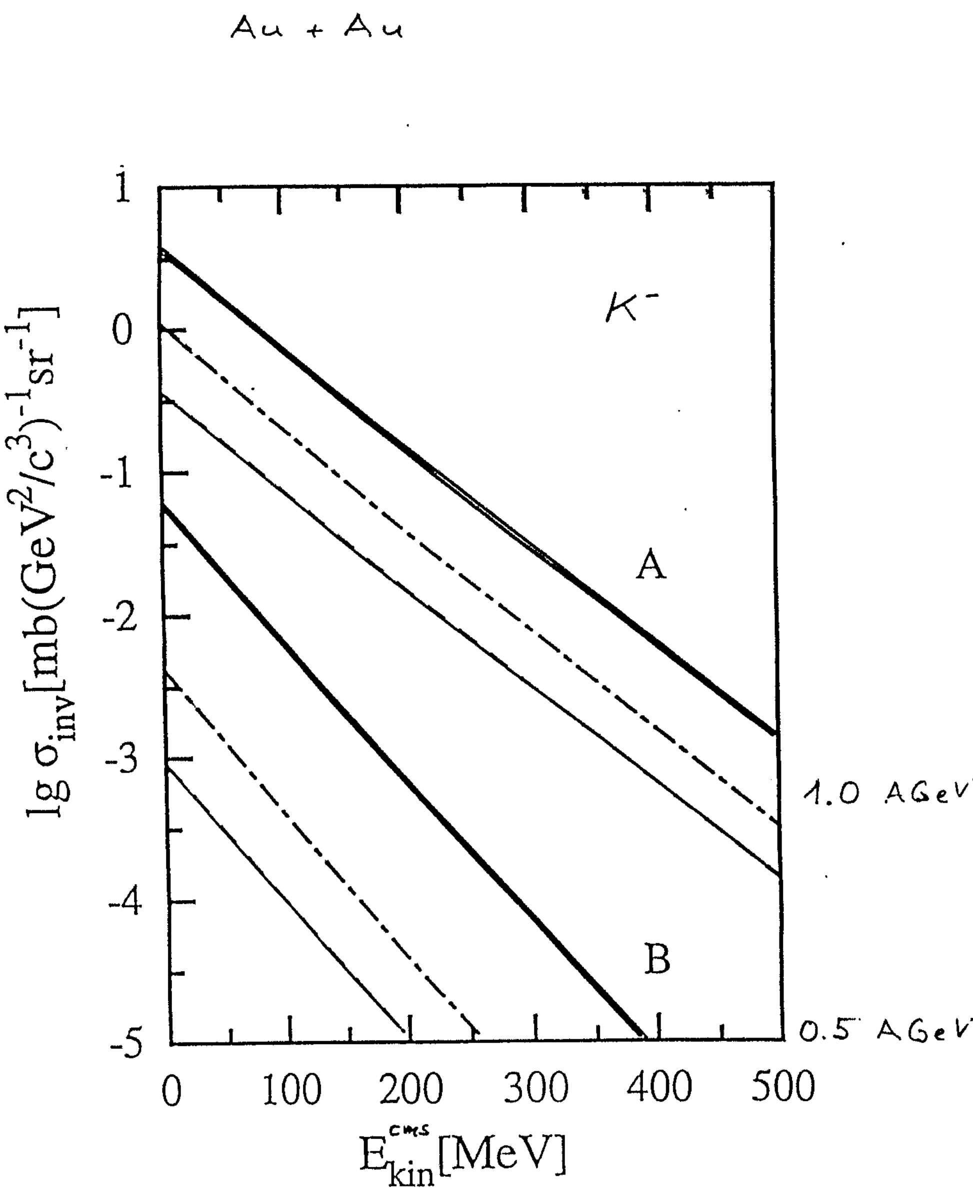

Au + Au
K-
lg σinv[mb(GeV2/c3)-1sr-1]
Ekin cms [MeV]
A
B
1.0 AGeV
0.5 AGeV

Li/Ko

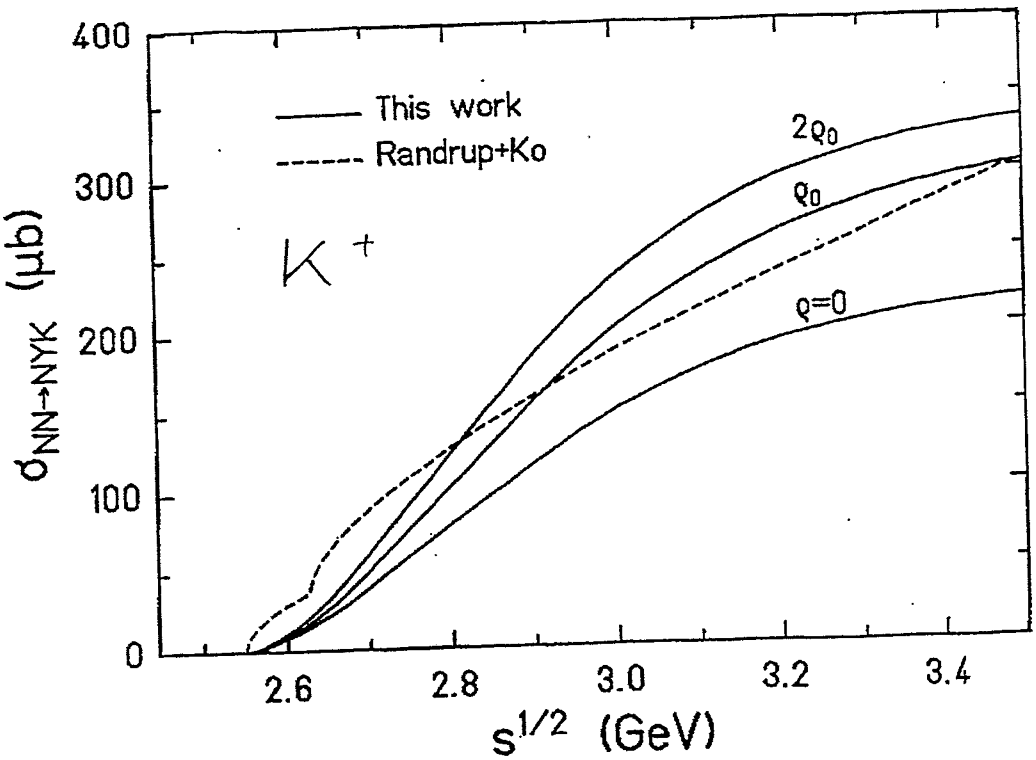

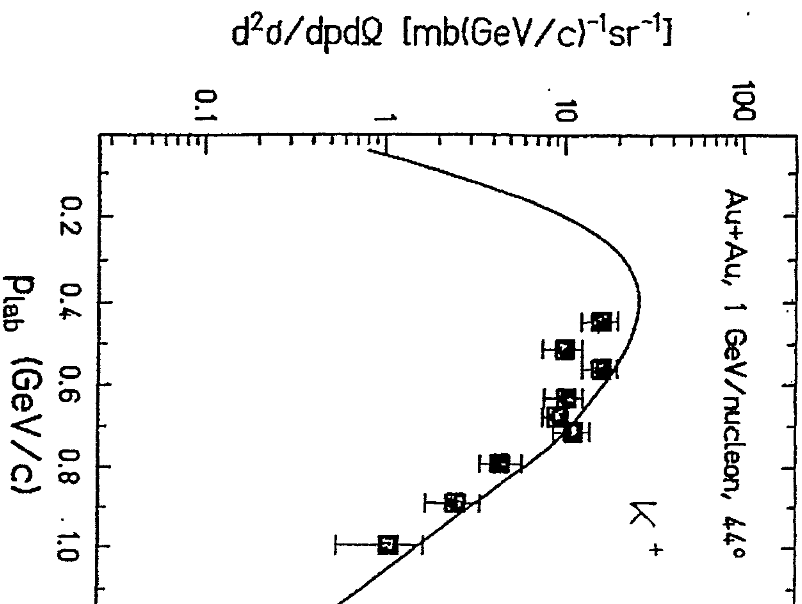

Kaos

Li/Ko